A DISSERTATION

FOR THE DEGREE OF DOCTOR OF PHILOSOPHY

Control of Macrophage Phenotypic Polarization by TSG-6 Secreted from Human and Canine Adipose Tissue-derived Mesenchymal Stem Cells in Mouse Models of Inflammatory Bowel Disease

염증성 장질환 마우스 모델에서 사람과 개의 지방유래 중간엽줄기세포가 분비하는 TSG-6 에 의한 대식세포 표현형 조절

By

Woojin Song

MAJOR IN VETERINARY CLINICAL SCIENCE

(VETERINARY INTERNAL MEDICINE)

COLLEGE OF VETERINARY MEDICINE

GRADUATE SCHOOL OF SEOUL NATIONAL UNIVESITY

February, 2019

염증성 장질환 마우스 모델에서 사람과 개의 지방유래 중간엽줄기세포가 분비하는 TSG-6 에 의한 대식세포 표현형 조절

지도교수 윤 화 영

이 논문을 수의학박사학위논문으로 제출함
2018 년 11 월

서울대학교 대학원
수의과대학 임상수의학 (수의내과학) 전공
송 우 진

송우진의 박사학위논문을 인준함
2018 년 12 월

위 원 장 김 용 백 (인)

부 위 원 장 윤 화 영 (인)

위 원 신 남 식 (인)

위 원 서 경 원 (인)

위 원 정 진 영 (인)

Control of Macrophage Phenotypic Polarization by TSG-6 Secreted from Human and Canine Adipose Tissue-derived Mesenchymal Stem Cells in Mouse Models of Inflammatory Bowel Disease

Woojin Song

(Supervised by Prof. Hwa-Young Youn)

Major in Veterinary Clinical Science
(Veterinary Internal Medicine)
College of Veterinary Medicine
Graduate School of Seoul National University

Abstract

Inflammatory bowel disease (IBD) is an intractable autoimmune disorder that markedly deteriorates quality of life. Mesenchymal stem cells (MSCs) alleviate inflammation by modulating inflammatory cytokines in inflamed tissues, and have been suggested as a promising alternative for IBD treatment in human and veterinary cases. Furthermore, tumor necrosis factor-α-induced gene/protein 6 (TSG-6) is a key factor influencing MSC immunomodulatory properties; however, the precise mechanism of TSG-6

release from human and canine MSCs in IBD remains unclear. This study aimed to assess therapeutic effects of human adipose tissue-derived (hAT)- and canine adipose tissue-derived (cAT)-MSC-produced TSG-6 in an IBD mouse model and explore the mechanisms underlying the immunomodulatory properties.

This dissertation is composed of three parts. The first part of the study was performed to investigate to assess therapeutic effects of hAT-MSC and explore their mechanisms in dextran sulfate sodium (DSS)-induced colitis mice. DSS-induced colitis mice were infused with hAT-MSCs intraperitoneally and colon tissues were collected. hAT-MSCs were shown to induce the expression of M2 macrophage markers and to regulate the expression of pro- and anti-inflammatory cytokines in the colon. Quantitative real time-PCR analyses demonstrated that less than 20 hAT-MSCs, 0.001% of all intraperitoneally injected hAT-MSCs, were detected in the inflamed colon. To investigate the effects of hAT-MSC-secreted factors *in vitro*, transwell co-culture system was used, demonstrating that tumor necrosis factor-α-induced gene/protein 6 (TSG-6) released by hAT-MSCs induces M2 macrophages. *In vivo*, hAT-MSCs transfected with TSG-6 small interfering RNA, administered intraperitoneally, were not able to induce M2 macrophage phenotype switch in the inflamed colon and had no significant effects on IBD severity.

The second part of the dissertation was designed to evaluate whether cAT-MSC-secreted TSG-6 could ameliorate IBD and regulated colonic expression of pro- and anti-inflammatory cytokines such as tumor necrosis factor-α, interleukin-6, and interleukin-10. To investigate the effect of cAT-MSC-secreted TSG-6 on activated macrophages *in vitro*, a transwell co-culture system was used; TSG-6 released by cAT-MSCs induced macrophage phenotypic switch from M1 to M2. The cAT-MSC-secreted TSG-6 increased M2 macrophages in the inflamed colon *in vivo*.

The last part of the dissertation was designed to demonstrate whether cAT-MSCs stimulated with TNF-α could exert enhanced therapeutic effects in IBD mice models. DSS- or dinitrobenzene sulfonic acid (DNBS)-induced colitis mice were treated with cAT-MSCs pre-treated with TNF-α intraperitoneally. Colitis severity was assessed and colon tissues were collected for histopathological, enzyme-linked immunosorbent assay, and flow cytometry analysis cAT-MSCs stimulated with TNF-α secreted higher concentrations of immunomodulatory factors such as TSG-6 and PGE2, which play a key role in inducing macrophages phenotypic alteration. In consequence, TNF-α pre-treated cAT-MSCs further regulated colonic inflammatory cytokines such as interleukin (IL)-1β, IL-6, and IL-10, and ameliorated DSS- or DNBS-induced colitis in mice. Also, I demonstrated that M1 macrophages ($F4/80^+/iNOS^+$ cells) were more decreased and M2 macrophages ($F4/80^+/CD206^+$ cells) were more increased in colon tissues

from mice treated with TNF-α pre-treated cAT-MSCs rather than those treated with naïve cAT-MSCs.

In conclusion, I demonstrated here that TSG-6 released from human or canine AT-MSCs can alleviate IBD in mice. Furthermore, pre-treatment with TNF-α enhanced anti-inflammatory effects of MSCs by secreting high concentrations of immunomodulatory factors (such as TSG-6 and PGE2) and inducing M2 macrophage phenotypic alteration. These findings might provide cell-based therapeutic options in IBD dogs.

Key words: / inflammatory bowel disease / auto-immune disease / mesenchymal stem cells / TSG-6 / immunomodulation / anti-inflammation

Student number: 2013-21558

CONTENTS

LIST OF FIGURES

LIST OF TABLES

ABBREVIATIONS

APC	Allophycocyanin
cAT-MSC	Canine adipose tissue-derived mesenchymal stem cell
cPBMC	Canine peripheral blood mononuclear cell
DSS	Dextran
ELISA	Enzyme-linked immunosorbent assay
FITC	Fluorescein isothiocyante
GAPDH	Glyceraldehyde 3-phosphate dehydrogenase
IACUC	Institutional Animal Care and Use Committee
IBD	Inflammatory bowel disease
IF	Immunofluorescence
IL	Interleukin
iNOS	Inducible nitric oxide synthase
LPS	Lipopolysaccharide
PE	Phycoerythrin
PGE2	Prostaglandin E2
PI	Propidium iodide
qRT-PCR	Quantitative reverse transcription-polymerase chain reaction
siRNA	Small interfering ribonucleic acid
TNF	Tumor necrosis factor
TSG-6	Tumor necrosis factor-α-induced gene/protein-6

LITERATURE REVIEW

1. Generalities of mesenchymal stem cells (MSCs)

Mesenchymal stem cells (MSCs) are a heterogeneous population of cells that proliferate *in vitro* as plastic-adherent cells, have fibroblast-like morphology, and can differentiate into adipocytes, osteocytes, and chondrocytes. MSCs have been successfully isolated from nearly every organ and many tissues including brain, liver, kidney, lung, bone marrow, muscle, thymus, pancreas, skin, aorta, vena cava, adipose tissue, fetal tissue, umbilical cord, Wharton's jelly and placenta (da Silva Meirelles et al., 2006; N Momin et al., 2010; Romanov et al., 2003). MSCs are regarded to be promising candidates for clinical application due to the ease of isolation from adult donors, thus obviating the ethical concerns concerning embryonic stem cell research.

MSCs potently modulate immune responses and have paracrine effects through secretion of growth factors, cytokines and antifibrotic or angiogenic mediators (Uccelli et al., 2008). Thus, MSCs have a broad prospect of clinical application in regenerative medicine. Recent studies also have demonstrated that MSCs show anti-inflammatory effects and can alleviate the symptoms in various inflammatory disease models, including rheumatoid arthritis, peritonitis, and pancreatitis, as well as IBD (Gonzalez-Rey et al., 2009; Jung et al., 2011; Liu et al., 2010; Prockop and Oh, 2012). Currently, the mechanisms underlying the anti-inflammatory effects are being

investigated, in order to establish the basis for effective clinical application of MSCs. In addition, MSCs derived from dogs, cats, or horses were shown to have immunomodulatory effects on activated immune cells and that cell-based therapy using MSCs is a potential treatment or intractable inflammatory diseases in veterinary medicine (Carrade Holt et al., 2014; Chae et al., 2017; Kim et al., 2016).

2. Properties of canine MSCs

Canine MSCs could be derived from various stromal tissues such as adipose tissue, bone marrow, umbilical cord blood, and amniotic fluid. Among them, canine adipose tissue or bone marrow derived MSCs have been used mainly for research and application. The samples can be obtained by appropriate general and local anesthesia. For collecting adipose tissue samples, our group use medetomidine (400-500 μg/m^2, IV), tramadol (4 mg/kg, IV), and lidocaine (local injection). For bone marrow samples, our group use alfaxalone (2 mg/kg, IV) for induction and 2% isoflurane inhalation with oxygen flow (2 L/min) for maintenance of general anesthesia.

Using protocols by professor Youn (supervisor of this dissertation), MSCs are isolated from adipose tissues as following procedure: The fat tissue are washed with PBS containing penicillin and streptomycin, and then cut into small pieces and digested for 1-2 h at 37°C with collagenase type IA. Then, enzymatic activity should be inhibited with Dulbecco's Modified Eagle's Medium (DMEM) containing 10% fetal bovine serum (FBS). After centrifugation at 1200 ×*g* for 5-10 min, the pellet should be filtered through a 100-μm cell strainer to remove debris and then incubated overnight in DMEM containing 20% FBS at 37°C in a humidified atmosphere of 5% CO_2. Then, the cultures are washed with PBS to remove non-adherent cells and incubated with fresh medium (DMEM containing 10% FBS), which should be changed

every 48-72 h until cells reached 70–80% confluence, after which they should be repeatedly sub-cultured under standard conditions (Yang et al., 2018b).

In addition, MSCs from bone marrow are isolated as following procedure: Bone marrow samples are diluted with PBS, and then gently layered over Ficoll-Paque PLUS (GE Healthcare Life Sciences, Uppsala, Sweden) in a conical tube (50 mL). After centrifugation at 800×g for 30 min without brake, the buffy coat layer should be carefully collected and centrifuged at 1200×g for 10-20 min. The supernatant is discarded and the cells are resuspended in alpha modified Eagle's medium (αMEM) containing 20% FBS, then incubated overnight at 37°C in a humidified atmosphere of 5% CO_2. After that, the cultures should be washed and changed (αMEM containing 10% FBS) as previously described for canine adipose tissue-derived MSCs (Yang et al., 2018b).

MSCs derived from stromal tissues should be characterized before their use. The International Society for Cellular Therapy (ISCT) established minimal criteria of MSC in 2006 to standardize MSCs (Dominici et al., 2006). Briefly, MSCs should adhere to plastic cell culture dish with a fibroblast-like morphology. Also, MSCs should have multi-potency of differentiation into the 3 major mesenchymal lineages (adipocytes, osteocytes, and chondrocytes) in vitro. In addition, MSCs should express specific surface markers such as

CD73, CD90, Sca-1 and CD105, but not express the negative markers such as CD14 or CD11b, CD34, and CD45.

3. Immunomodulatory effects of canine MSCs

MSCs are considered to show hypo-immunogenicity because of their low or lack of expression level in major histocompatibility complex class I and II molecules, which enables MSCs to be safely used without potential risks for immune rejection even in allogeneic environments. Furthermore, xenogeneic infusion of canine MSCs into mouse and rat models has been also reported to be well-tolerated and effective, suggesting that canine MSCs can exert cross-species immunomodulatory effects.

The immunomodulatory effects of MSCs have been demonstrated in immune-mediated disease models (Kim et al., 2016; Le Blanc et al., 2004). For example, human MSCs have been used in studies on treatment of graft-vs.-host disease, inflammatory bowel disease, systemic lupus erythematosus, and rheumatoid arthritis (Dave et al., 2015; Glenn and Whartenby, 2014). In addition, canine MSCs in particular have been used for the treatment of severe acute pancreatitis, inflammatory bowel disease, osteoarthritis, pemphigus, and atopic dermatitis (Ferrer et al., 2016; Hoffman and Dow, 2016). Moreover, several studies reported that even when MSCs do not migrate directly to the site of inflammation or the injured tissue, they can still exert anti-inflammatory actions through secretory factors (Lee et al., 2011; Silini et al., 2013). Recent investigations have reported that MSCs regulate the inflammatory processes through the activity of various soluble factors, such

as indoleamine 2,3-dioxygenase (IDO), TGF-β, PGE2, and TNF-α-induced gene/protein 6 (TSG-6) (Gonzalo-Gil et al., 2016; Kim et al., 2015; Liu et al., 2016; Liu et al., 2015). Among these factors, several studies have revealed that TSG-6 is pivotal in anti-inflammatory effects of MSCs against corneal inflammation, severe burn injury, acute lung injury, acute peritonitis, pancreatitis, and IBD (Danchuk et al., 2011; He et al., 2016; Liu et al., 2016; Roddy et al., 2011; Sala et al., 2015; Wang et al., 2012).

Furthermore, previous studies have revealed that human MSCs stimulated with pro-inflammatory cytokines (such as TNF-α and IL-1β) could improve secretory effects of immunomodulatory soluble factors (Broekman et al., 2016; Heo et al., 2011). TSG-6 and PGE_2 are well-known immunomodulatory factors secreted from human and canine MSCs, and recent studies have demonstrated that they play important roles in ameliorating atopic dermatitis, rheumatoid arthritis, acute pancreatitis, and IBD (Kim et al., 2016; Kim et al., 2015; Mao et al., 2017; Shin et al., 2016; Song et al., 2017).

4. Preclinical and clinical application of canine MSCs in non-infectious inflammatory diseases

4.1. Severe acute pancreatitis (SAP)

Acute pancreatitis is a common disease in dogs. Although most cases are self-limiting and fully reversible, some progress to severe acute pancreatitis (SAP), which leads to systemic complications such as multi-organ failure and diffuse intravascular coagulation (Cook et al., 1993; Mansfield, 2012). Mortality rates among dogs with SAP are 27% to 42% (Cook et al., 1993; Mansfield, 2012). To date, no effective treatment strategies have been developed, indicating the need for a better understanding of the pathophysiology of SAP. A breed predisposition has been reported for acute pancreatitis that deteriorates into SAP, implying that the disease is related to hereditary mutations (Hess et al., 1998), including those that cause auto-activation of trypsin, resulting in pancreatic edema, death of acinar cells (Whitcomb et al., 1996), and an inflammatory response mediated by cytokines such as TNF-α, IL-1β, -6, -12, -4, and -10, IFN-γ released by macrophages and T cells (Pandiyan et al., 2007; Tsuda et al., 2014). Overproduction of these inflammatory cytokines can lead to systemic manifestations, ulti-organ failure, or death (Norman, 1998).

I have demonstrated the therapeutic effects of canine adipose tissue-derived MSCs in a SAP rat model (not included in this dissertation). Canine

MSCs improved SAP in rats by inhibiting pro-inflammatory cytokines and stimulating anti-inflammatory cytokine production. In addition, canine MSCs suppressed the proliferation of co-cultured cPBMCs as well as rat splenocytes treated with ConA in a ratio-dependent manner. Similarly, CM containing soluble factors inhibited the proliferation of both cPBMCs and rat splenocytes in the present study. In addition, canine MSCs blocked the infiltration of $CD3^+$ T cells and increased the $FoxP3^+$ regulatory T cell population in the injured pancreas of SAP rats. Although the identity of the soluble factors and anti-inflammatory mechanisms of canine MSCs require more detailed study, I speculate that cAT-MSCs inhibit inflammation by regulating T cells via paracrine mechanisms as well as cell-to-cell contact. Therefore, canine MSCs could be an attractive candidate for cell-based clinical therapy in SAP dogs.

4.2. Inflammatory bowel disease (IBD)

IBD is an intractable autoimmune disease, leading to a chronic inflammation of the digestive system, which can be classified as either ulcerative colitis or Crohn's disease, depending on the site and pattern of inflammation (Bouma and Strober, 2003; van Beelen Granlund et al., 2013). And, IBD leads to abdominal pain, diarrhea, fever, or other symptoms that may be caused by chronic inflammation of the digestive system. Although the exact pathogenesis of IBD remains unknown, it is believed to be associated

with genetic and environmental factors, as well as inflammatory responses towards gut flora (Knights et al., 2013; Manichanh et al., 2012). Intestinal inflammatory response is known to be regulated through the secretion of inflammatory cytokines, such as TNF-α, IFN-γ, TGF-β, IL-1β, -4, -6, -10, -17 and -23 which are secreted by macrophages and T-cells (Neurath, 2014). In addition, the disease occurs naturally in dogs by a similar pathogenesis, and data from therapeutic trials for canine IBD may be excellent references for human IBD (Maeda et al., 2016). Although IBD leads to a decreased quality of life in both humans and dogs, no effective treatments for IBD have been developed.

In an open label baseline controlled study by Perez-Merino et al. (Perez-Merino et al., 2015), 12 dogs that were partially tolerant to corticosteroids with histologically confirmed lymphocytic-plasmocytic IBD, received a single intravenous injection of allogeneic, single donor sourced adipose tissue-derived MSCs (2×10^6 / kg) (Allenspach et al., 2007; Jergens et al., 2003). These patients were monitored for 42 days after transplantation using two different clinical scoring systems which incorporated laboratory and clinical observations (including owner observations of attitude, appetite, stool consistency and frequency, vomiting, pruritus) along with ascites, peripheral edema, body weight, and serum albumin as well as biomarkers folate, cobalamin, and C-reactive protein (CRP). Treatment significantly

improved clinical scores, serum albumin, and biomarkers (although not CRP) compared to baseline values. The absence of a control group obscures understanding of the magnitude of effects achieved with MSCs, and the open label design may contribute to observer (owner, veterinarian) bias. However, these data support the safety and therapeutic activity of allogeneic canine MSCs in partially refractory canine IBD at the selected dosage, one that mirrors the dosage range employed in past human studies (1-2 × 10^6 /kg).

4.3. Pemphigus

Canine pemphigus foliaceus is an autoimmune antibody mediated skin disease characterized by acantholysis. The pathogenesis involves the production of autoantibodies against a target protein in the adhesion molecules of keratinocytes (Craig, 2013). Desmoglein I is the main antigen implicated in pemphigus foliaceus in dogs and humans (Gross et al., 2008; Morris, 1994). Binding of antibodies to adhesion molecules such as Desmoglein I disrupts the intercellular cohesion of keratinocytes. This results in acantholysis and the typical lesions seen in pemphigus, including formation of blisters and intra-epidermal pustules. The cause is usually unknown. However, some cases are possibly drug-induced (White et al., 2002) or a sequel to a chronic inflammatory skin disease (Medleau and Hnilica, 2006). The most successful treatment for canine pemphigus foliaceus is

immunosuppression with corticosteroids or cyclosporine. In recent studies, however, side effects of this treatment such as diarrhea, polyuria/polydipsia, weight gain, and recurrent infections have been described (Gomez et al., 2004). Moreover, it has been reported that only 53% of treated cases survive for more than 1 year after initiation of treatment (Gomez et al., 2004).

Youn (supervisor of this dissertation) and colleagues have described the clinical application of cytotoxic T-lymphocyte antigen 4 (CTLA4) overexpressing canine MSCs and/or naive canine MSCs in steroid refractory pemphigus foliaceus. Initial treatment comprised immunosuppressive doses of prednisolone after the diagnosis of pemphigus foliaceus. Treatment with prednisolone alone did not have the desired effect and combinations with cyclosporine and azathioprine were prescribed, with no improvement in the clinical signs. Side effects of the immunosuppression included melena and anorexia and the skin condition deteriorated, with lesions spreading over the whole body. After the first administration of CTLA4 overexpressing canine MSCs, the skin lesions improved. CLTA4 overexpressing canine MSCs and/or naive canine MSCs were administered 21 times over a period of 20 months with an interval of 2 to 8 weeks. A tapering dose of prednisolone was given concurrently. After termination of canine MSC treatment, the skin lesions were well controlled with a low dose of prednisolone and remained under control for 12 months.

4.4. Atopic dermatitis

Atopic dermatitis is a condition that afflicts 8.7% dogs (Hillier et al., 2001) similar to children (10%-20%) and adults (3%-4%), that is associated with breed predilections, polymorphisms at specific gene loci, altered gene expression, and specific allergens. The concept behind employing MSC for immunomodulation of atopic dermatitis, led Hall et al. (Hall et al., 2010) to implement an open label baseline controlled clinical trial employing a single dose of autologous canine adipose tissue-derived MSC (1×10^6 cells / dog, IV) in five canine patients, using established clinical scores to record the effects. While the injections were found to be safe, no benefits of canine MSC treatment were observed in this trial. The dosage of canine MSC was lower than employed in other studies, and lower than dosages typically employed in human studies (2×10^6 /kg). It is unclear if any preclinical studies were performed to establish the immune modulatory capacity of the canine MSC used in this study. To discuss therapeutic effects of canine MSCs in atopic dermatitis, additional in vivo study using canine MSCs and/or large-scale clinical trials will be necessary.

CHAPTER I.

TSG-6 Secreted by Human Adipose Tissue-derived Mesenchymal Stem Cells Ameliorates Inflammatory Bowel Disease by Inducing M2 Macrophage Polarization in Mice

Introduction

Inflammatory bowel disease (IBD) is an intractable autoimmune disease, leading to a chronic inflammation of the digestive system, which can be classified as either ulcerative colitis or Crohn's disease, depending on the site and pattern of inflammation (Bouma and Strober, 2003; van Beelen Granlund et al., 2013). Although the exact pathogenesis of IBD remains unknown, it is believed to be associated with genetic and environmental factors, as well as inflammatory responses towards gut flora (Knights et al., 2013; Manichanh et al., 2012). Intestinal inflammatory response is known to be regulated through the secretion of inflammatory cytokines, such as tumor necrosis factor (TNF)-α, interferon (IFN)-γ, transforming growth factor (TGF)-β, interleukin (IL)-1β, -4, -6, -10, -17 and -23 which are secreted by macrophages and T-cells (Neurath, 2014). Even though there are numerous patients worldwide who suffer from IBD, which leads to a diminished quality of life, effective treatment for IBD has not been developed yet.

Recent studies have demonstrated that mesenchymal stem cells (MSCs) show anti-inflammatory effects and can alleviate the symptoms in various inflammatory disease models, including rheumatoid arthritis, peritonitis, and pancreatitis, as well as IBD (Gonzalez-Rey et al., 2009; Jung et al., 2011; Liu et al., 2010; Prockop and Oh, 2012). Currently, the mechanisms underlying the anti-inflammatory effects are being investigated,

in order to establish the basis for effective clinical application of MSCs. Moreover, several studies reported that even when MSCs do not migrate directly to the site of inflammation or the injured tissue, they can still exert anti-inflammatory actions through secretory factors (Heo et al., 2011; Silini et al., 2013). TNF-α-induced gene/protein 6 (TSG-6) is one of the best-known secretory factors responsible for anti-inflammatory activity, and recently, it was demonstrated that it plays crucial roles in the regulation of inflammatory responses in IBD, peritonitis, myocardial infarction, lung injury, corneal injury, and skin wound healing (Choi et al., 2011; Danchuk et al., 2011; Lee et al., 2009; Qi et al., 2014; Roddy et al., 2011; Sala et al., 2015).

Macrophages represent one of the key immune cells of the innate immunity and play a role as the link with immune cells responsible for the acquired immune response, such as the lymphocytes (Locati et al., 2012). According to several recently published studies, macrophages in the inflamed tissues can be classified into two distinct types: M1 and M2 macrophages (Chávez-Galán et al., 2015; Martinez et al., 2006). M1 macrophages trigger inflammatory response by secreting cytokines such as TNF-α and IL-1β, whereas M2 macrophages induce anti-inflammatory responses by secreting cytokines such as IL-10 (Murray and Wynn, 2011). Recent *in vitro* and inflammation-induced animal model studies demonstrated that MSCs can induce M1 to M2 macrophage phenotypic switch (Cho et al., 2014; Geng et

al., 2014; Nakajima et al., 2012), but the mechanisms underlying this process are not clearly understood.

In this study, I assessed the effects of human adipose tissue-derived (hAT)-MSCs on a dextran sulfate sodium (DSS)-induced colitis model in mice, together with the effect on phenotypic switch in macrophages. Additionally, I aimed to elucidate the mechanisms underlying these processes.

Materials and Methods

Cell preparations

Human adipose tissue was obtained from the abdominal subcutaneous fat of donor that provided an informed, written consent for research use. Cells isolated were prepared under a protocol approved by the Institutional Review Board of the R Bio (IRB No. RBIO-2015-04-002). Subcutaneous adipose tissues were digested with collagenase I (1 mg/mL; Gibco/Life Technologies, Grand Island, NY, USA) under gentle agitation for 60 min at 37ºC and filtered through a 100-mm nylon sieve to remove cellular debris, followed by centrifugation at 470 g for 5 min. After centrifugation, the pellet was resuspended in Dulbecco's modified eagle's medium (DMEM; Invitrogen, Carlsbad, CA, USA)–based media and cultured overnight at 37°C in a humidified atmosphere with 5% CO_2. After 24 h, the cell adhesion was checked under an inverted microscope, and non-adherent cells were removed by washing with phosphate buffered saline (PBS; PAN biotech, Aidenbach, Germany). The cell medium was changed to keratinocyte-serum free medium (SFM; Invitrogen) based media containing 0.2 mM ascorbic acid, 0.09 mM calcium, 5 ng/mL recombinant epidermal growth factor (rEGF; Prospec, East Brunswick, NJ, USA), and 5% fetal bovine serum (FBS; PAN biotech). The cells were maintained for 4 to 5 days until confluent (passage 0). When the cells reached 90% confluency, they were subculture-expanded in

Keratinocyte-SFM-based media containing 0.2 mM ascorbic acid, 0.09 mM calcium, 5 ng/mL rEGF, and 5% FBS. Isolated hAT-MSCs were used at passage 3-5 for the following experiments.

Cells isolated were characterized for the expression of stem cell markers by flow cytometry using fluorescein isothiocyante (FITC)-, or phycoerythrin (PE)-conjugated antibodies against the following proteins: CD31-FITC, CD34-PE, CD45-FITC, CD73-PE, and CD90-PE (all from BD Biosciences, Franklin Lakes, NJ, USA). Cells were analyzed using a FACSCalibur flow cytometer (BD Biosciences) with the CELLQuest software (BD Biosciences). Cellular differentiation was evaluated using the StemPro Adipogenesis Differentiation, StemPro Osteogenesis Differentiation, and StemPro Chondrogenesis Differentiation kits (all from Gibco/Life Technologies, Carlsbad, CA, USA) according to the manufacturer's instructions followed by Oil Red O staining, Alizarin Red staining, and Alcian Blue staining, respectively. The expression of several stem cell markers on these cells was determined by flow cytometry (Fig. 1). Additionally, cellular differentiation was observed (Fig. 2), and the isolated hAT-MSCs at passage 3-5 were used in the following experiments.

RAW 264.7 cells, murine macrophage-like cell line, were purchased from the Korean Cell Line Bank (Seoul, Korea). Macrophages were cultured in Dulbecco's Modified Eagle's Medium (DMEM; PAN Biotech, Aidenbach,

Germany) containing 10% foetal bovine serum (FBS; PAN Biotech) at 37°C in a humidified atmosphere with 5% CO_2.

Stimulation of hAT-MSCs with TNF-α

Before further co-culture experiments, hAT-MSCs were stimulated with TNF-α, in order to induce TSG-6 expression. hAT-MSCs were plated at the density of 2×10^5 cells per well in six-well plates or 1×10^6 in 100-mm culture dishes, and incubated for 24 h. Afterwards, the medium was changed and 50 ng/mL of the recombinant human TNF-α (PeproTech, Rocky Hill, NJ, USA) was added, and the incubation was continued for another 24 h. TSG-6 mRNA expression level of these cells were determined using qRT-PCR.

Transfection of hAT-MSCs with small interfering RNA (siRNA)

When they reach approximately 40% confluence, hAT-MSCs were transfected with TSG-6 siRNA or control siRNA (sc-39819 and sc-37007, respectively; Santa Cruz Biotechnology, Santa Cruz, CA, USA) for 48 h using Lipofectamine 2000 (Invitrogen, Carlsbad, CA, USA) according to the manufacturers' instructions. TSG-6 knockdown was confirmed by q RT-PCR assays before the use of these cells in further experiments.

Animal experiments

Male C57BL/6J mice aged 6-8 weeks were purchased from the Central Lab Animal Inc. (Seoul, Korea) and they were housed under controlled conditions of temperature (20°C), humidity (50%) and light cycle (7 am lights on, 7 pm lights off). The study and all experimental procedures involving animals were approved by the Institutional Animal Care and Use Committee of Seoul National University (SNU-151007-3-1), and the animal study protocol was performed in accordance with the approved guidelines. Colitis was induced by the *ad libitum* administration of 3% DSS (36-50 kDa, MP biomedical, Solon, OH, USA) in the drinking water from day 0 to day 7. On day 1, the following procedure was performed: hAT-MSCs (2×10^6 cells in 200 μL PBS) or the identical PBS volume were injected intraperitoneally into mice; 2×10^6 hAT-MSCs transfected with TSG-6 siRNA in 200 μL of PBS, 2×10^6 hAT-MSCs transfected with scrambled siRNA control in 200 μL of PBS, 2×10^6 control hAT-MSCs in 200 μL of PBS, or the identical volume of PBS was injected intraperitoneally into mice for systemic siRNA-hAT-MSC experiments. And hAT-MSCs transfected with si-RNA were used just after completion of the transfection protocol described above. In each experiment, mice receiving normal drinking water were used as the naïve group. Body weight of each mouse was measured every 24 h, mice were sacrificed on day 10, and the colon samples were collected for further processing.

Assessment of colitis severity

The DAI was calculated by scoring the body weight loss (grades, 0-4: 0, none; 1, < 10% loss of the initial body weight; 2, 10-15% loss of the initial body weight; 3, 15-20% loss of the initial body weight; 4, >20% loss of the initial body weight), stool consistency (grades, 0-2: 0, none; 1, mild diarrhoea; 2, moderate to severe diarrhoea), rectal bleeding (grades, 0-2: 0, none; 1, mild bleeding; 2, moderate to severe bleeding), and general activity (grades, 0-2: 0, normal; 1, mildly depressed; 2, moderately to severely depressed).

Histological analysis

Colon samples were fixed in 10% formaldehyde for 24 h, embedded in paraffin, and cut into 4-μm sections, which were stained with H&E. A total of 30 fields per group was selected randomly and histological examinations were performed in a blinded manner (magnification, 200×). The severity of symptoms was determined by scoring the extent of bowel wall thickening (grades, 0-3: 0, none; 1, mucosa; 2, mucosa and submucosa; 3, transmural), the damage of crypt (grades, 0-3: 0, none; 1, loss of goblet cells; 2, only surface epithelium intact; 3, loss of entire crypt and epithelium), and the infiltration of inflammatory cells (grades, 0-2: 0, none; 1, mild to moderate; 2, severe).

Co-culturing of Raw 264.7 macrophages with hAT-MSCs

Raw 264.7 cells were stimulated with 200 ng/mL of LPS (Sigma-Aldrich, St. Louis, MO, USA) for 6 h before further experiments. The LPS-stimulated macrophages were plated at the density of 1×10^6 cells per well in six-well plates and 2×10^5 hAT-MSCs, control siRNA-hAT-MSCs, or TSG-6 siRNA-hAT-MSCs were seeded onto 0.4-μm pore-sized transwell inserts (SPL Life Science, Pocheon, Korea). After 48 h of incubation, total RNA and proteins were extracted from the Raw 264.7 macrophages following their trypsinization.

RNA extraction, cDNA synthesis, and qRT-PCR

Total RNA was extracted from homogenised colon tissue or Raw 264.7 cells using the Easy-BLUE Total RNA Extraction kit (Intron Biotechnology, Seongnam, Korea) according to the manufacturer's instructions. cDNA was synthesised using LaboPass M-MuLV Reverse Transcriptase (Cosmo Genetech, Seoul, Korea) and the samples were analysed in duplicate using 10 μL of AMPIGENE qPCR Green Mix Hi-ROX with SYBR Green dye (Enzo Life Sciences, Farmingdale, NY, USA) and 400 nM forward and reverse primers (Cosmo Genetech). Expression levels of the target genes were normalised to that of glyceraldehyde 3-phosphate

dehydrogenase (GAPDH). Primer sequences used in this study are listed in Table 1.

Determination of TSG-6 expression by MSCs in the conditioned medium (CM)

TSG-6 secreted by naïve hAT-MSCs, TNF-α-stimulated hAT-MSCs, siCTL-hAT-MSCs, or siTSG6-hAT-MSCs grown in the CM was quantified by ELISA kit (MyBiosource, San Diego, CA, USA), according to the manufacturer's instructions.

Western blot analysis

Total proteins were extracted from Raw 264.7 cells using PRO-PREP Protein Extraction Solution (Intron Biotechnology) according to the manufacturer's instructions. The concentrations of the protein samples were measured using Bio-Rad DC Protein Assay Kit (Bio-Rad, Hercules, CA, USA). The proteins were separated by sodium dodecyl sulfate-polyacrylamide gel electrophoresis and transferred to polyvinylidene difluoride membranes (Millipore, Billerica, MA, USA). The membranes were blocked by 5% non-fat dry milk in Tris-buffered saline containing 0.1% Tween 20 and incubated with primary antibodies against CD206 (1:1000; Abcam, Cambridge, MA, USA) and Arg1 (1:1000; Cell Signaling Technology, Beverly, MA, USA) at 4°C overnight. The membranes were incubated with

secondary antibodies at room temperature for 1 h. The immunoreactive bands were visualised using enhanced chemiluminescence (Advansta, Menlo Park, CA, USA) and normalised to β-actin levels (Santa Cruz Biotechnology).

Immunofluorescence(IF) analyses

Paraffin-embedded 4-μm thick colon tissue sections were deparaffinised in xylene and rehydrated sequentially in 100%, 95%, 80%, and 70% ethanol. After antigen retrieval using 10 mM citrate buffer (Sigma-Aldrich), the sections were blocked with blocking buffer containing 5% bovine serum albumin and 0.3% Triton X-100 (both from Sigma-Aldrich) for 1 h. Afterwards, the slides were incubated overnight at 4°C with antibodies against phycoerythrin-conjugated CD11b (1:100; Abcam) and CD206 (1:200; Santa Cruz Biothechnology). For the sections incubated with CD206 antibody, after three washes, they were incubated with fluorescein isothiocyante-conjugated secondary antibody (1:200; Santa Cruz Biotechnology) for 1 h at room temperature in the dark. Then, the colon sections stained with either antibody against CD11b or CD206 were washed three times and mounted in Vectashield mounting medium containing 4',6-diamidino-2-phenylindole (Vector Laboratories, Burlingame, CA, USA). The samples were observed using EVOS FL microscope (Life Technologies, Darmstadt, Germany). Immunoreactive cells were counted in 20 random fields per group and the

ratio of CD206/CD11b positive cells was calculated with colon sections from same mice.

Generation of GAPDH standard curve

Standard curves for the evaluation of the migratory ability of intraperitoneally injected cells were produced by delivering serial dilutions of hAT-MSCs to mouse tissues as described previously[14,16]. Briefly, 2×10, 2×10^2, 2×10^3, 2×10^4, or 2×10^5 hAT-MSCs were added to the whole mouse organs prior to the homogenization. After the total RNA was extracted from the samples (Easy-BLUE Total RNA Extraction kit; Intron Biotechnology), cDNA was synthesised (LaboPass M-MuLV Reverse Transcriptase; Cosmo Genetech) using 1 μg of RNA. qRT-PCR for human-specific GAPDH (forward primer, TGC TTT TAA CTC TGG TAA AGT GGA TA; reverse primer, GTG GAA TCA TAT TGG AAC ATG TAA AC) was performed in order to generate the standard curve, which was corrected by performing parallel qRT-PCR with primers used to amplify both human and mouse GAPDH (forward primer, CAG CGA CAC CCA CTC CTC CAC CTT; reverse primer, CAT GAG GTC CAC CAC CCT GTT GCT).

Statistical analysis

Data are shown as mean ± standard deviation. Group means were compared by one-way analysis of variance (ANOVA) using the GraphPad Prism v.6.01 software (GraphPad Inc., La Jolla, CA, USA). P value of < 0.05 was considered statistically significant.

Results

Intraperitoneally administered hAT-MSCs ameliorate IBD

Intraperitoneal injection of hAT-MSCs was shown to lead to a significant reduction in body weight loss, in comparison with that measured in mice injected with the phosphate-buffered saline (PBS) from day 7 (Fig. 3). On day 10, the disease activity index (DAI) of mice treated with hAT-MSCs was significantly decreased, in comparison with that in the mice treated with PBS (Fig. 4). To evaluate length and histology of the colon, mice were sacrificed on day 10. Compared with that in the PBS-treated group, colon length was significantly improved in hAT-MSC-treated group (Fig. 5). Histological examination of the DSS-induced colitis mouse colons showed severe submucosal or transmural thickening, destruction of entire epithelium, and severe inflammatory cell infiltration. In contrast, the extent of bowel wall thickening, crypt damage, and the infiltration of inflammatory cells were reduced in colon sections obtained from mice injected with hAT-MSCs, compared with those in the PBS-treated mice (Fig. 6). The analysis for haematoxylin and eosin (H&E)-stained colon sections showed a significant decrease in the histologic scores of hAT-MSC-treated group, in comparison with those in the PBS-treated group (Fig. 6).

hAT-MSCs reduce the inflammatory response by increasing the percentage of M2 macrophages in colon

I explored whether intraperitoneally injected hAT-MSCs modulate inflammatory cytokines related to development of DSS-induced colitis. In colon tissues of the PBS-treated colitis mice, TNF-α, IL-1β, IFN-γ, and IL-17 mRNA expression levels were considerably increased, whereas that of IL-10 was increased slightly (Fig. 7). However, the administration of hAT-MSCs not only significantly decreased the expression levels of these genes but also significantly increased that of IL-10, in comparison with those in the PBS-treated animals (Fig. 7). Furthermore, protein levels of TNF-α and IL-10 in the colon samples also exhibited similar tendencies in the colitis mice (Fig. 8).

Considering that hAT-MSCs may affect the activity of inflammatory cytokines, I examined the presence of M2 macrophages in the colon tissues. The expression levels of CD206, Arg1, Fizz1, and Ym1 (well-known M2 macrophage markers) were decreased or slightly increased in the colons of colitis model mice treated with PBS (Fig. 9). However, the injection of hAT-MSCs led to a significant increase in the expression of M2 macrophage markers, compared with that in the PBS-treated mice (Fig. 9). Furthermore, infiltrated total macrophages and M2 macrophages were detected in colon tissue sections, using the antibodies specific for CD11b and CD206,

respectively (Fig. 10). And I calculated the percentage of CD206-positive cells to CD11b-positive cells using colon sections from the same mice. The percentage of M2 macrophages in the PBS-treated group was 14.50% ± 2.65%, whereas it was 59.25% ± 1.71% in the hAT-MSC-treated group (Fig. 10).

Intraperitoneally injected hAT-MSCs do not migrate into the colon

I next tracked and quantified the hAT-MSCs administered intraperitoneally (2×10^6 cells) by constructing standard curves using quantitative real time (qRT)-PCR (Figs. 11, 12, and Table 1). After 1 day of hAT-MSC administration, approximately 0.002%, 0.12%, 0.02%, 0.06% and 0.09% of the cells were detected in the heart, lung, liver, spleen, and kidney of the colitis mice, respectively (Fig. 13). After 3 days of hAT-MSC injection, percentages of the cells detected in the five organs were decreased compared with day 1 (Fig. 13). However, intraperitoneally infused hAT-MSCs were hardly detected in the brain and the inflamed colon tissues of the colitis mice at day 1 as well as day 3 (Figs. 11, 13).

hAT-MSC-produced TSG-6 induces the phenotypic switch to M2 macrophages in vitro

I further investigated whether TSG-6, one of well-known immunomodulatory factors secreted by hAT-MSCs, can alter macrophage phenotype to M2. To test the hypothesis, TNF-α-stimulated hAT-MSCs were used. TSG-6 gene expression was considerably induced in these cells, in comparison with that in the naïve hAT-MSCs (Fig. 14). Additionally, TSG-6 concentration determined in the supernatant collected from the culture of TNF-α-stimulated hAT-MSCs was significantly higher than that measured using the naïve hAT-MSCs (Fig. 14). Afterwards, lipopolysaccharide (LPS)-stimulated Raw 264.7 cells were co-cultured with the naïve or TNF-α-stimulated hAT-MSCs in a transwell system for 48 h, and M2 macrophage marker gene expression levels were shown to be significantly increased in the LPS-stimulated Raw 264.7 cells co-cultured with naïve hAT-MSCs, compared with those determined using the LPS-stimulated Raw 264.7 cells alone (Fig. 15). Interestingly, the expression levels of the M2 macrophage markers were shown to be further increased in the LPS-stimulated Raw 264.7 cells co-cultured with TNF-α-stimulated hAT-MSCs, in comparison with those in the cells co-cultured with naïve hAT-MSCs (Fig. 15). CD206 and Arg1 levels were determined as well, and LPS-stimulated Raw 264.7 cells co-cultured with naïve hAT-MSCs was shown to express CD206 and Arg1 (Fig. 16). Furthermore, the expression of both proteins was significantly increased in LPS-stimulated Raw 264.7 cells co-cultured with TNF-α-stimulated hAT-

MSCs compared with that in the cells co-cultured with naïve hAT-MSCs (Fig. 16).

Furthermore, TSG-6 expression in hAT-MSCs was knocked down by transient transfection with siRNAs. hAT-MSCs transfected with siRNAs maintained their fibroblast-like shape, proliferative ability, and differentiation potential *in vitro* (Fig. 2). TSG-6 expression was shown to be suppressed in hAT-MSCs transfected with TSG-6 siRNA (siTSG6-hAT-MSCs), whereas there was no significant change in TSG-6 expression levels in hAT-MSCs transfected with the control siRNA (siCTL-hAT-MSCs), compared with those in the naïve hAT-MSCs (Fig. 17). Additionally, the concentration of TSG-6 protein secreted by siTSG6-hAT-MSCs was significantly decreased compared with that by the naïve or siCTL-hAT-MSCs (Fig. 17). Afterwards, I co-cultured LPS-stimulated Raw 264.7 cells with naive or siRNA transfected hAT-MSCs in a transwell system for 48 h, and showed that M2 macrophage marker gene expression levels were significantly reduced in LPS-stimulated Raw 264.7 cells co-cultured with siTSG6-hAT-MSCs compared with those in the naïve hAT-MSCs (Fig. 18). Furthermore, CD206 and Arg1 levels were significantly decreased as well in the LPS-stimulated Raw 264.7 cells co-cultured with siTSG6-hAT-MSCs (Fig. 19). In contrast to this, siCTL-hAT-MSCs, with normal TSG-6 secretion levels, did not affect the gene or protein

expression of M2 macrophage markers in LPS-stimulated Raw 264.7 cells (Figs. 18, 19).

Intraperitoneal administration of hAT-MSCs with TSG-6 knockdown cannot alleviate IBD

I further investigated whether siRNA-transfected hAT-MSCs can alleviate DSS-induced colitis in mice. siTSG6-hAT-MSCs had no effect on body weight loss and DAI. In contrast, siCTL-hAT-MSCs were shown to significantly reduce body weight loss and DAI (Figs. 20, 21). Additionally, no significant improvement in the length and histologic score of colons obtained from the mice that received siTSG6-hAT-MSCs was observed. However, the administration of siCTL-hAT-MSCs led to a significant improvement in length and histologic score of these mice (Figs. 22, 23).

Next, I assessed the expression level of M2 macrophages in colons of colitis mice. Intraperitoneal administration of siTSG6-hAT-MSCs had no effect on the expression level of the M2 macrophage markers in the colon, in comparison with those measured in the PBS-treated mice (Fig. 24). In contrast, siCTL-hAT-MSCs injection led to a significant increase in M2 macrophage marker expression in the colon, in comparison with that in the PBS-treated mice (Fig. 24). Furthermore, the percentage of CD206-positive M2 macrophages to CD11b-positive total macrophages was significantly

increased in the colon tissue sections of mice injected with siCTL-hAT-MSCs, whereas there was no significant difference in the percentage of M2 macrophages in the colons of mice injected with siTSG6-hAT-MSCs, compared with that in the PBS-treated mice (Fig. 25).

Discussion

Recently, hAT-MSCs, which can be obtained relatively easily in large quantities, have shown promising anti-inflammatory effects in studies that used different inflammatory disease models (Choi et al., 2016; González et al., 2009; Lopez-Santalla et al., 2015; Shin et al., 2016; van den Broek et al., 2013). For chronic diseases, such as IBD, hAT-MSC administration may represent an important treatment option. Here, I showed that the application of hAT-MSCs to DSS-induced colitis mouse model may alleviate the symptoms of this disease, and that the weight loss and DAI were improved. Furthermore, by measuring the length of colon and assigning the scores based on the microscopic observation of the colon tissue obtained during the mouse autopsy, I showed that the intraperitoneal administration of hAT-MSCs has therapeutic effects against DSS-induced colitis in mice. In addition, I analysed the mechanisms underlying this process, in order to help the development of efficient cell therapies and their clinical application.

For these experiments, I injected human MSCs into immunocompetent mice model of IBD. I used this strategy to focus on immune cells of mice after human MSC application. Also, human MSCs are immunoprivileged partly due to low expression of major histocompatibility complex class II (Le Blanc et al., 2003). Furthermore, similar strategy applying human MSCs to immunocompetent animal models has been

successfully performed by several groups, and obvious cross-species-induced immunological responses have not been reported (Kim et al., 2013; Kim et al., 2015; Qi et al., 2014; Roddy et al., 2011).

Macrophages observed in the inflamed tissue may appear as either M1 or M2 macrophages, with distinct roles in the regulation of inflammatory response (Jang et al., 2014; Nishikawa et al., 2014; Wang et al., 2007; Wynn et al., 2013; Zhu et al., 2014). Macrophages have very important roles in innate and acquired immune response, and consequently, macrophage type changes have a major impact on the inflammatory conditions in the inflamed tissue. It is well known that M2 macrophages can be induced by IL-4 and IL-13, which induce the expression of CD206, Arg1, Fizz1, and Ym1 (Murray and Wynn, 2011; Sica et al., 2015). Moreover, recent studies demonstrated that MSCs might have ability to elicit the phenotypic switch from M1 to M2 macrophages in animal models for acute kidney injury, spinal cord injury and skin wound as well as *in vitro* (Cho et al., 2014; Geng et al., 2014; Nakajima et al., 2012; Vasandan et al., 2016; Ylöstalo et al., 2012; Zhang et al., 2010). Consistent with these reports, I found here that colon tissues obtained from the hAT-MSC-injected group showed a considerably higher expression of M2 macrophage markers than the colon tissues obtained from the PBS-treated group. Moreover, the percentage of M2 macrophages to total macrophages identified using IF staining the in colon tissue sections was increased in the

hAT-MSC-treated group compared with the PBS-treated group. Gene expression levels of pro-inflammatory cytokines TNF-α, IL-1β, IFN-γ, and IL-17 were significantly reduced in the colons of the hAT-MSC-treated group, while the expression of anti-inflammatory cytokine IL-10 was significantly induced. These findings indicated that the intraperitoneally administration of hAT-MSCs modulates the expression of the inflammatory cytokines by inducing the cell differentiation into M2 macrophages in the colon, alleviation the inflammatory responses. In addition, my results might complement previous findings that MSCs infused into colitis mice reduced inflammation by altering macrophages (Anderson et al., 2012; Parekkadan et al., 2011).

According to previous studies that have revealed therapeutic effects of MSCs in the DSS-induced colitis mice model, I determined the optimal procedure, that is, 2×10^6 hAT-MSCs were administered intraperitoneally (Kim et al., 2013; Wang et al., 2016). Also, I examined the distribution of hAT-MSCs intraperitoneally injected using qRT-PCR assays. At 1 day and 3 days after hAT-MSC administration, less than 0.5% of injected cells were detected in total for heart, lung, liver, spleen, kidney, and brain tissues. In addition, less than 0.001% of injected cells were detected in colon tissues despite inflammatory response. In addition, similar results obtained after siCTL- and siTSG6-hAT-MSC administration in colitis mice. These findings are related to several previous studies (Bazhanov et al., 2016; Sala et al.,

2015). Sala *et al*. reported that less than 1% of mouse bone marrow- and adipose-derived MSCs injected intraperitoneally to DSS-induced colitis mice model were detected in inflamed colon, whereas high frequency of injected cells formed aggregates with immune cells in the peritoneal cavity within 3 days (Sala et al., 2015). Bazhanov *et al*. also showed that the majority of human bone marrow-derived MSCs infused intraperitoneally into immunocompetent mice aggregated quickly and the aggregates were attached in the peritoneal cavity (Bazhanov et al., 2016). Based on these previous studies, my findings indicated that most of hAT-MSCs administered intraperitoneally might form aggregates in the peritoneal cavity and reduce colitis by inducing M2 macrophages distant from the inflamed colon through secretory factors.

Consistent with the findings, recent investigations have reported that MSCs regulate the inflammatory processes through the activity of various soluble factors, such as indoleamine 2,3-dioxygenase, TGF-β, prostaglandin E2 (PGE2), and TSG-6 (Gonzalo-Gil et al., 2016; Kim et al., 2015; Liu et al., 2016; Liu et al., 2015). Among these factors, several studies have revealed that TSG-6 is pivotal in anti-inflammatory effects of MSCs against corneal inflammation, severe burn injury, acute lung injury, acute peritonitis, pancreatitis, and IBD (Broekman et al., 2016; Danchuk et al., 2011; Liu et al., 2016; Roddy et al., 2011; Sala et al., 2015; Wang et al., 2012). In addition,

Mittal *et al.* recently showed that TSG-6 prevented lung injury by inducing macrophage phenotype switch, although TSG-6 used in the study was not a protein released by stem cells (Mittal et al., 2016). Based on these previous findings and my results, it is tempting to speculate that TSG-6 secreted from hAT-MSCs plays a key role in inducing M2 macrophage polarization in the inflamed colon.

Thus, I conducted *in vitro* experiments to examine whether TSG-6 secreted by hAT-MSCs has ability to induce macrophage phenotype switch. LPS-stimulated Raw 264.7 cells exhibit a conventional M1 macrophage pattern, and these cells were co-cultured with hAT-MSCs with TNF-α-induced or inhibited TSG-6 expression, or with the naive hAT-MSCs. The co-culturing of TSG-6 overexpressing hAT-MSCs with M1 macrophages led to a significant increase in the expression of M2 macrophage markers. However, because it is possible that other factors secreted by hAT-MSCs may affect this process as well, I performed additional experiments using TSG-6 targeting siRNAs. hAT-MSCs with TSG-6 knockdown were cultured with M1 macrophages, and the expression of M2 macrophage markers was shown to be decreased in these cells. Taken together, these findings suggest that TSG-6 secreted by hAT-MSCs plays a crucial role in the regulation of M1 to M2 phenotypic switch *in vitro*.

In order to analyse effects of TSG-6 released by hAT-MSCs *in vivo* as well, I administered siRNA-treated hAT-MSCs to the experimental animals, and showed that, in comparison with those in the control group, siTSG6-hAT-MSC administration did not lead to significant changes in M2 macrophage marker expression levels in the colon. However, the expression of these markers was shown to be induced in the siCTL-hAT-MSC-treated group and naive hAT-MSC-treated group, in comparison with that in the PBS-treated group. Taken together, I confirmed that TSG-6 secreted by hAT-MSCs plays an important role in the alteration of macrophages to M2 phenotype in the inflamed mouse colons. Moreover, the percentage change of M2 macrophages to total macrophages in colon affected the severity of DSS-induced colitis symptoms in mice. In the siTSG6-hAT-MSC-treated group, weight loss rate, DAI, colon length, and histologic scores were not improved, in comparison with those in the PBS-treated group, but the animals treated with siCTL-hAT-MSCs showed considerable improvements in these parameters, which were similar to those observed in the naive hAT-MSC-treated group.

Even so, my results do not exclude the possibility that one or more other secretory factors released from hAT-MSCs increased ability to induce M2 macrophage polarization in colitis mice. Interestingly, recent investigations showed that human MSCs altered macrophage phenotype by

producing PGE2 *in vitro* (Vasandan et al., 2016; Ylöstalo et al., 2012). Additional experiments related to other MSC-secreted factors such as PGE2 are required to determine their effects on macrophages in IBD models. However, my findings suggest that TSG-6 plays a key role in M2 macrophage polarization *in vitro* and DSS-induced colitis mice.

In conclusion, I present here a possible mechanism underlying TSG-6-induced effects in various inflammatory disease models, including IBD, which were previously described. I demonstrated that hAT-MSC-secreted TSG-6 induces the phenotypic switch of macrophages that infiltrated into colon to M2 type, which leads to the regulation of inflammatory cytokine expression and the alleviation of DSS-induced colitis symptoms in mice. I believe that these findings may help the understanding and the development of stem cell therapies for the treatment of IBD.

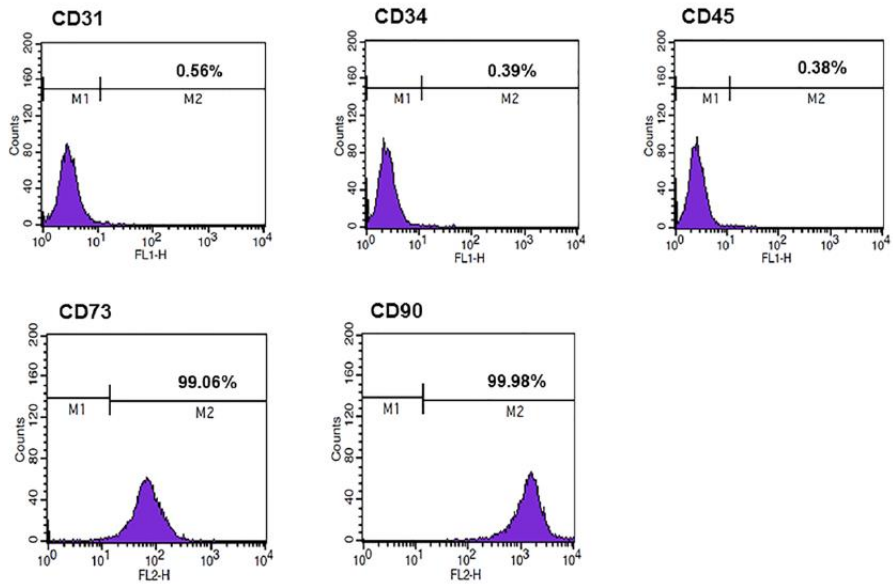

Figure 1. Immunophenotypic analysis of hAT-MSCs by flow cytometry.

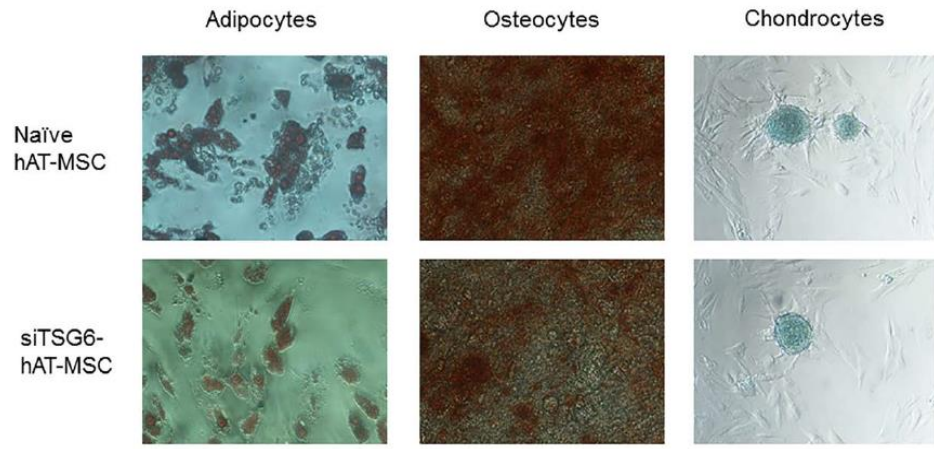

Figure 2. Adipogenic (Oil Red O staining), osteogenic (Alizarin Red S staining), and chondrogenic (Alcian Blue staining) differentiation of naïve and siTSG6-hAT-MSCs.

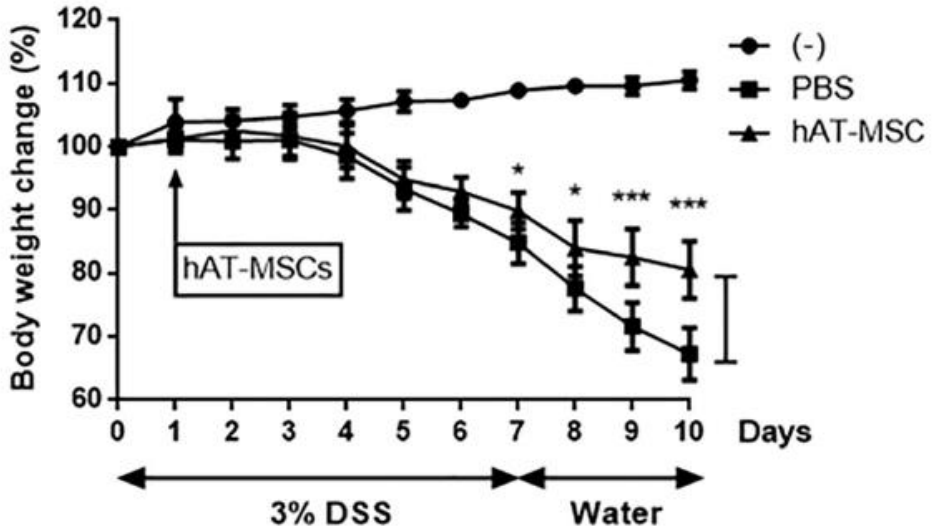

Figure 3. Intraperitoneally injected hAT-MSCs ameliorate IBD. DSS-induced colitis mice were infused hAT-MSCs or PBS (vehicle control) on day 1. Body weight, measured every day and expressed as the relative change from day 0. Results are shown as mean ± standard deviation. *P < 0.05, ***P < 0.001.

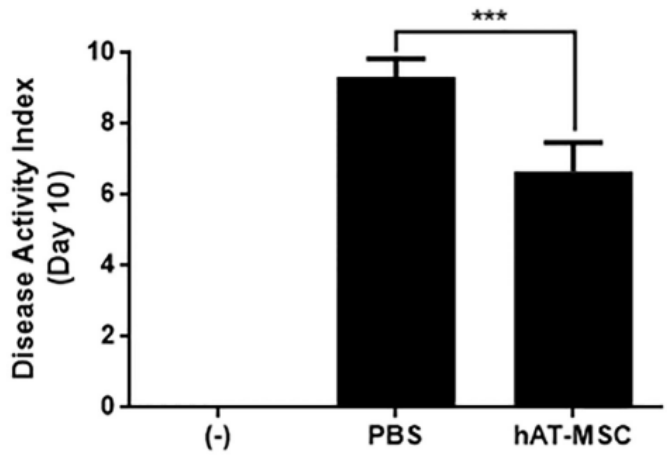

Figure 4. Intraperitoneally injected hAT-MSCs ameliorate IBD. DSS-induced colitis mice were infused hAT-MSCs or PBS (vehicle control) on day 1. Mice were sacrificed on day 10 and DAI was assessed. Results are shown as mean ± standard deviation. ***P < 0.001.

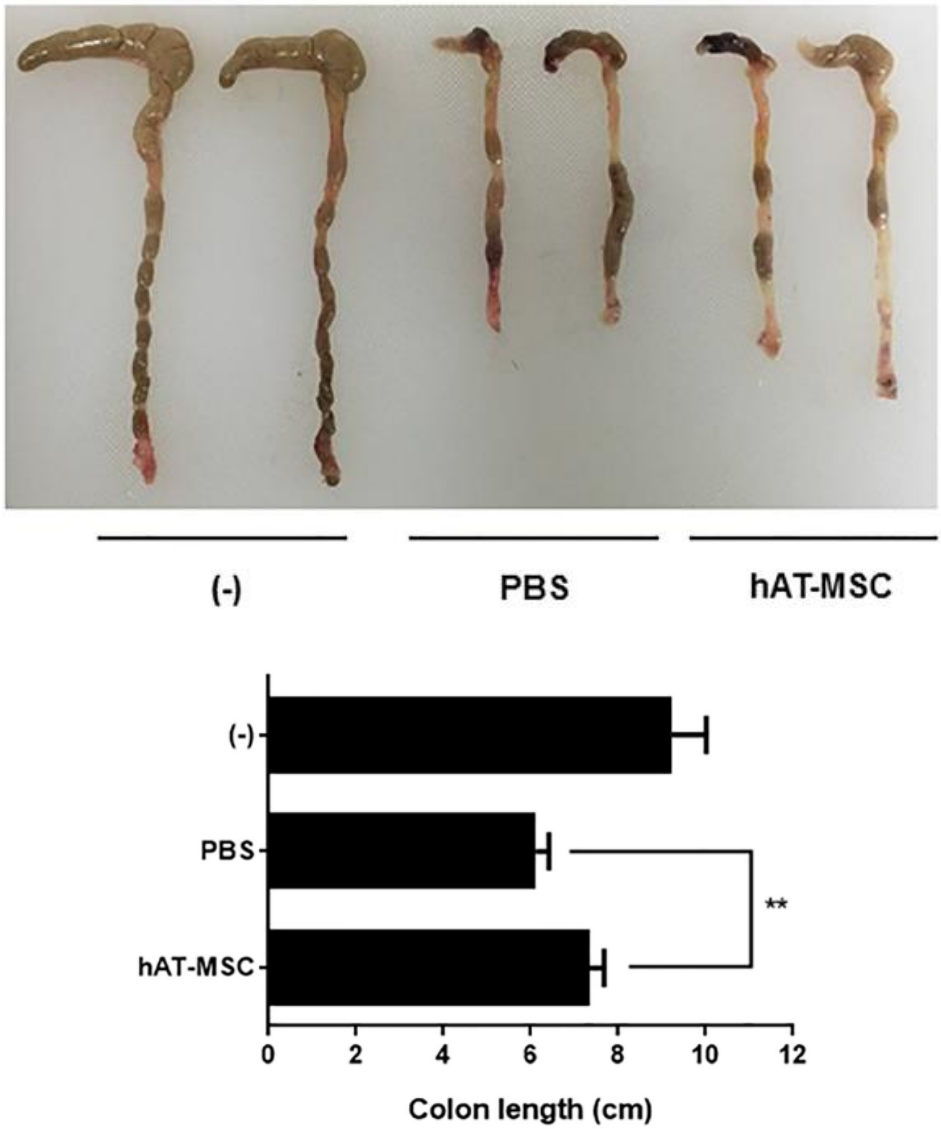

Figure 5. Intraperitoneally injected hAT-MSCs ameliorate IBD. DSS-induced colitis mice were infused hAT-MSCs or PBS (vehicle control) on day 1. Mice were sacrificed on day 10 and colon length was assessed. Results are shown as mean ± standard deviation. **P < 0.01.

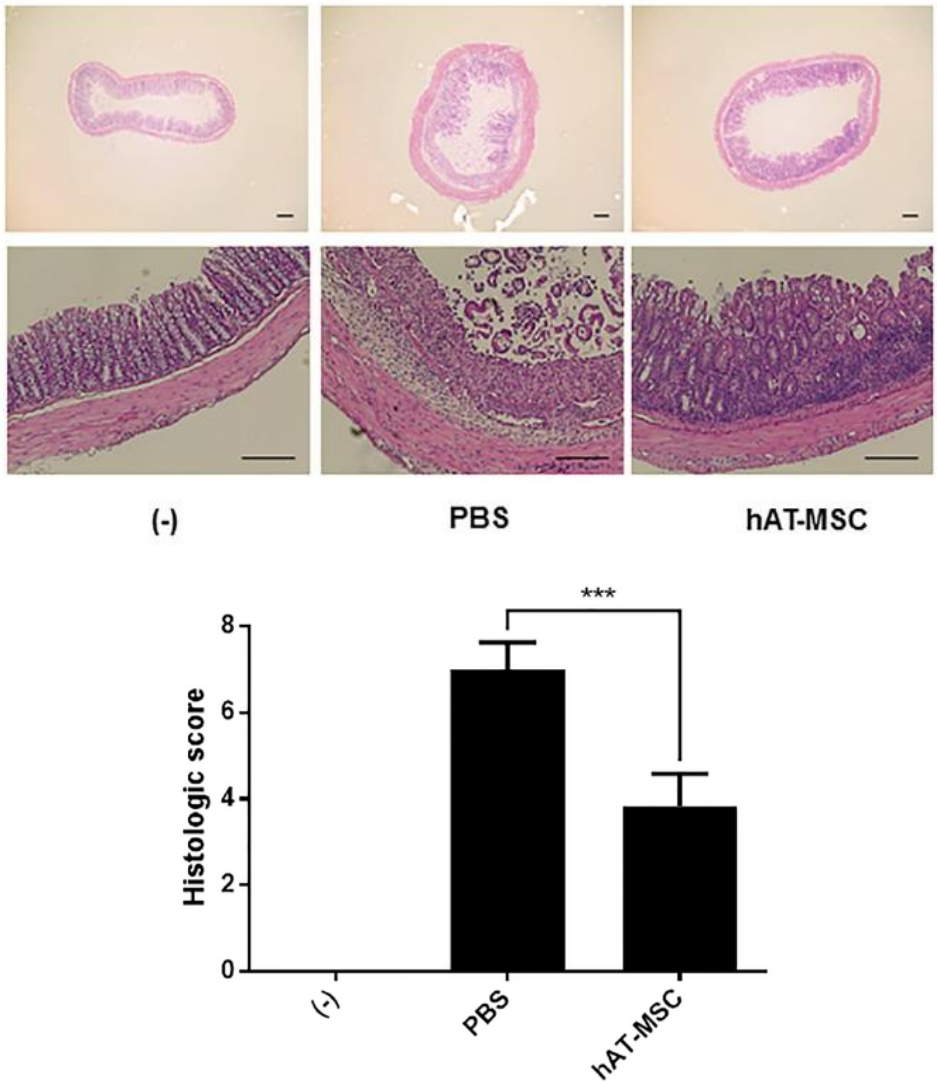

Figure 6. Intraperitoneally injected hAT-MSCs ameliorate IBD. DSS-induced colitis mice were infused hAT-MSCs or PBS (vehicle control) on day 1. Representative H&E staining of the colon sections, and their histological scores are shown. Bars = 100 μm. Results are shown as mean ± standard deviation. ***P < 0.001.

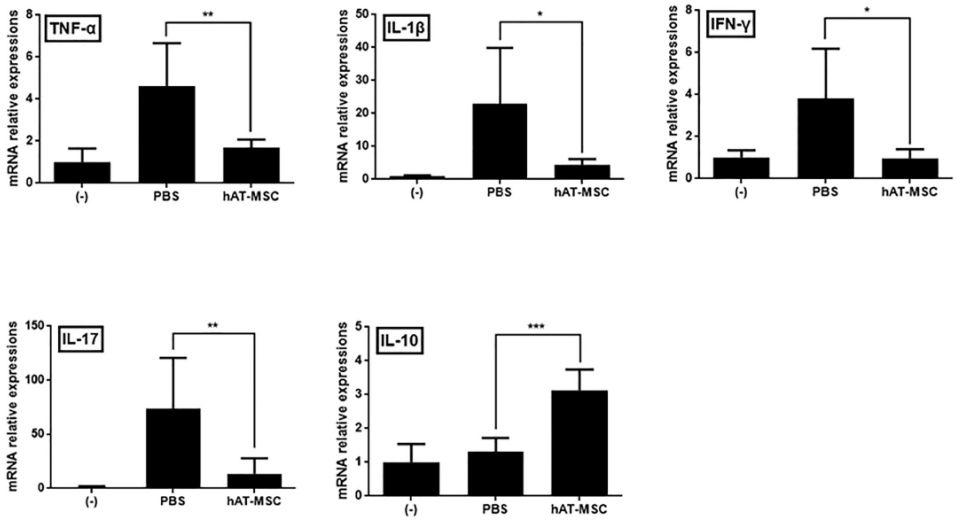

Figure 7. hAT-MSCs inhibit inflammatory response in the colon. mRNA expression levels of pro- and anti-inflammatory cytokines in colons were determined by qRT-PCR. Results are presented as mean ± standard deviation. *P < 0.05, **P < 0.01, ***P < 0.001.

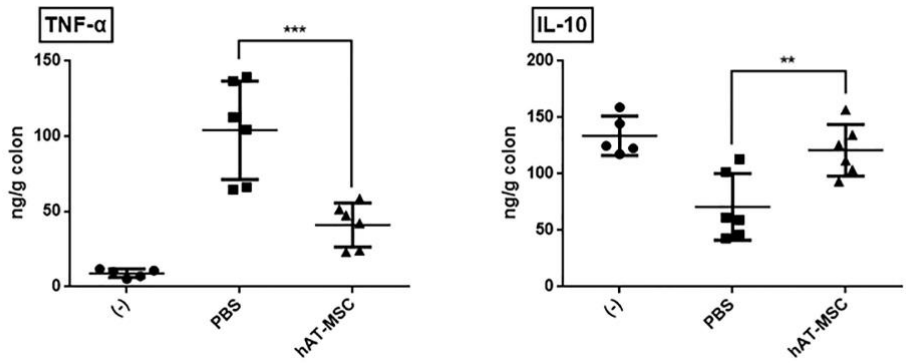

Figure 8. hAT-MSCs inhibit inflammatory response in the colon. Levels of TNF-α and IL-10 in colons were assessed using ELISA. Results are presented as mean ± standard deviation. **P < 0.01, ***P < 0.001.

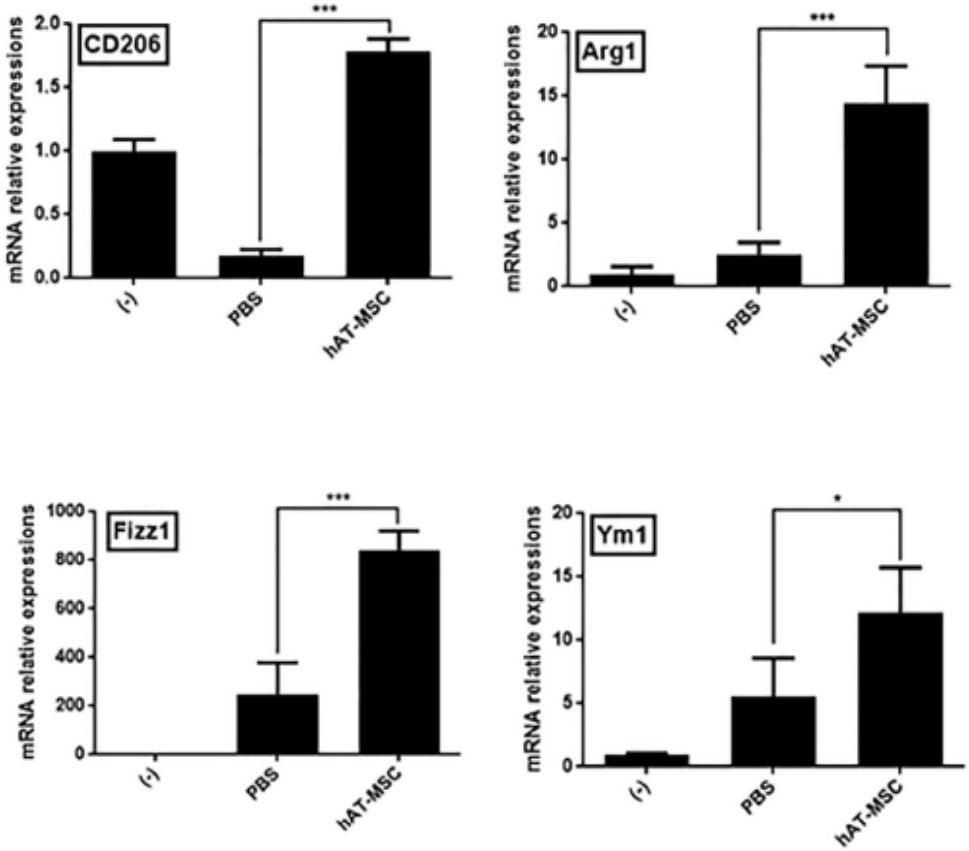

Figure 9. hAT-MSC administration leads to an increase in the percentage of M2 macrophages in the colon. Expression levels of CD206, Arg1, Fizz1, and Ym1 were determined using qRT-PCR. Results are presented as mean ± standard deviation. *P < 0.05, ***P < 0.001.

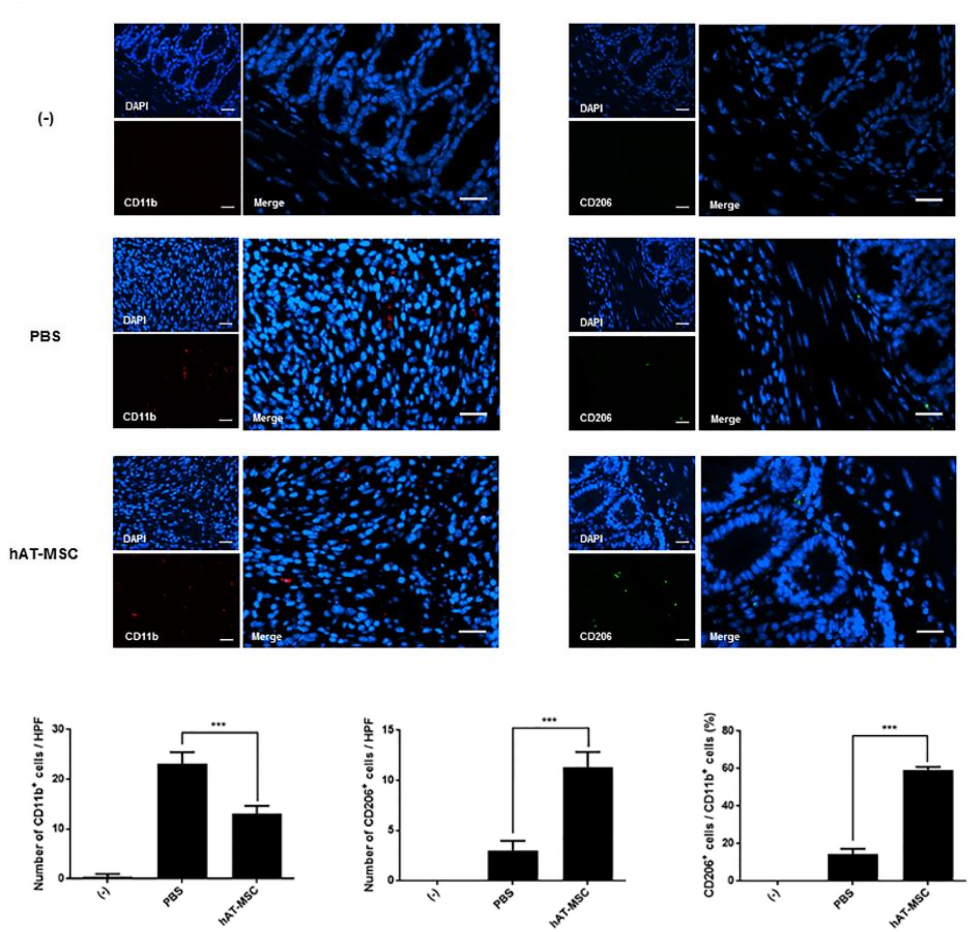

Figure 10. hAT-MSC administration leads to an increase in the percentage of M2 macrophages in the colon. Representative immunofluorescence staining using anti-CD11b or anti-CD206 antibodies. Bars = 30 μm. Also, the number of CD11b- or CD206-positive cells within the inflammatory infiltrates, and the calculated percentage of CD206-positive cells among the CD11b-positive cells are shown. Results are presented as mean ± standard deviation. ***P < 0.001.

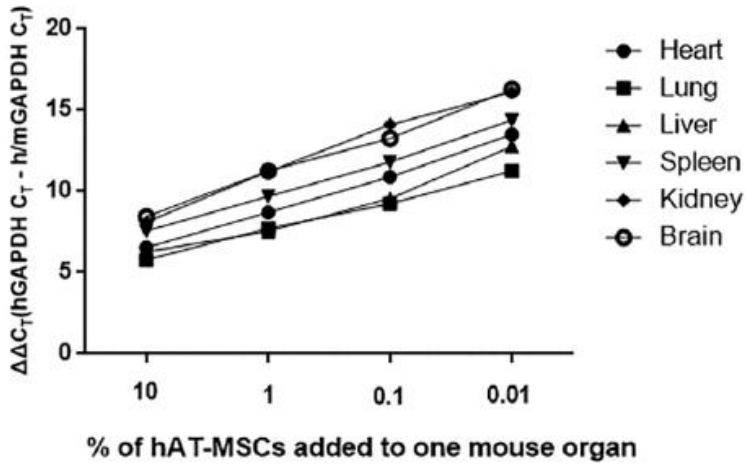

Heart	y = 2.3074x + 4.1409	(R^2 = 0.9979)
Lung	y = 1.7951x + 4.008	(R^2 = 0.9973)
Liver	y = 2.1481x + 3.6681	(R^2 = 0.9959)
Spleen	y = 2.2642x + 5.2034	(R^2 = 0.9975)
Kidney	y = 2.6842x + 5.678	(R^2 = 0.9907)
Brain	y = 2.559x + 5.915	(R^2 = 0.9945)

Figure 11. Standard curves for qRT-PCR assays of human mRNA for GAPDH. The results are representative of three independent experiments.

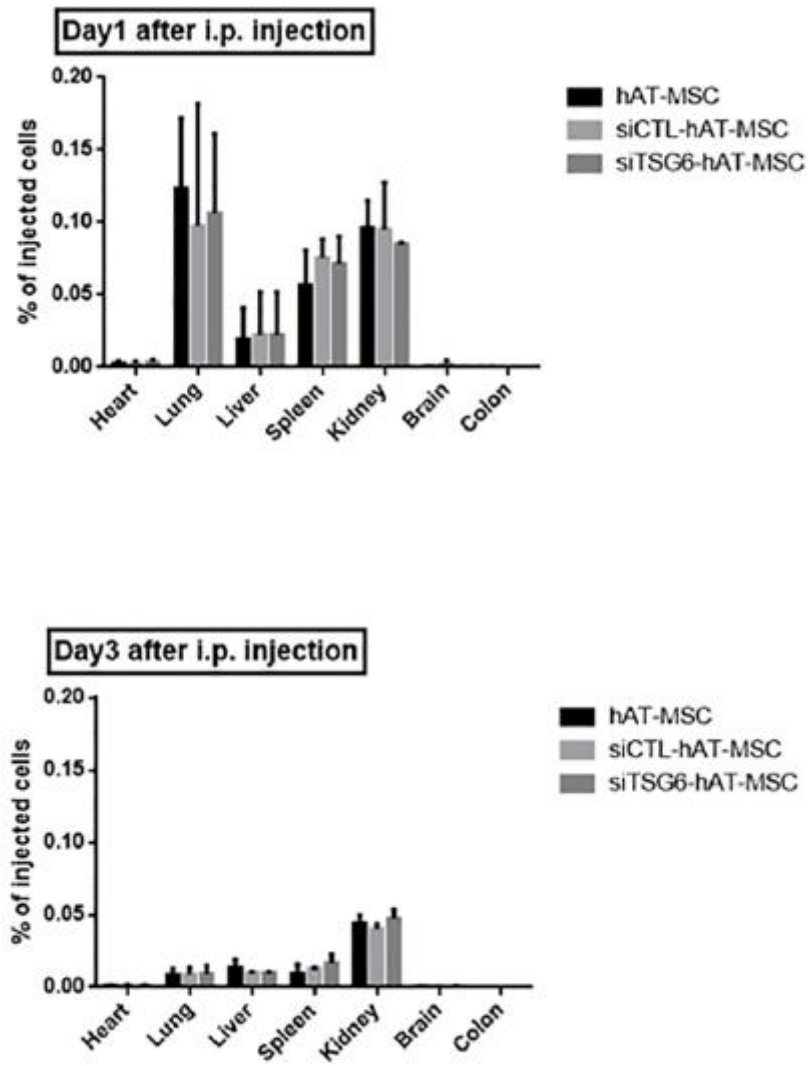

Figure 12. Distribution of hAT-MSCs in colitis mice after intraperitoneally infusion. The results are representative of three independent experiments.

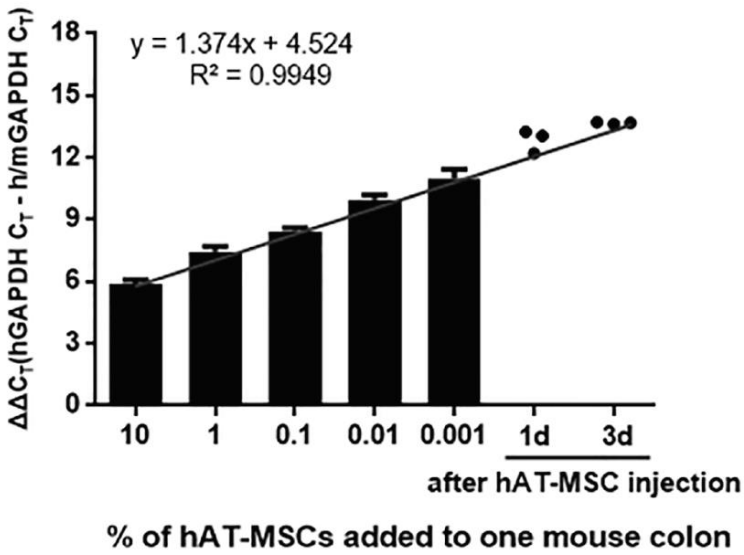

Figure 13. Intraperitoneally administered hAT-MSCs do not migrate into the colon. Serial dilutions of hAT-MSCs were administered to the investigated mice and the expression of human-specific GAPDH was evaluated. The results are representative of three independent experiments.

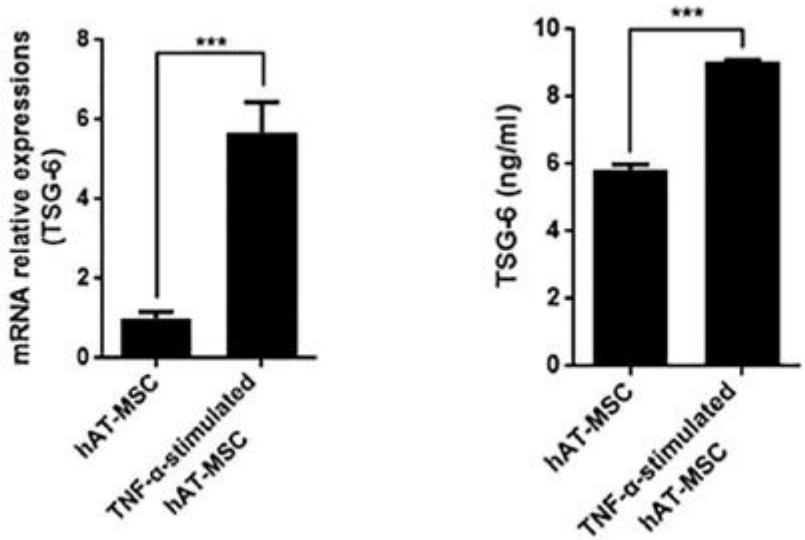

Figure 14. TSG-6 gene and protein expression levels in TNF-α-stimulated hAT-MSCs and naïve hAT-MSCs. Results are presented as mean ± standard deviation of the data obtained in three independent experiments. ***$P < 0.001$.

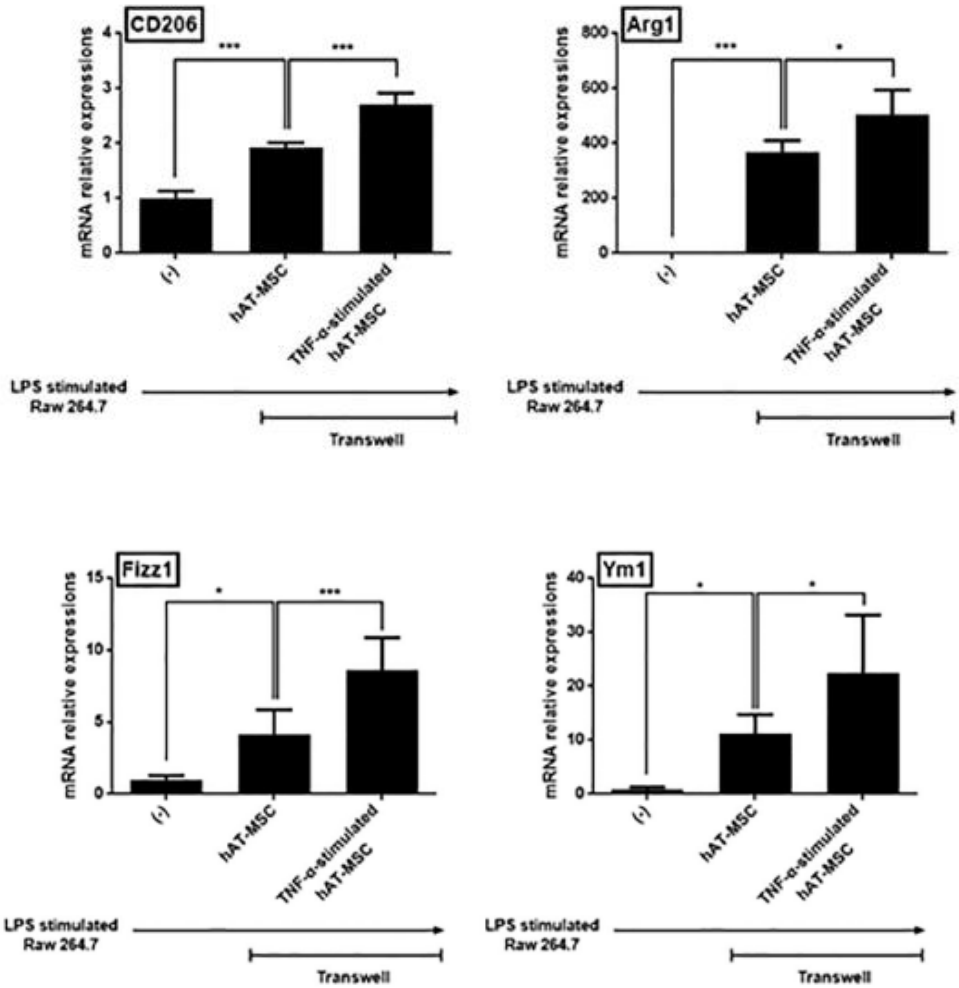

Figure 15. TNF-α-stimulated hAT-MSCs induce the expression of the M2 macrophage markers. LPS-stimulated Raw 264.7 macrophages were co-cultured with naïve or TNF-α-stimulated hAT-MSCs in a transwell system for 48 h. CD206, Arg1, Fizz1, and Ym1 mRNA expression levels are shown. Results are presented as mean ± standard deviation of the data obtained in three independent experiments. *P < 0.05, ***P < 0.001.

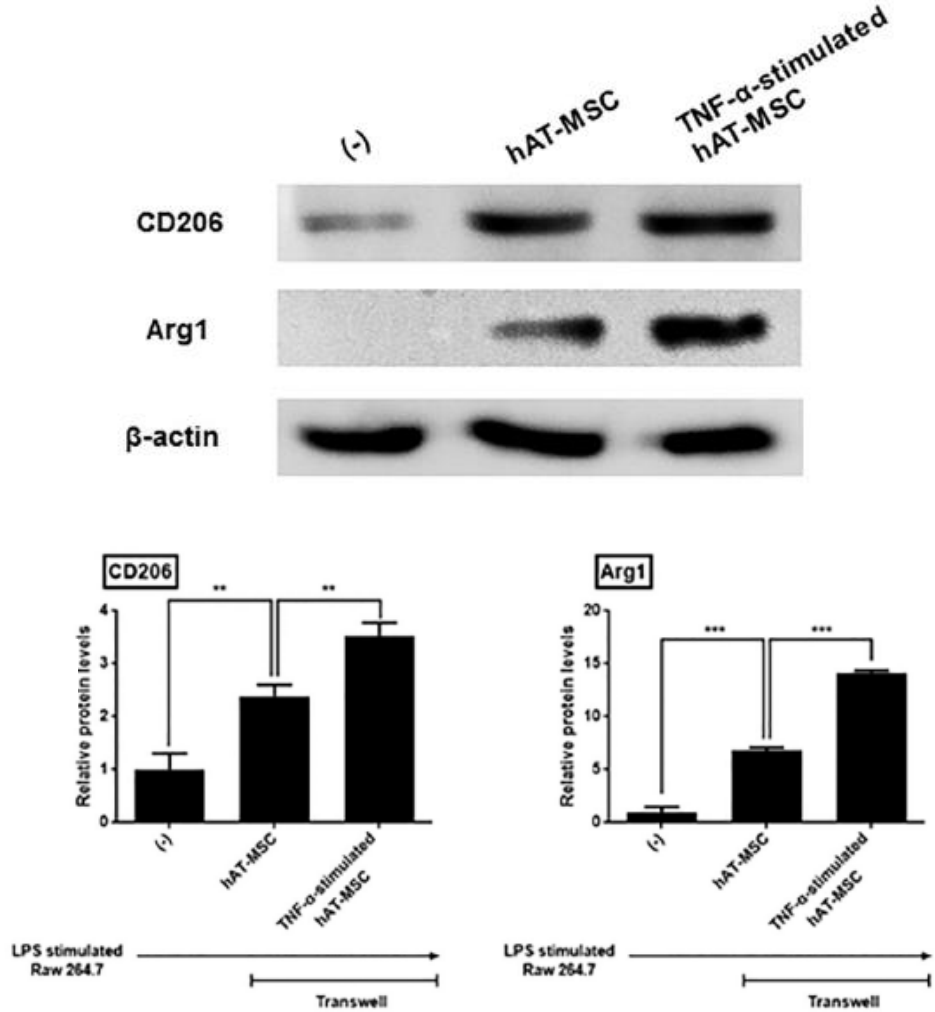

Figure 16. TNF-α-stimulated hAT-MSCs induce the expression of the M2 macrophage markers. LPS-stimulated Raw 264.7 macrophages were co-cultured with naïve or TNF-α-stimulated hAT-MSCs in a transwell system for 48 h. CD206 and Arg1 protein expression levels in these cells are shown. Results are presented as mean ± standard deviation of the data obtained in three independent experiments. **P < 0.01, ***P < 0.001.

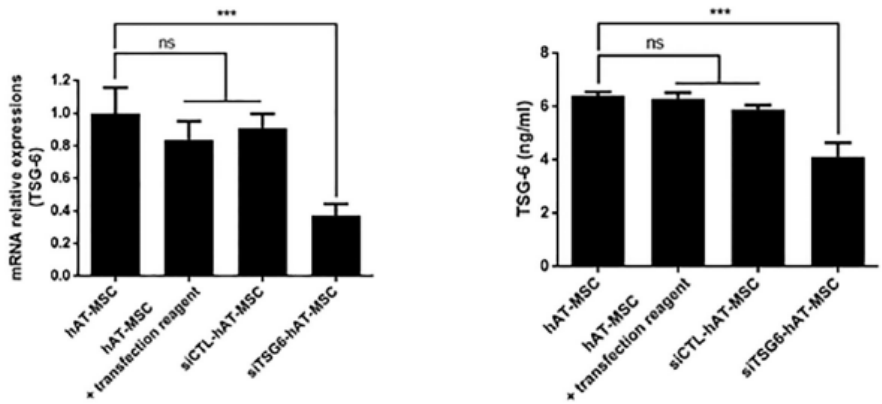

Figure 17. TSG-6 mRNA and protein expression levels in hAT-MSCs transfected with TSG-6 siRNA (siTSG6-hAT-MSCs), hAT-MSCs transfected with control siRNA (siCTL-hAT-MSCs), hAT-MSCs with transfection reagent, and naïve hAT-MSCs. Results are presented as mean ± standard deviation obtained in three independent experiments. ***P < 0.001.

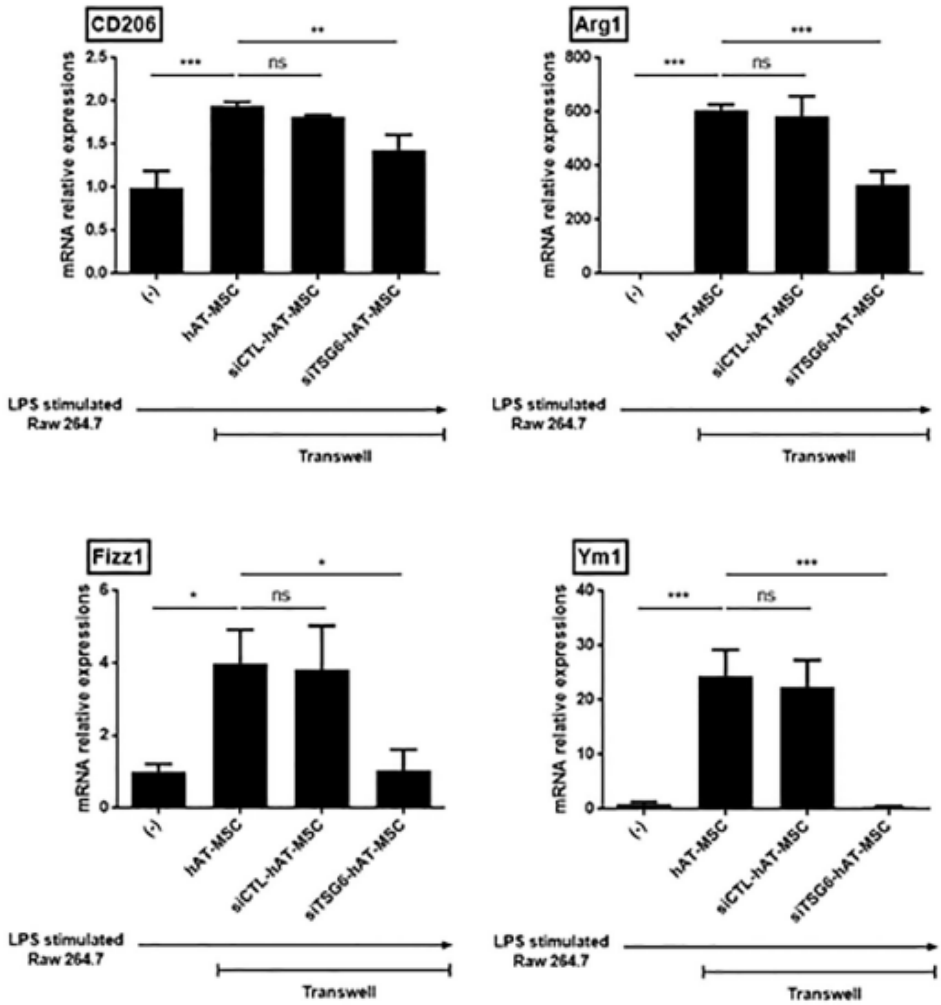

Figure 18. Expression of M2 macrophage markers decreases in hAT-MSCs transfected with TSG-6 siRNA. LPS-stimulated Raw 264.7 macrophages were co-cultured with naïve or siCTL- or siTSG6-hAT-MSCs for 48 h. CD206, Arg1, Fizz1, and Ym1 mRNA expression levels in these cells are shown. Results are presented as mean ± standard deviation obtained in three independent experiments. *P < 0.05, **P < 0.01, ***P < 0.001.

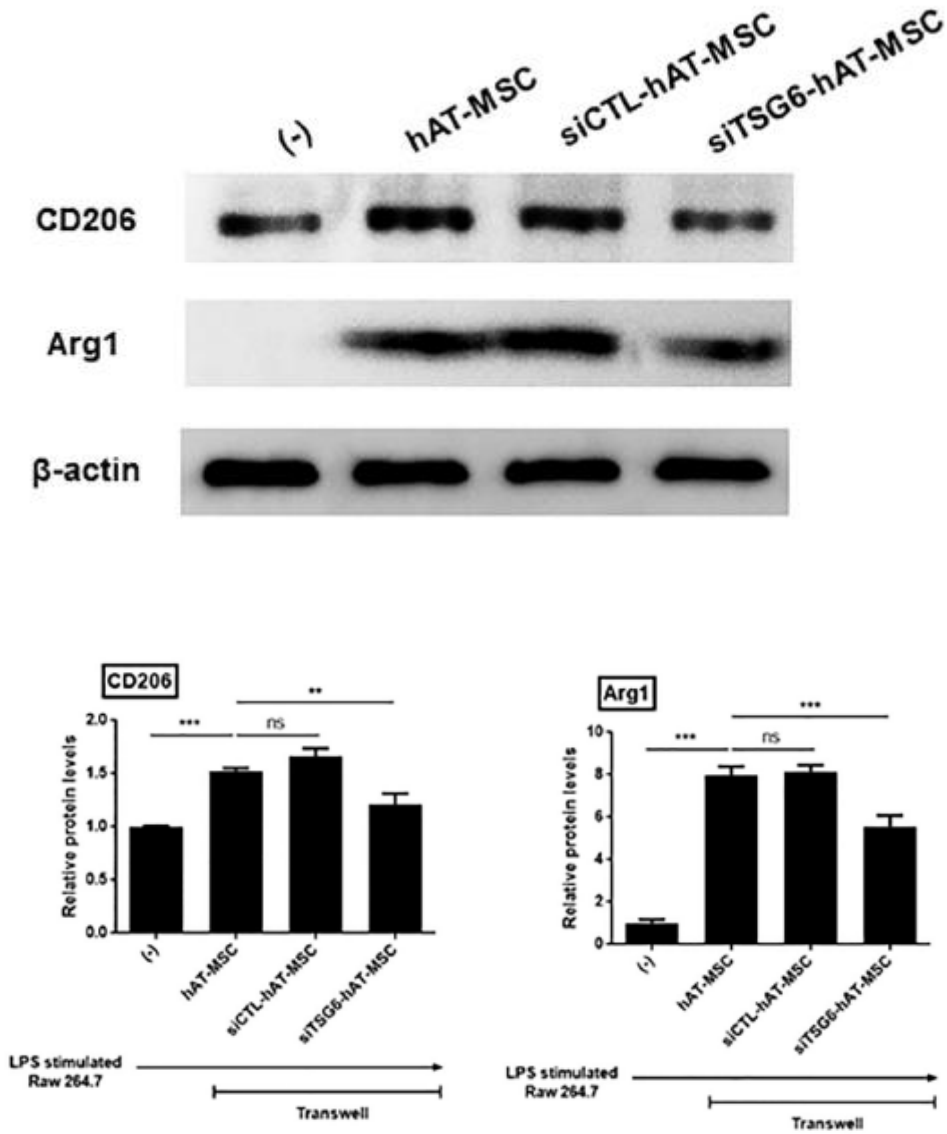

Figure 19. Expression of M2 macrophage markers decreases in hAT-MSCs transfected with TSG-6 siRNA. LPS-stimulated Raw 264.7 macrophages were co-cultured with naïve or siCTL- or siTSG6-hAT-MSCs for 48 h. CD206 and Arg1 protein expression levels are shown. Results are

presented as mean ± standard deviation obtained in three independent experiments. **P < 0.01, ***P < 0.001.

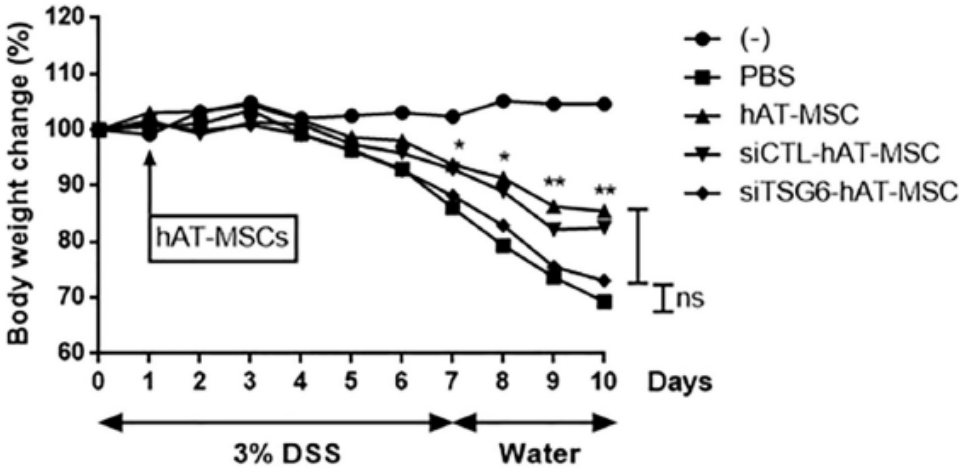

Figure 20. TSG-6 knockdown in hAT-MSCs inhibits their effect on IBD.

Body weight of animals injected with siTSG6-hAT-MSCs, siCTL-hAT-MSCs, or naïve hAT-MSCs was measured every day during the experiment, and expressed in terms of the relative change from the weight measured on day 0. Results are presented as mean ± standard deviation. *P < 0.05, **P < 0.01.

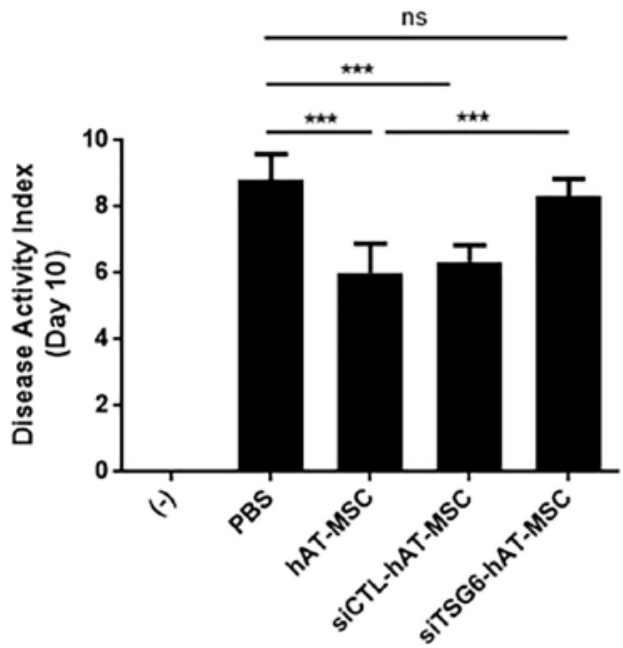

Figure 21. TSG-6 knockdown in hAT-MSCs inhibits their effect on IBD.

Mice were sacrificed on day 10 to evaluate clinical severity. DAI is shown. Results are presented as mean ± standard deviation. ***P < 0.001.

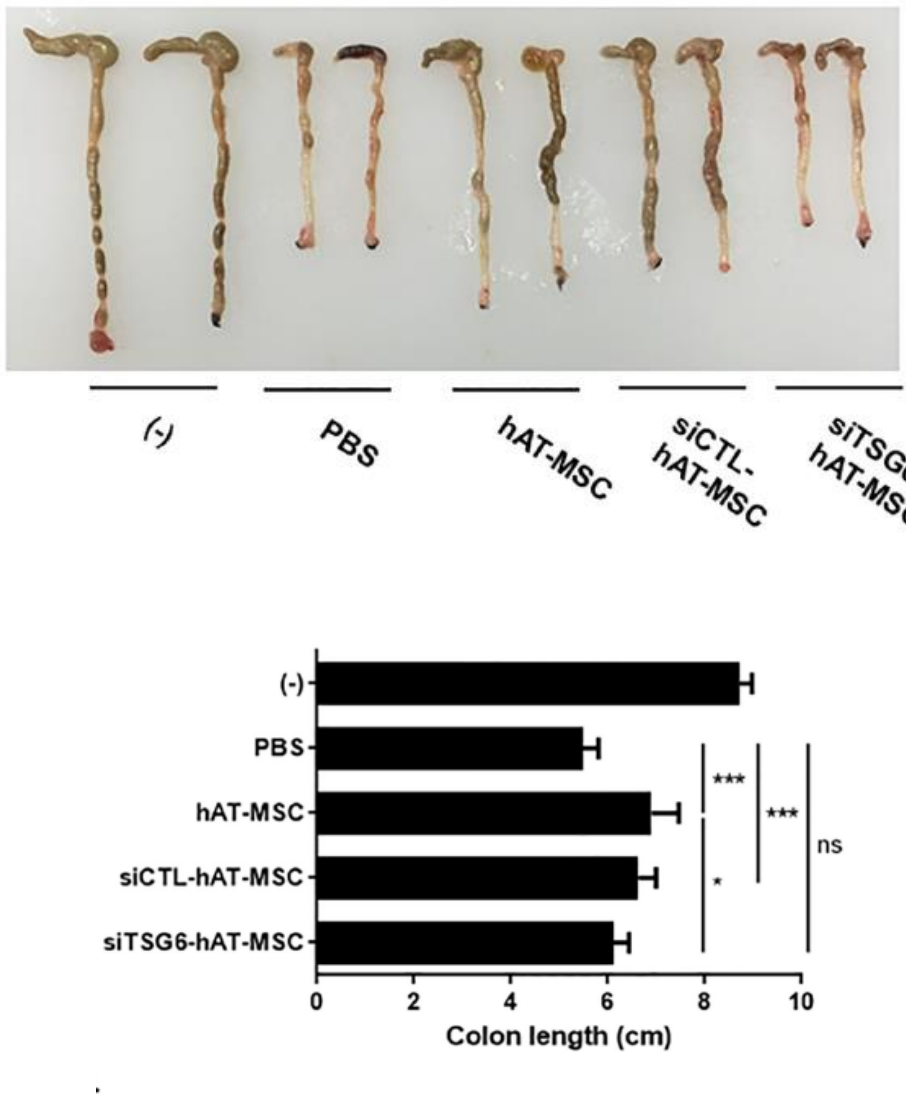

Figure 22. TSG-6 knockdown in hAT-MSCs inhibits their effect on IBD. Mice were sacrificed on day 10 to evaluate clinical severity. Colon length is shown. Results are presented as mean ± standard deviation. *P < 0.05, ***P < 0.001.

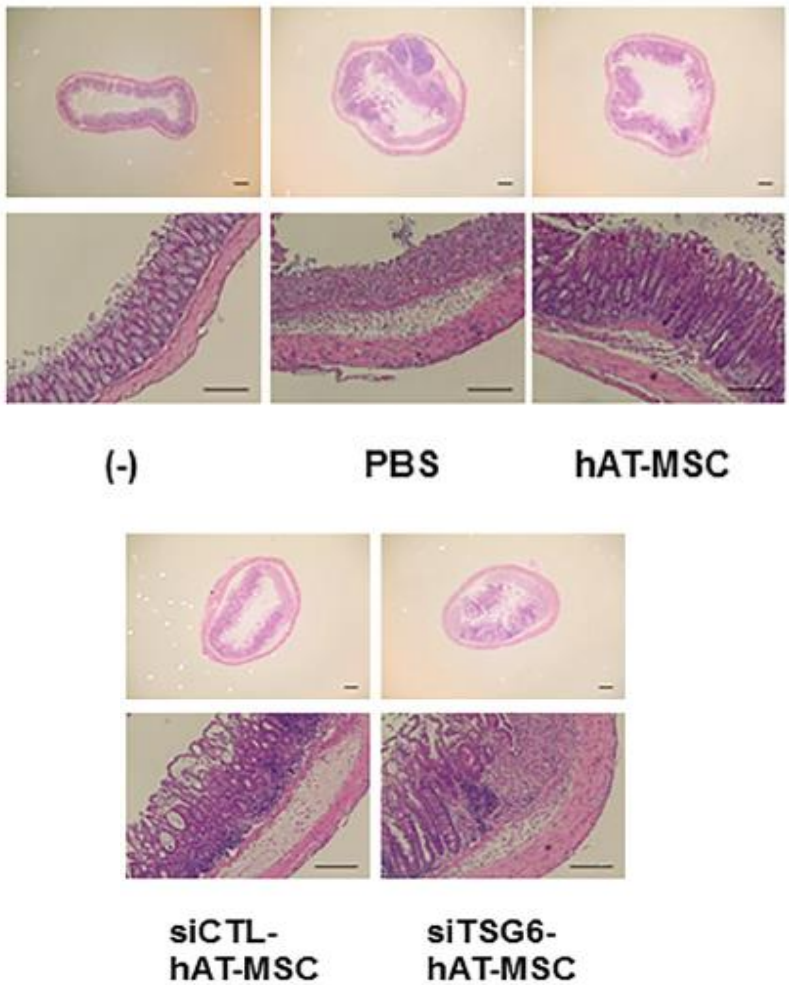

Figure 23. (see legends on next page)

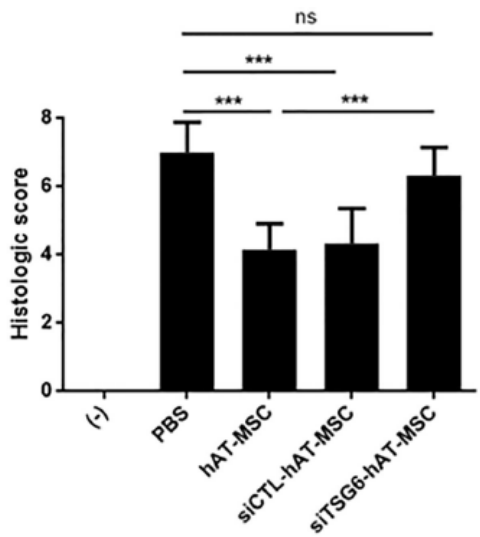

(see figures on previous page)

Figure 23. TSG-6 knockdown in hAT-MSCs inhibits their effect on IBD. Mice were sacrificed on day 10 to evaluate clinical severity. Representative colon tissue sections stained with H&E and histological scores are shown. Bars = 100 μm. Results are presented as mean ± standard deviation. ***P < 0.001.

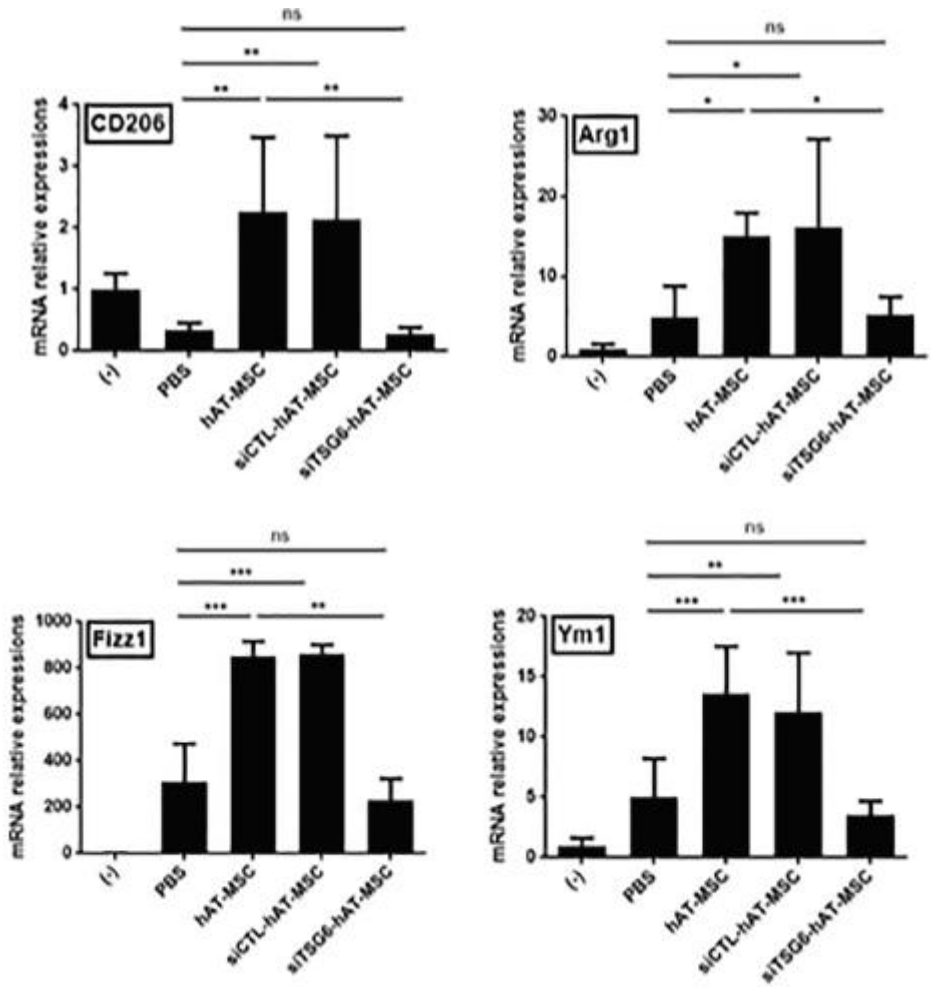

Figure 24. TSG-6 knockdown in hAT-MSCs inhibits their effect on M2 macrophage phenotypic switch. The gene expression levels of CD206, Arg1, Fizz1, and Ym1 in the colon samples of mice injected with siTSG6-hAT-MSCs, siCTL-hAT-MSCs, or naïve hAT-MSCs. Results are presented as mean ± standard deviation. *P < 0.05, **P < 0.01, ***P < 0.001.

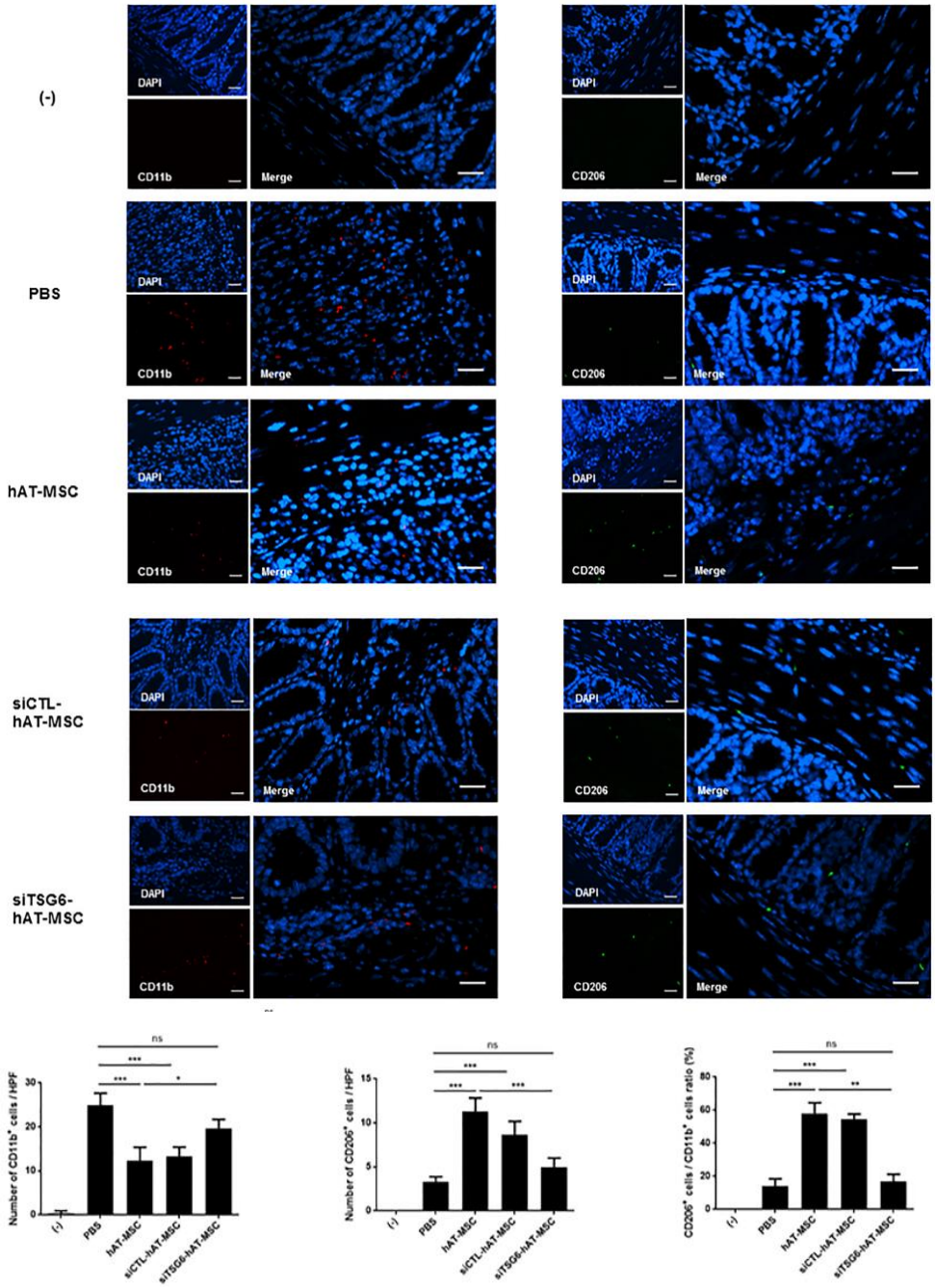

Figure 25. TSG-6 knockdown in hAT-MSCs inhibits their effect on M2 macrophage phenotypic switch. Representative immunofluorescence

staining using CD11b- or CD206-specific antibodies. Bars = 30 μm. The number of CD11b- or CD206-positive cells within the inflammatory infiltrates, and the calculated percentage of CD206-positive cells among the CD11b-positive cells are shown. Results are presented as mean ± standard deviation. *P < 0.05, **P < 0.01, ***P < 0.001.

Table 1. List for primers for qRT-PCR used in the first part of this dissertation

Gene	Forward (5′-3′)	Reverse (5′-3′)
Mouse		
TNF-α	CCCTCACACTCAGATCATCTTCT	GCTACGACGTGGGCTACAG
IL-1β	GTCTTTCCCGTGGACCTTC	TGTTCATCTCGGAGCCTGT
IFN-γ	CTCTTCTTGGATATCTGGAGGAACT	GCTGTTGCTGAAGAAGGTAGTAATC
IL-17	GGTCAACCTCAAAGTCTTTAACTCC	GAGGGATATCTATCAGGGTCTTCAT
IL-10	GTGATTTTAATAAGCTCCAAGACCA	GATCATCATGTATGCTTCTATGCAG
CD206	AACGGAATGATTGTGTAGTTCTAGC	TACAGGATCAATAATTTTTGGCATT
Arg1	CAGAAGAATGGAAGAGTCAG	CAGATATGCAGGGAGTCACC
Fizz1	GAATCTATTGTGGAGAAAAAGGTCA	AGCCGTGATACTAGTACAGGAGAAA
Ym1	GTGTACTCACCTGATCTATGCCTTT	CAGGAGAGTTTTTAGCTCAGTGTTC
GAPDH	AGTATGTCGTGGAGTCTACTGGTGT	AGTGAGTTGTCATATTTCTCGTGGT
Human		
TSG-6	AAAAACTGGCATTATTGATTATGGA	CAGTAGCAGATTTGGTTATCTTCGT
GAPDH	TGCTTTTAACTCTGGTAAAGTGGATA	GTGGAATCATATTGGAACATGTAAAC

CHAPTER II.

TSG-6 Released from Intraperitoneally Injected Canine Adipose Tissue-derived Mesenchymal Stem Cells Ameliorate Inflammatory Bowel Disease by Inducing M2 Macrophage Switch in Mice

Introduction

Inflammatory bowel disease (IBD) is an intractable autoimmune disease that leads to abdominal pain, diarrhea, fever, or other symptoms that may be caused by chronic inflammation of the digestive system. Depending on the pattern and site of inflammation, IBD can be categorized as either Crohn's disease or ulcerative colitis (Bouma and Strober, 2003). Although the exact underlying pathogenesis of IBD is unknown, it is thought to be associated with genetic and environmental factors and gut flora (Knights et al., 2013; Manichanh et al., 2012). In addition, the disease occurs naturally in dogs by a similar pathogenesis, and data from therapeutic trials for canine IBD may be excellent references for human IBD (Maeda et al., 2016). Although IBD leads to a decreased quality of life in both humans and dogs, no effective treatments for IBD have been developed.

Macrophages are important immune cells related to inflammatory diseases and release inflammatory cytokines which associated with acquired immune cells, such as lymphocytes (Locati et al., 2012). In inflamed tissues, macrophages can be classified into two subtypes: M1 and M2 macrophages (Mantovani et al., 2013; Sica et al., 2015). M1 macrophages induce inflammatory responses by secreting cytokines such as tumor necrosis factor (TNF)-α, interleukin (IL)-1β, and IL-6, whereas M2 macrophages exert anti-inflammatory responses by releasing anti-inflammatory cytokines such as IL-

10 (Murray and Wynn, 2011). According to several recent studies, M1 macrophages are present dominantly in inflamed tissues of inflammatory disease model animals; however, the percentage of M2 macrophages increased markedly when the model animals recovered.

Mesenchymal stem cells (MSCs) have been suggested as a promising tool for treating various inflammatory diseases, including pancreatitis, peritonitis, rheumatoid arthritis, and atopic dermatitis, as well as IBD (Choi et al., 2011; Gonzalez et al., 2009; Jung et al., 2011; Kim et al., 2015; Shin et al., 2016). In addition, the mechanisms underlying the therapeutic effects have been investigated and several studies showed that MSCs exert anti-inflammatory effects through secretory factors. TNF-α-induced gene/protein 6 (TSG-6) is a well-known secretory factor responsible for immunomodulation, and several recent studies showed that it plays important roles in reducing inflammatory responses in lung injury, corneal injury, skin wound, peritonitis, and pancreatitis (Danchuk et al., 2011; He et al., 2016; Legaki et al., 2016; Qi et al., 2014; Sala et al., 2015). Moreover, MSCs derived from dogs, cats, or horses were shown to have immunomodulatory effects on activated immune cells and that cell-based therapy using MSCs is a potential treatment or intractable inflammatory diseases in veterinary medicine (Carrade Holt et al., 2014; Chae et al., 2017; Kim et al., 2016).

In canine medicine, however, few studies have characterized secretory factors from canine MSCs, and cross-talk mechanisms between canine MSCs and immune cells are not well-understood. Evaluating the efficacy of canine MSCs and accumulating therapeutic results from canine medicine would be useful in human medicine as well as veterinary medicine, particularly for intractable inflammatory diseases such as IBD. Therefore, in this study, I assessed the anti-inflammatory effects and their mechanisms of canine adipose tissue-derived (cAT)-MSCs in a dextran sulfate sodium (DSS)-induced colitis model.

Materials and Methods

Isolation and characterization of cAT-MSCs

Canine adipose tissue was obtained from a healthy dog <1-year-old under a protocol approved by the Institutional Animal Care and Use Committee (IACUC) of Seoul National University (SNU; protocol no. 170724-6). The tissue was washed three times with PBS (PAN Biotech) containing penicillin and streptomycin, and then cut into small pieces and digested for 1 h at 37°C with collagenase type IA (1 mg/mL; Sigma-Aldrich). Enzymatic activity was inhibited with Dulbecco's Modified Eagle's Medium (DMEM; PAN Biotech) containing 10% fetal bovine serum (FBS; PAN Biotech). After centrifugation at 1200 ×*g* for 5 min, the pellet was filtered through a 100-μm Falcon cell strainer (Fisher Scientific, Waltham, MA, USA) to remove debris and then incubated in DMEM containing 10% FBS at 37°C in a humidified atmosphere of 5% CO_2. After 48 h, the cultures were washed with PBS to remove non-adherent cells and incubated with fresh medium, which was changed every 48 h until cells reached 70–80% confluence, after which they were repeatedly subcultured under standard conditions.

Isolated cells were characterized for the expression of stem cell markers by flow cytometry using fluorescein isothiocyante (FITC)- or phycoerythrin (PE)-conjugated antibodies against the following proteins: CD29-FITC, CD31-FITC, CD34-PE, and CD73-PE (BD Biosciences) and

CD44-FITC, CD45-FITC, and CD90-APC (eBiosciences). Cells were analyzed with a FACSAria II system (BD Biosciences). Cellular differentiation was evaluated using the StemPro Adipogenesis Differentiation, StemPro Osteogenesis Differentiation, and StemPro Chondrogenesis Differentiation kits (all from Gibco/Life Technologies, Carlsbad, CA, USA) according to the manufacturer's instructions followed by Oil Red O staining, Alizarin Red staining, and Alcian Blue staining, respectively. Cells were assessed for the expression of several stem cell markers by flow cytometry (Fig. 26). Additionally, the differentiation ability of the cells was confirmed (Fig. 27), and isolated cAT-MSCs at passage 3–4 were used in the following experiments.

Small interfering RNA (siRNA) transfection of cAT-MSCs

When cAT-MSCs reached approximately 70% confluence, they were transfected with TSG-6 siRNA or control siRNA (sc-39819 and sc-37007, respectively; Santa Cruz Biotechnology, Santa Cruz, CA, USA) for 24 h using Lipofectamine RNAiMAX (Invitrogen, Carlsbad, CA, USA) according to the manufacturers' instructions. TSG-6 knockdown was confirmed by quantitative reverse transcription (qRT)-PCR (Fig. 28). cAT-MSCs transfected with siRNA were used for further experiments immediately after the transfection protocol was completed.

Animal experiments

Male C57BL/6J mice aged 6 weeks were purchased from the Nara Biotech (Seoul, Korea) and housed under controlled temperature, humidity, and light cycle conditions. All experimental procedures involving animals were approved by the IACUC of SNU (protocol no. SNU-170804-2), and the protocols were performed in accordance with approved guidelines. Colitis was induced by *ad libitum* administration of 3% DSS (36–50 kDa, MP Biomedical, Solon, OH, USA) in the drinking water from day 0 to 7, whereas mice receiving normal drinking water were used as the naïve group. On day 1, the following procedure was performed: 2×10^6 cAT-MSCs transfected with TSG-6 siRNA in 200 μL of PBS, 2×10^6 cAT-MSCs transfected with scrambled siRNA control in 200 μL of PBS, 2×10^6 control cAT-MSCs in 200 μL of PBS, or the identical volume of PBS was injected intraperitoneally into colitis mice. The body weight of each mouse was assessed every 24 h. The mice were sacrificed on day 10 and colon tissues were collected for further processing.

Evaluating colitis severity

The disease activity index was determined by scoring the body weight loss (grades, 0–4: 0, none; 1, <5% loss of the initial body weight; 2, 5–10% loss of the initial body weight; 3, 10–20% loss of the initial body

weight; 4, >20% loss of the initial body weight), stool consistency (grades, 0–2: 0, none; 1, mild to moderate diarrhea; 2, severe diarrhea), rectal bleeding (grades, 0–2: 0, none; 1, mild to moderate bleeding; 2, severe bleeding), and general activity (grades, 0–2: 0, normal; 1, mildly to moderately depressed; 2, severely depressed).

Histological analysis

Colon tissues were fixed in 10% formaldehyde for 48 h, embedded in paraffin, and cut into 4-μm sections. The sections were stained with hematoxylin and eosin. A total of 20 fields per group was selected randomly and histological examinations were performed in a blinded manner. The severity of symptoms was calculated by scoring the extent of bowel wall thickening (grades, 0–3: 0, none; 1, mucosa; 2, mucosa and submucosa; 3, transmural), damage to the crypt (grades, 0–3: 0, none; 1, loss of goblet cells; 2, only surface epithelium intact; 3, loss of entire crypt and epithelium), and infiltration of inflammatory cells (grades, 0–2: 0, none; 1, mild to moderate; 2, severe).

Enzyme-linked immunosorbent assay (ELISA)

Total proteins were extracted from the colon tissue using PRO-PREP Protein Extraction Solution (Intron Biotechnology, Seongnam, Korea)

according to the manufacturer's instructions and stored at -80°C until use. The concentrations of TNF-α, IL-6, and IL-10 were measured using a commercial ELISA kit (all from eBiosciences, San Diego, CA, USA) according to the manufacturer's instructions.

Obtaining canine peripheral blood mononuclear cell (cPBMC)-derived macrophages

Canine macrophages were obtained from the peripheral blood as previously described (Viana et al., 2013). Briefly, the blood of healthy canine donors was obtained from the SNU Veterinary Medical Teaching Hospital and PBMCs were isolated using Ficoll-Paque PLUS (GE Healthcare Life Sciences, Little Chalfont, UK). Canine PBMCs were resuspended in Roswell Park Memorial Institute-1640 medium (PAN Biotech, Aidenbach, Germany) containing 20% fetal bovine serum (PAN Biotech) and 20% macrophage colony-stimulating factor medium obtained from the supernatant of L929 immortalized cells. The canine PBMCs were plated at 2×10^6 cells/well in 24-well plates and incubated at 37°C in a humidified atmosphere of 5% CO_2. After 24 h, the wells were washed to remove non-adherent cells. The remaining adherent cells were incubated with fresh medium for 5 days for differentiation into macrophages.

Co-culture of canine PBMC-derived macrophages with cAT-MSCs

After canine PBMC-derived macrophages were stimulated with 200 ng/mL of lipopolysaccharide (LPS; Sigma-Aldrich, St. Louis, MO, USA) for 24 h, the LPS-stimulated macrophages were plated at a density of 2×10^5 cells per well in 24-well plates. Subsequently, 2×10^4 cAT-MSCs, control siRNA-cAT-MSCs, or TSG-6 siRNA-cAT-MSCs were seeded onto 0.4-μm pore-sized Transwell inserts (SPL Life Science, Pocheon, Korea) and incubated for 48 h. The macrophages were harvested for further experiments.

RNA extraction, cDNA synthesis, and qRT-PCR

Total RNA was extracted from homogenized colon tissue or canine PBMC-derived macrophages using the Easy-BLUE Total RNA Extraction kit (Intron Biotechnology) according to the manufacturer's instructions. cDNA was synthesized using LaboPass M-MuLV Reverse Transcriptase (Cosmo Genetech, Seoul, Korea) and the samples were analyzed using 10 μL of AMPIGENE qPCR Green Mix Hi-ROX with SYBR Green dye (Enzo Life Sciences, Farmingdale, NY, USA) and 400 nM forward and reverse primers (Cosmo Genetech). Expression levels of the target genes were normalized to that of glyceraldehyde 3-phosphate dehydrogenase (GAPDH). Primer sequences used in the present study are listed in Table 2.

Flow cytometric analysis

Flow cytometry was conducted using a FACSAria II system (BD Biosciences, Franklin Lakes, NJ, USA) and analyzed using FlowJo software (Tree Star, Ashland, OR, USA). To characterize mesenchymal stem cells derived from canine adipose tissues, the cells were harvested and resuspended in PBS. Subsequently, the cells were stained with fluorescein isothiocyante (FITC)-, phycoerythrin (PE)-, or allophycocyanin (APC)-conjugated antibodies against the following proteins: CD29-FITC, CD34-PE, and CD73-PE (BD Biosciences); and CD44-FITC, CD45-FITC, and CD90-APC (eBiosciences). To evaluate M2 macrophage polarization, PBMC-derived macrophages co-cultured with cAT-MSCs were detached and resuspended in PBS. Next, the macrophages were stained with PE-conjugated CD11b (Abcam, Cambridge, UK) and FITC-conjugated CD206 (Santa Cruz Biotechnology).

Immunofluorescence (IF) analysis

Paraffin-embedded colon tissue sections were cut at a thickness of 4 μm. Sections were deparaffinized in xylene and rehydrated sequentially in 100%, 95%, and 80% ethanol solutions, and antigen retrieval was carried out using 10 mM citrate buffer (Sigma-Aldrich). After the sections were washed, they were blocked with blocking buffer containing 5% bovine serum albumin and 0.3% Triton X-100 (both from Sigma-Aldrich) for 1 h. The sections were

incubated overnight at 4°C with antibodies against F4/80 (1:250) or FITC-conjugated CD206 (1:250; both from Santa Cruz Biotechnology). After three washes, the slides incubated with F4/80 antibody were incubated with PE-conjugated secondary antibody (1:500; Santa Cruz Biotechnology) for 1 h at 20°C in the dark. The colon sections stained with antibody against either F4/80 or CD206 were washed three times and mounted in Vectashield mounting medium containing 4',6-diamidino-2-phenylindole (Vector Laboratories, Burlingame, CA, USA). The slides were visualized with a confocal laser scanning microscope (LSM710; Carl Zeiss, Jena, Germany), and immunoreactive cells were counted in 20 random fields per group.

Annexin-V and propidium iodide (PI) staining

Colon tissue slides were stained with FITC-conjugated annexin-V and PI using the Annexin V-FITC apoptosis detection kit plus (Enzo Life Sciences) according to the manufacturer's instructions. The slides were observed using an EVOS FL microscope (Life Technologies, Carlsbad, CA, USA). Apoptotic cells identified as FITC-positive cells were counted in 20 random fields per group.

Generation of the GAPDH standard curve

Standard curves for evaluating the migratory ability of intraperitoneally injected canine MSCs were generated by administering serial dilutions of cAT-MSCs to mouse organs as described previously [24]. Briefly, 2×10^2, 2×10^3, 2×10^4, or 2×10^5 cAT-MSCs were added to whole mouse organs prior to homogenization. Total RNA was extracted from the samples using the Easy-BLUE Total RNA Extraction kit (Intron Biotechnology), and cDNA was synthesized (LaboPass M-MuLV Reverse Transcriptase; Cosmo Genetech) using 1 μg of RNA. Next, qRT-PCR using canine-specific mitochondrial cytochrome b primers (forward primer, 5′-CCT TAC TAG GAG TAT GCT TG-3′; reverse primer, 5′-TGG GTG ACT GAT GAA AAA G-3′) was performed to generate the standard curves. The curves were corrected by performing parallel qRT-PCR with primers for universal eukaryotic 18S ribosomal RNA (forward primer, 5′-GCT ACT ACC GAT TGG ATG GTT TAG-3′; reverse primer, 5′-CTA CGG AAA CCT TGT TAC GAC TTT-3′).

Statistical analysis

Data are shown as the mean ± standard deviation. Mean values among different groups were compared by one-way analysis of variance using the GraphPad Prism v.6.01 software (GraphPad, Inc., La Jolla, CA, USA). A P value of < 0.05 was considered statistically significant.

Results

Intraperitoneally administered cAT-MSC-secreted TSG-6 played a crucial role in ameliorating IBD

I previously showed the therapeutic effects of TSG-6 released from human AT-MSCs against colitis in the first part of this dissertation. In this chapter, I first investigated whether cAT-MSC-secreted TSG-6 exerted anti-inflammatory effects in DSS-induced colitis mice. Intraperitoneally infused cAT-MSCs significantly reduced body weight loss compared to in mice injected with PBS from day 7 (Fig. 29). On day 10, the disease activity index of colitis mice treated with cAT-MSCs was significantly improved compared to in mice treated with PBS (Fig. 30). On day 10, mice were sacrificed to evaluate the length and histology of the colon. The shortening of colon length was significantly improved in the cAT-MSC-treated group compared to in the PBS-treated group (Fig. 31). Upon histological examination, severe submucosal or transmural thickening, destruction of the entire epithelium, and severe inflammatory cell infiltration were observed in DSS-induced colitis mouse colons. In colon sections from mice treated with cAT-MSCs, the extent of bowel wall thickening, crypt damage, and infiltration of inflammatory cells were improved compared to in PBS-treated mice (Fig. 32). However, colitis mice administered cAT-MSCs transfected with TSG-6 siRNA did not show improvements in body weight loss, disease activity index,

colon length, and histologic scores compared to colitis mice injected PBS (Figs. 29-32).

cAT-MSC-secreted TSG-6 reduced inflammatory response and apoptosis in the colon

I next evaluated the effect of cAT-MSCs on the modulation of inflammatory cytokines associated with inflammatory bowel disease or DSS-induced colitis. Production of TNF-α and IL-6 was considerably increased in the colon of DSS-treated mice, whereas that of IL-10 was slightly decreased (Fig. 33). Treatment of cAT-MSCs not only significantly decreased TNF-α and IL-6, but also significantly increased IL-10 (Fig. 2A). However, siRNA-induced down regulation of TSG-6 significantly reduced the anti-inflammatory abilities of cAT-MSCs to modulate TNF-α, IL-6, and IL-10 in the colon (Fig. 33).

In addition, I examined apoptosis that could be induced by TNF-α in colon sections. Annexin-V-positive cells were increased markedly in the colons of DSS-induced mice (Fig. 34). Administration of cAT-MSCs led to a significant decrease in annexin-V positive cells in the colon sections compared to in PBS-treated groups, which was abolished by knockdown of TSG-6 with siRNA transfection (Fig. 34).

Intraperitoneally infused cAT-MSCs did not migrate to inflamed colon

Next, I tracked and quantified intraperitoneally injected cAT-MSCs (2×10^6 cells) by constructing standard curves by qRT-PCR (Fig. 35). After 2 h of cAT-MSC injection, approximately 0.07%, 0.11%, 0.26%, 0.25%, 0.08%, and 0.06% of the cells were detected in the heart, lung, liver, spleen, kidney, and colon of DSS-induced colitis mice, respectively (Fig. 36). At days 1 and 3 after cAT-MSC administration, these percentages were lower than they were at 2 h after cell infusion. Furthermore, infused cAT-MSCs were not detected in inflamed colons at days 1 and 3 (Fig. 36).

TSG-6 produced by cAT-MSCs induced phenotypic switching from M1 to M2 macrophages in vitro

Given that cytokines such as TNF-α, IL-6, and IL-10 modulated in the above study are largely derived from macrophages, I further investigated whether cAT-MSCs could switch the macrophage phenotype from M1 to M2. Macrophages derived from cPBMCs were stimulated with LPS (200 ng/mL) for 24 h to induce the M1 phenotype. Next, macrophages were co-cultured with cAT-MSCs in a transwell system for 48 h. The proportion of $CD11b^+$ cells expressing CD206, a well-known M2 marker, was significantly increased in the cAT-MSCs group compared to in the control group (Fig. 37). In addition, cAT-MSCs transiently transfected with TSG-6 siRNA were co-

cultured with LPS-stimulated cPBMC-derived macrophages to determine whether TSG-6 mediates macrophage polarization. Interestingly, the phenotypic switching effect was significantly decreased in cAT-MSCs transfected with TSG-6 siRNA compared to cAT-MSCs transfected with control siRNA or naïve cAT-MSCs (Fig. 4A). Furthermore, a reduction in mRNA expression of inducible nitric oxide synthase (iNOS) and IL-6 was observed in LPS-stimulated cPBMC-derived macrophages co-cultured with cAT-MSCs compared to in those incubated alone, which was abrogated by co-culture with cAT-MSCs transfected with TSG-6 siRNA (Fig. 38). Additionally, the CD206 and IL-10 mRNA expression levels of LPS-stimulated cPBMC-derived macrophages were increased in the cAT-MSC group compared to in the control group, which were restored in the TSG-6 siRNA-transfected cAT-MSC group (Fig. 38).

cAT-MSC-secreted TSG-6 increased M2 macrophages in inflamed colon

I next assessed the expression level of M2 macrophages in inflamed colons. Quantitative analysis of macrophages detected in colon tissue sections by immunofluorescence examination showed that the percentage of $F4/80^+$ total macrophages was decreased significantly, whereas that of $CD206^+$ M2 macrophages was increased significantly in the cAT-MSCs group compared to in the PBS group (Fig. 39). Furthermore, the mRNA expression level of

not only iNOS was significantly decreased, but also those of M2 markers, CD206, Arg1, Fizz1, and Ym1, were markedly increased in colon tissues of DSS-induced colitis mice infused with cAT-MSCs compared to in PBS-treated mice (Fig. 40). However, the M2 polarization effect of cAT-MSCs in colon tissue was abrogated when TSG-6 was inhibited (Figs. 39, 40).

Discussion

Numerous studies have shown that MSC administration may be an important treatment option for IBD (Abdel Salam et al., 2014; Ando et al., 2008; Bassi et al., 2012; Castelo-Branco et al., 2012; Liang et al., 2011; Zhang et al., 2013). Although they are not fully understood, the mechanisms underlying the anti-inflammatory effects of MSC have been described previously (Gonzalo-Gil et al., 2016; Liu et al., 2015; Shin et al., 2017). It is well-known that the anti-inflammatory ability and mechanisms of MSCs vary depending on their source (Kern et al., 2006). Moreover, inflammatory cytokines released by activated immune cells are important triggers of MSCs to exert immunomodulatory properties, indicating that the disease-specific inflammatory microenvironment is crucial for the therapeutic effects of administered MSCs (Wang et al., 2014). In this study, I first demonstrated the anti-inflammatory effects of cAT-MSCs and determined the underlying mechanisms in a DSS-induced colitis mouse model.

Recent studies reported that MSCs reduce inflammation through soluble factors such as indoleamine 2,3-dioxygenase, transforming growth factor-β, prostaglandin E2 (PGE2), hepatocyte growth factor, and TSG-6 (Gonzalo-Gil et al., 2016; Kennelly et al., 2016; Kim et al., 2015; Liu et al., 2016; Liu et al., 2015). Among these, TSG-6 has been shown to be pivotal for the immunomodulatory effects of MSCs in several inflammatory disease

models such as corneal inflammation, wound injury, acute lung injury, peritonitis, and pancreatitis (Choi et al., 2011; He et al., 2016; Qi et al., 2014; Roddy et al., 2011; Wang et al., 2012). I also previously demonstrated that MSCs derived from human adipose tissue exert therapeutic effects against DSS-induced colitis by secreting TSG-6 in the first part of this dissertation. Here, I showed that TSG-6 secreted from intraperitoneally infused cAT-MSCs may ameliorate the symptoms of DSS-induced colitis and that weight loss and disease activity indices were reduced. In addition, by evaluating the length of the colon and assessing the histologic scores of the colon tissue section, I demonstrated the therapeutic effects of cAT-MSC-secreted TSG-6 against DSS-induced colitis mice. Moreover, TSG-6 released from cAT-MSCs played an important role in modulating inflammatory cytokines such as TNF-α, IL-6, and IL-10 in the colon, and reduced TNF-α secretion led to a significant decrease in annexin V-positive apoptotic cells in colon tissue sections.

In the present study, I administered cAT-MSCs into an immunocompetent mouse model of IBD. I focused on alterations in mice immune cells after treatment with canine MSCs. Moreover, MSCs are immunoprivileged, partly because of the low expression of major histocompatibility complex class II molecules (Le Blanc et al., 2003). Similar approaches involving the injection of xenogeneic MSCs into immunocompetent mouse models have been used by several groups, and

cross-species-induced immunological responses have not been reported (Kim et al., 2013; Kim et al., 2016; Qi et al., 2014; Roddy et al., 2011). Additionally, in this study, none of the mice injected with cAT-MSCs showed any side effects or died until sacrifice. In addition, Wang *et al*. reported that intraperitoneal infusion of MSCs showed better amelioration of DSS-induced colitis compared to local anal injection, suggesting that systemic immunomodulation rather than reducing local inflammation is required for effective therapy (Wang et al., 2016). Therefore, I determined that the optimal conditions were 2×10^6 cAT-MSCs infused intraperitoneally.

I also evaluated the distribution of intraperitoneally administered cAT-MSCs using qRT-PCR, which is known to have relatively higher sensitivity and specificity compared to fluorescence-mediated cell tracking. Two hours after cAT-MSC infusion, less than 1% of the infused cells were detected in the heart, lung, liver, spleen, kidney, and colon tissues. At 1 and 3 days after cAT-MSC administration, the percentages of cells detected in the tissues were less than 0.5%. Furthermore, infused cAT-MSCs were not detected in colon tissues, despite inflammatory responses observed at day 1 and 3. Similar results were obtained when cAT-MSCs transiently transfected with control or TSG-6 siRNA were administered. These results are consistent with those of results from the first part of this dissertation, indicating that intraperitoneally injected cAT-MSCs formed aggregates in the peritoneal

cavity and alleviated DSS-induced colitis at sites distant from the colon through soluble factors, such as TSG-6.

Considering that inflammatory cytokines modulated in inflamed colon treated with cAT-MSCs were principally derived from macrophages, I carried out *in vitro* experiments to evaluate whether TSG-6 secreted from cAT-MSCs could switch the macrophage phenotype from M1 to M2. LPS-stimulated cPBMC-derived macrophages exhibit a conventional M1 type pattern and were co-cultured with cAT-MSCs transfected with siRNA or with naïve cAT-MSCs in a transwell system. CD206-expressing M2 macrophages were increased markedly in the cAT-MSC group, but were inhibited in the siTSG-6-cAT-MSC group. Moreover, TSG-6 secreted from cAT-MSCs contributed to the decrease in the expression levels of M1 markers such as iNOS and IL-6.

Next, I evaluated M2 macrophages in colon tissue sections of DSS-induced colitis mice treated with cAT-MSCs, to analyze the macrophage polarization ability of TSG-6 released by cAT-MSCs *in vivo*. Recent studies suggested that MSCs have the capacity to induce phenotypic alterations in macrophages in acute kidney injury, spinal cord injury, and skin wound animal models (Nakajima et al., 2012; Wise et al., 2014; Zhang et al., 2010). Consistent with these reports, the expression levels of M2 markers in the colon tissue were increased in the siCTL-cAT-MSC-treated group and naïve

cAT-MSC-treated group compared to in the PBS-treated group. However, the siTSG-6-cAT-MSC-treated group showed no significant changes in the expression levels of these markers compared to the PBS group. Taken together, I demonstrated that TSG-6 secreted by cAT-MSCs plays an essential role in the switching phenotype of macrophages from M1 to M2 in the inflamed colon.

I could not rule out the possibility that other factors secreted from cAT-MSCs contributed to M2 macrophage polarization in colitis mice. Interestingly, other groups recently showed that PGE2 released by human MSCs induced macrophage phenotypic alteration (Vasandan et al., 2016; Ylöstalo et al., 2012). Further experiments of other factors secreted from cAT-MSCs such as PGE2 are required to verify their effects on macrophages in IBD models. However, my findings suggest that TSG-6 released by cAT-MSCs plays an important role in switching the macrophage phenotype from M1 to M2 *in vitro* and in DSS-induced colitis mice.

In conclusion, I demonstrated that TSG-6 secreted by cAT-MSCs ameliorated DSS-induced colitis in mice by inducing macrophages to switch to the M2 phenotype. In addition, my findings reveal a possible mechanism underlying the TSG6-induced therapeutic effects in various inflammatory disease models previously published. These results may help in the development of cell-based therapies for treating IBD.

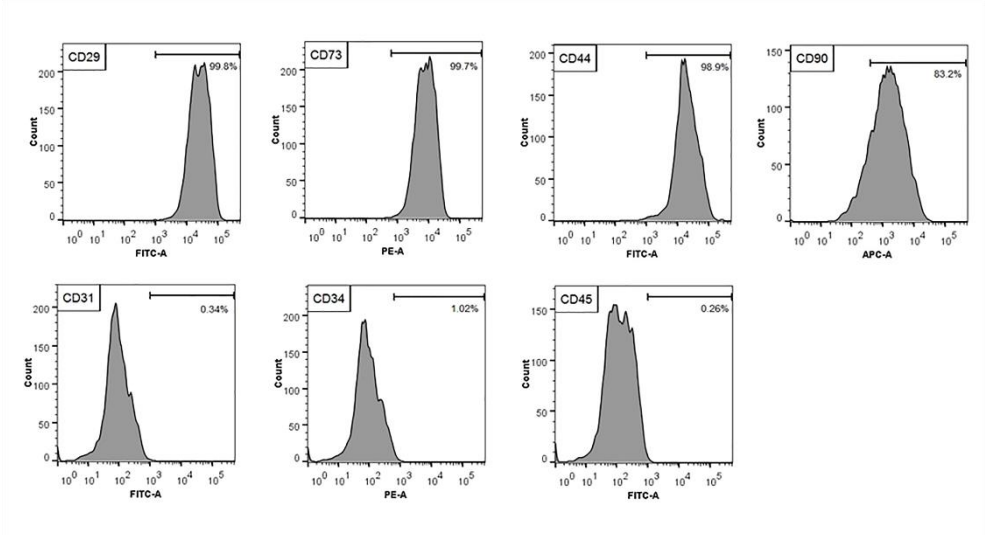

Figure 26. cAT-MSCs have high expression of CD29, CD73, CD44, and CD90, and do not express CD31, CD34, or CD45.

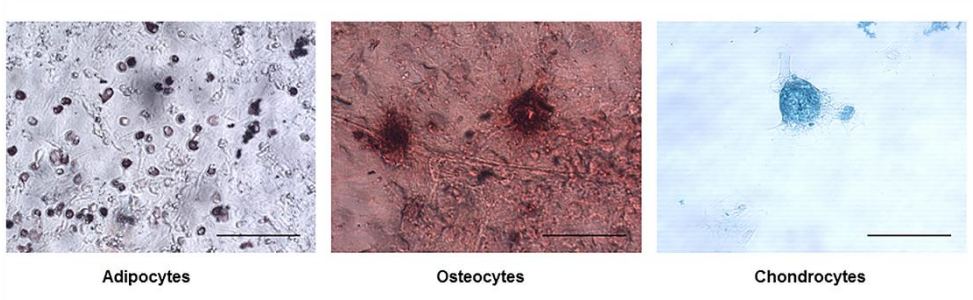

Figure 27. cAT-MSCs have the ability to differentiate into adipocytes (Oil Red O staining), osteocytes (Alizarin Red S staining), and chondrocytes (Alcian Blue staining). Bars = 200 µm.

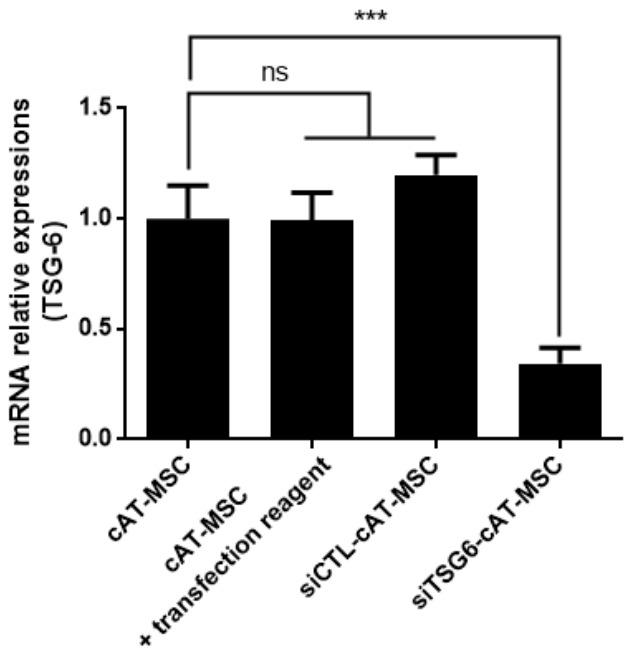

Figure 28. TSG-6 mRNA expression levels in cAT-MSCs transfected with TSG-6 siRNA (siTSG6-cAT-MSCs), cAT-MSCs transfected with control siRNA (siCTL-cAT-MSCs), cAT-MSCs with transfection reagent, and naïve cAT-MSCs. Results are presented as mean ± standard deviation obtained in three independent experiments. ***$P < 0.001$.

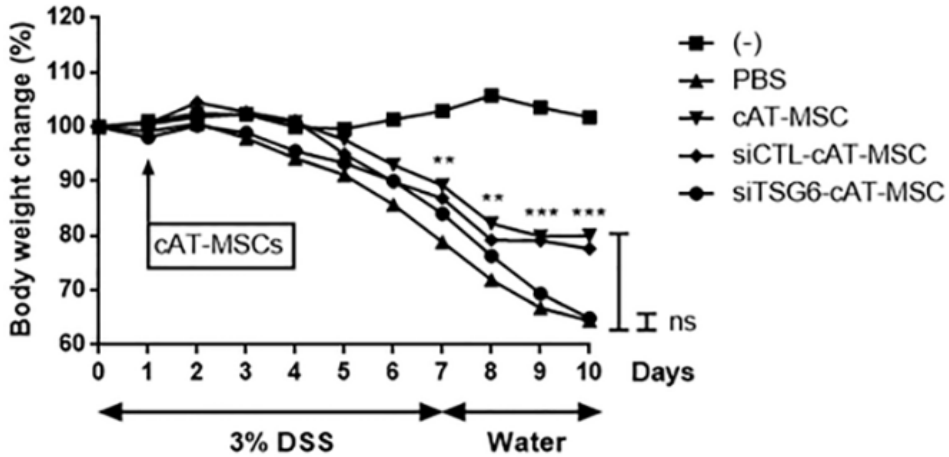

Figure 29. Intraperitoneally infused cAT-MSC-secreted TSG-6 plays an essential role in alleviating IBD. DSS-induced colitis mice were administered with cAT-MSCs transfected with TSG-6 siRNA (siTSG-6-cAT-MSC), cAT-MSCs transfected with scrambled siRNA (siCTL-cAT-MSC), naïve cAT-MSCs, or PBS (vehicle control) on day 1. Body weight was measured every day and expressed in terms of the relative change from the weight measured on day 0. Results are shown as the mean ± standard deviation. **P < 0.01, ***P < 0.001.

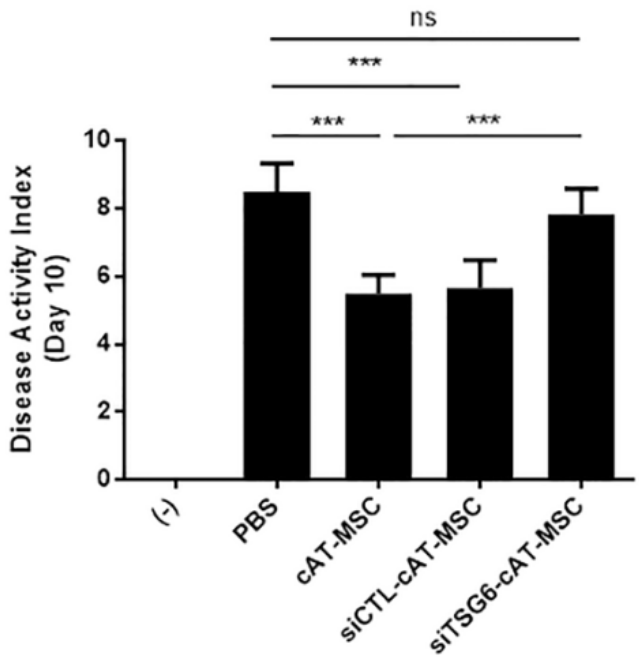

Figure 30. Intraperitoneally infused cAT-MSC-secreted TSG-6 plays an essential role in alleviating IBD. DSS-induced colitis mice were administered with cAT-MSCs transfected with TSG-6 siRNA (siTSG-6-cAT-MSC), cAT-MSCs transfected with scrambled siRNA (siCTL-cAT-MSC), naïve cAT-MSCs, or PBS (vehicle control) on day 1. Mice were sacrificed on day 10 and DAI was assessed. Results are shown as the mean ± standard deviation. ***P < 0.001.

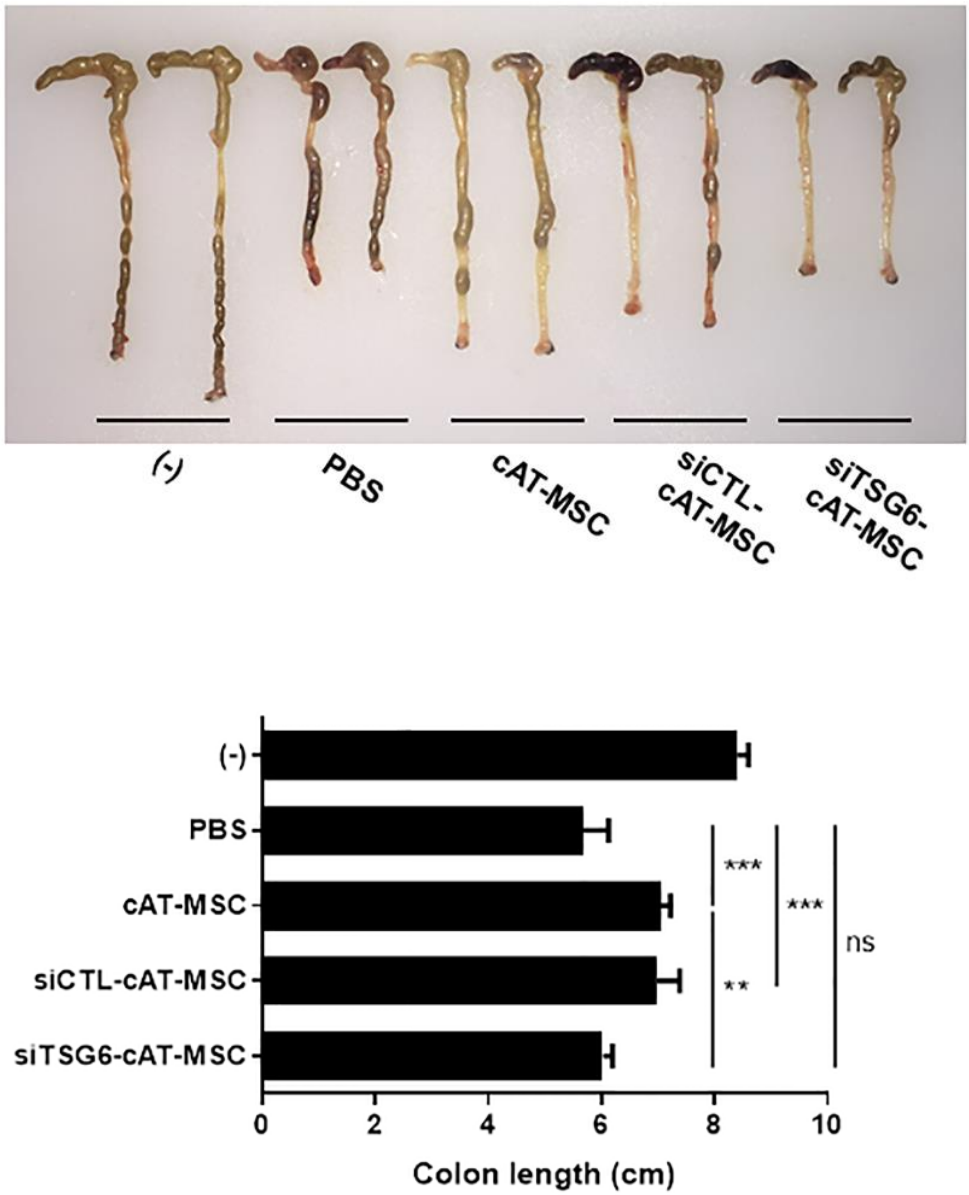

Figure 31. Intraperitoneally infused cAT-MSC-secreted TSG-6 plays an essential role in alleviating IBD. Mice were sacrificed on day 10 and colon length, were assessed. Results are shown as the mean ± standard deviation. **P < 0.01, ***P < 0.001.

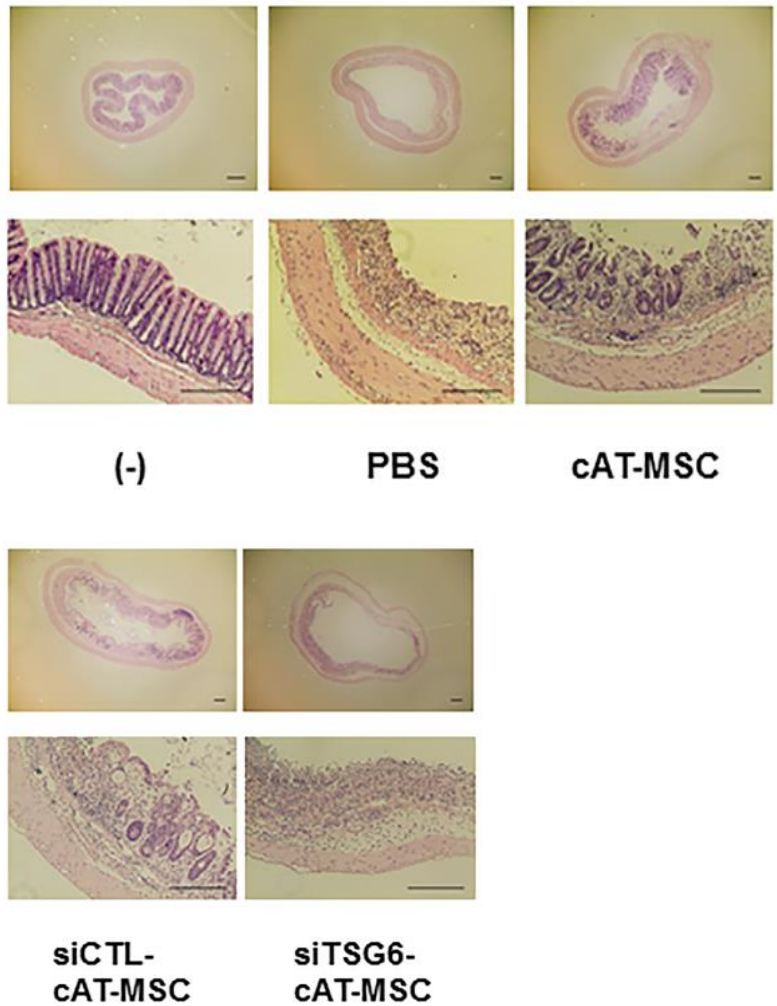

(See legends on next page)

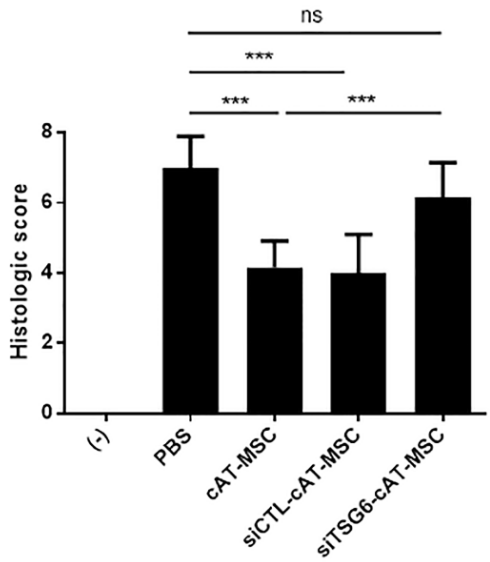

(See figures on previous page)

Figure 32. Intraperitoneally infused cAT-MSC-secreted TSG-6 plays an essential role in alleviating IBD. Representative hematoxylin and eosin staining of the colon tissue sections, and their histological scores are shown. Bars = 100 μm. Results are shown as the mean ± standard deviation. ***P < 0.001.

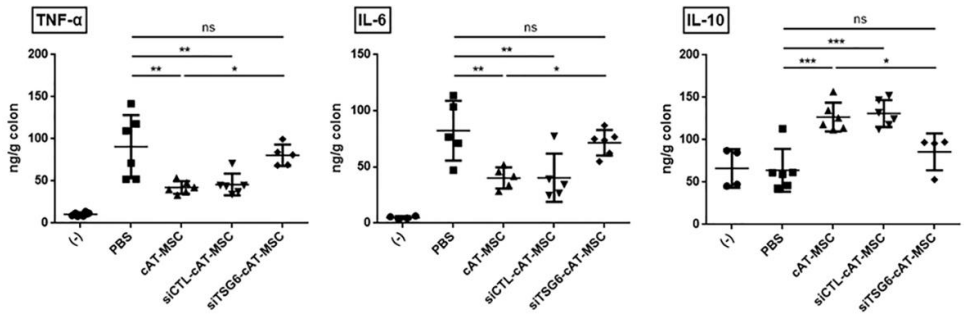

Figure 33. TSG-6 secreted by cAT-MSCs inhibits inflammatory response in the colon. Levels of TNF-α, IL-6, and IL-10 in colons were assessed by ELISA. Results are shown as the mean ± standard deviation. *P < 0.05, **P < 0.01, ***P < 0.001.

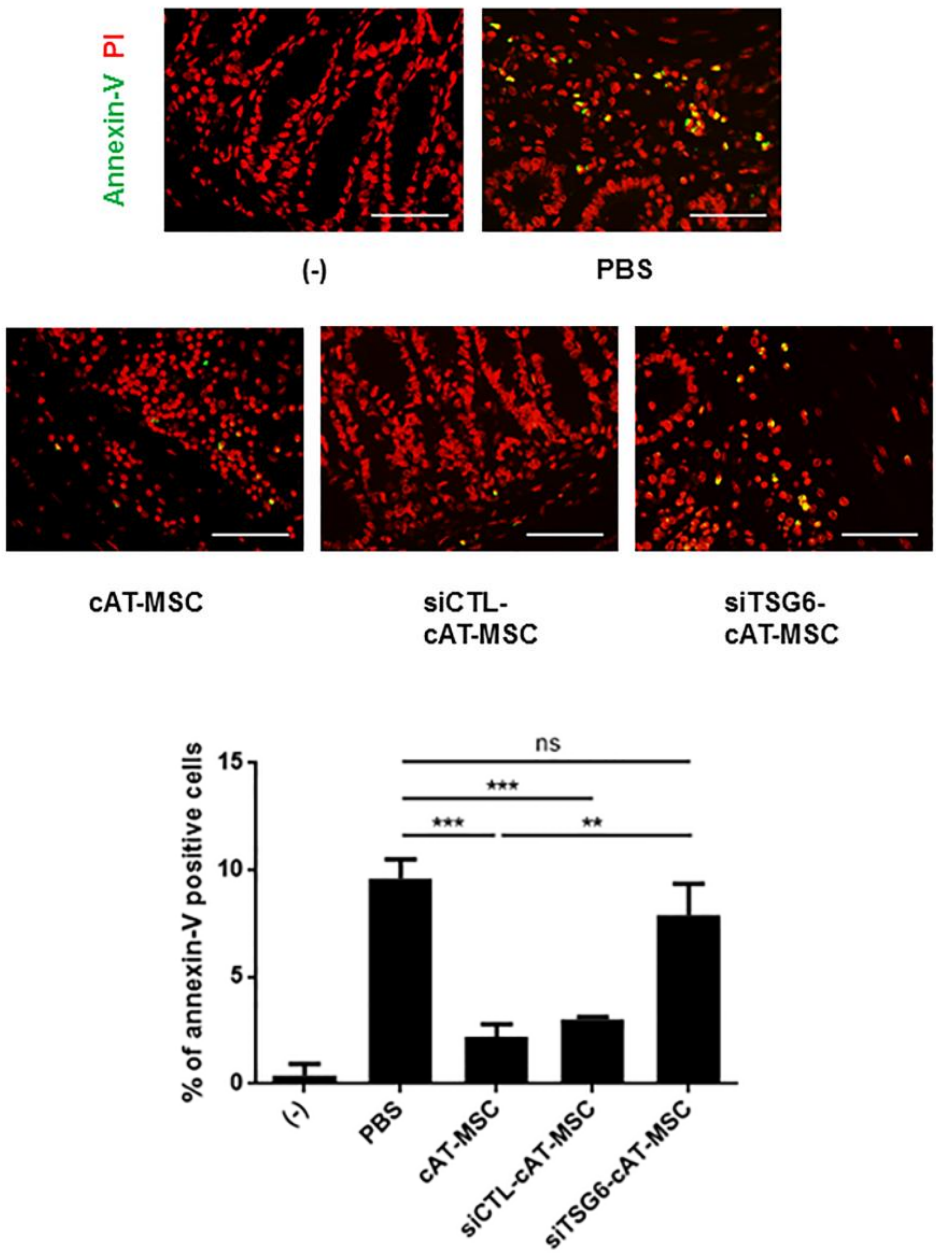

Figure 34. TSG-6 secreted by cAT-MSCs inhibits apoptosis in the colon. Representative immunofluorescence staining of colon tissue sections using annexin-V antibody or propidium iodide (PI), and the percentage of the

annexin-V positive cells are shown. Results are shown as the mean ± standard deviation. **P < 0.01, ***P < 0.001.

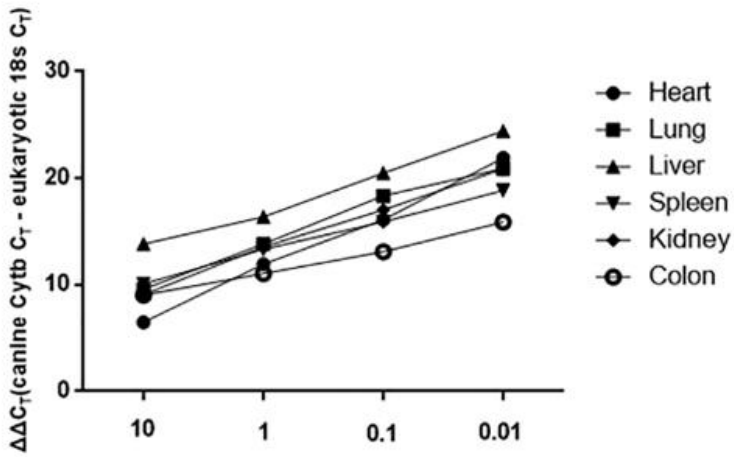

Heart	$y = 5.0451x + 1.5013$	$(R^2 = 0.9965)$
Lung	$y = 3.8546x + 6.0426$	$(R^2 = 0.9870)$
Liver	$y = 3.5865x + 5.8199$	$(R^2 = 0.9902)$
Spleen	$y = 2.8937x + 7.3147$	$(R^2 = 0.9982)$
Kidney	$y = 3.8981x + 5.3953$	$(R^2 = 0.9972)$
Colon	$y = 2.2626x + 6.6186$	$(R^2 = 0.9931)$

Figure 35. Standard curves for evaluating the migratory ability of intraperitoneally injected cells were generated by administering serial dilutions of cAT-MSCs to the mouse heart, lung, liver, spleen, kidney, and colon.

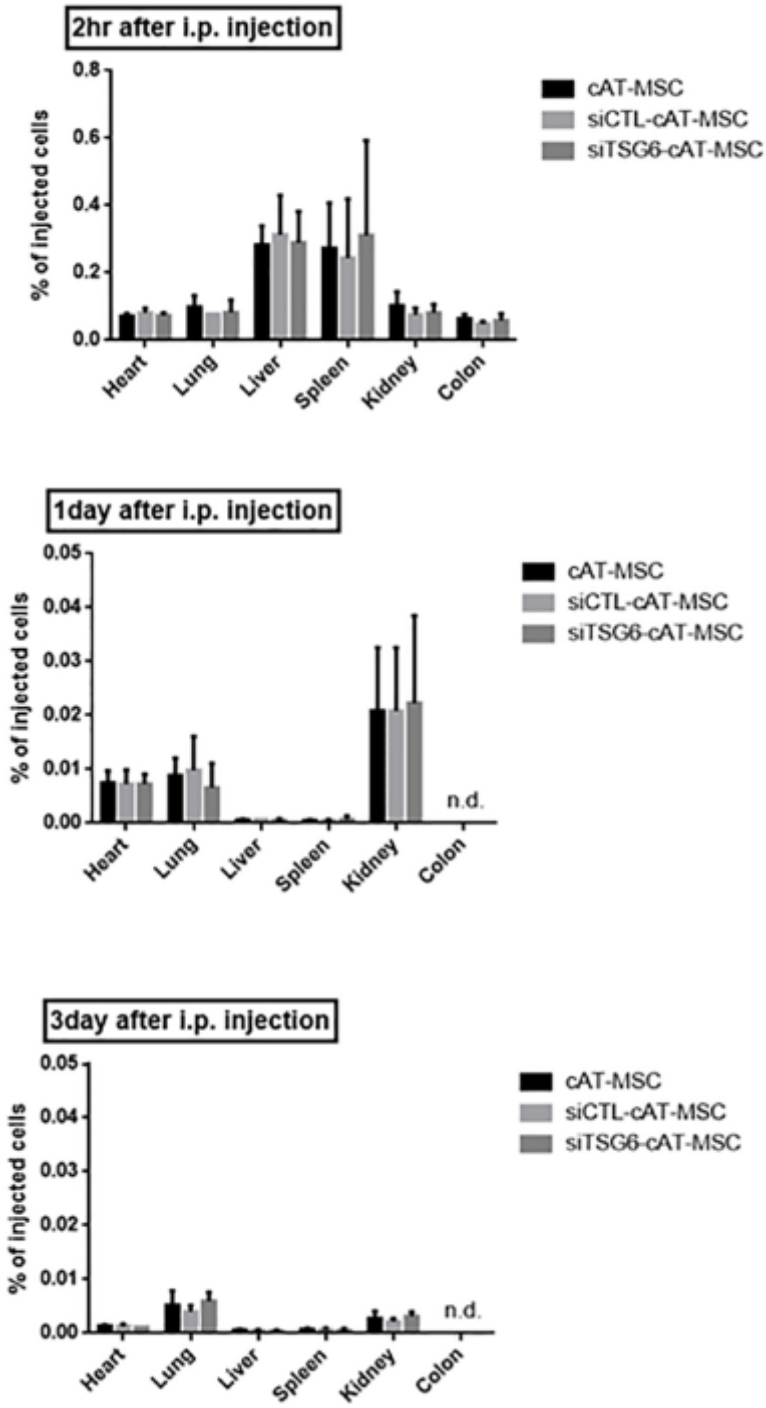

(See legends on next page)

(See figures on previous page)

Figure 36. Intraperitoneally administered cAT-MSCs do not migrate into the colon. The percentage of infused cAT-MSCs in the organs was evaluated at 2 h, 1 day, and 3 days after cell administration. Results are presented as the mean ± standard deviation of the data obtained in three independent experiments

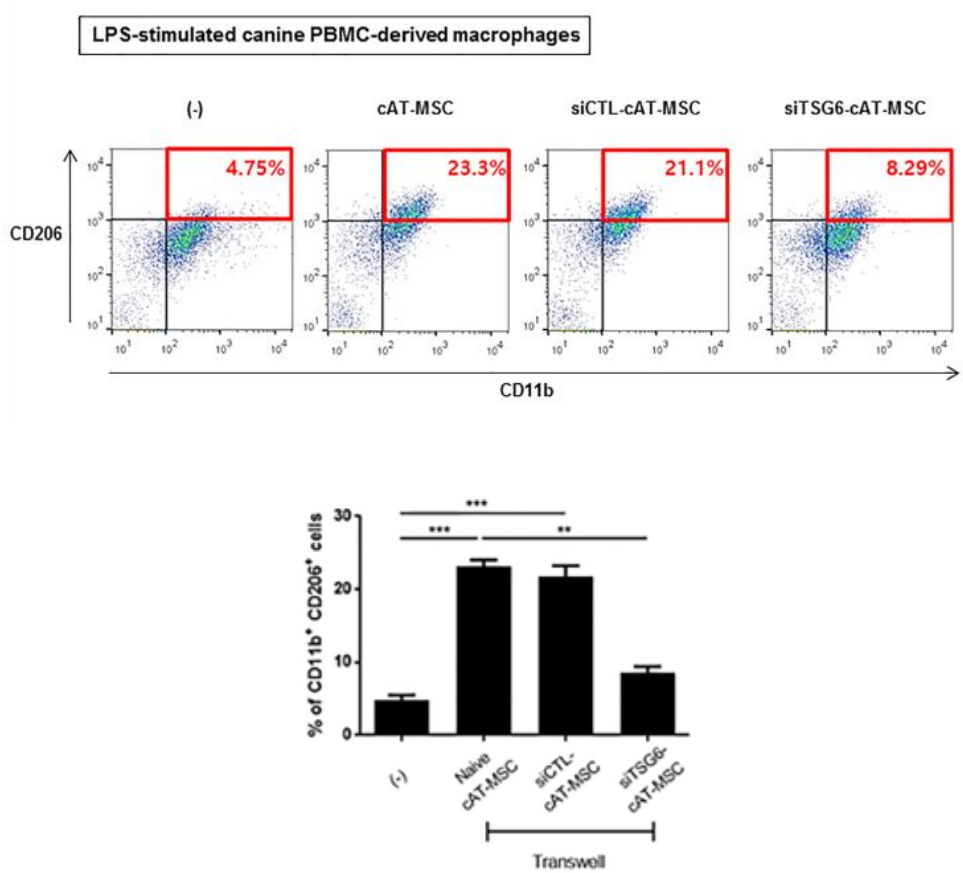

Figure 37. cAT-MSC-secreted TSG-6 induce macrophage phenotypic switching from M1 to M2 *in vitro*. LPS-stimulated cPBMC-derived macrophages were co-cultured in transwell system with cAT-MSCs transfected with TSG-6 siRNA (siTSG-6-cAT-MSC), cAT-MSCs transfected with scrambled siRNA (siCTL-cAT-MSC), or naïve cAT-MSCs for 48 h. M2 macrophage population was determined by measuring CD11b- and CD206-double positive cells by flow cytometry. Results are presented as the mean ± standard deviation of three independent experiments. **P < 0.01, ***P < 0.001.

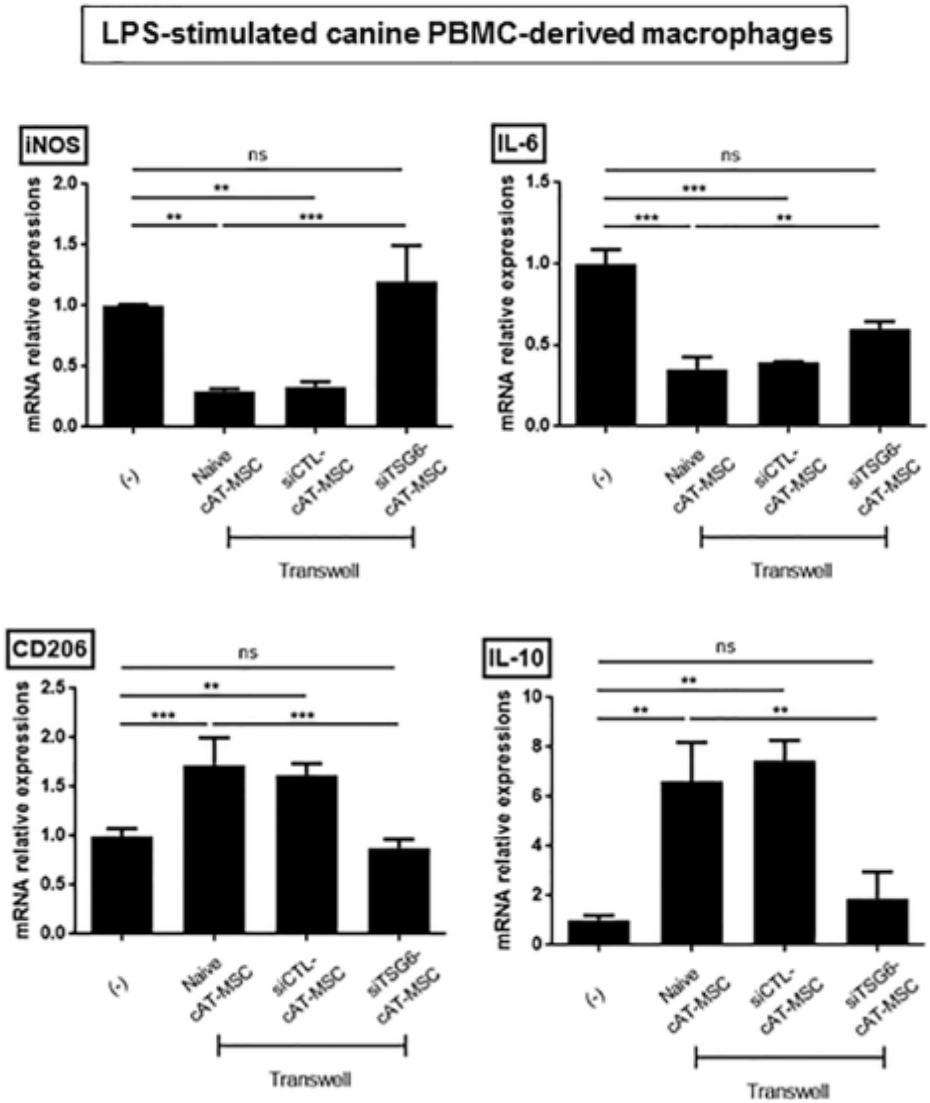

Figure 38. cAT-MSC-secreted TSG-6 induce macrophage phenotypic switching from M1 to M2 *in vitro*. LPS-stimulated cPBMC-derived macrophages were co-cultured in transwell system with cAT-MSCs transfected with TSG-6 siRNA (siTSG-6-cAT-MSC), cAT-MSCs transfected with scrambled siRNA (siCTL-cAT-MSC), or naïve cAT-MSCs for 48 h.

iNOS, IL-6, CD206, and IL-10 mRNA expression levels in the macrophages were evaluated. Results are presented as the mean ± standard deviation of three independent experiments. **P < 0.01, ***P < 0.001.

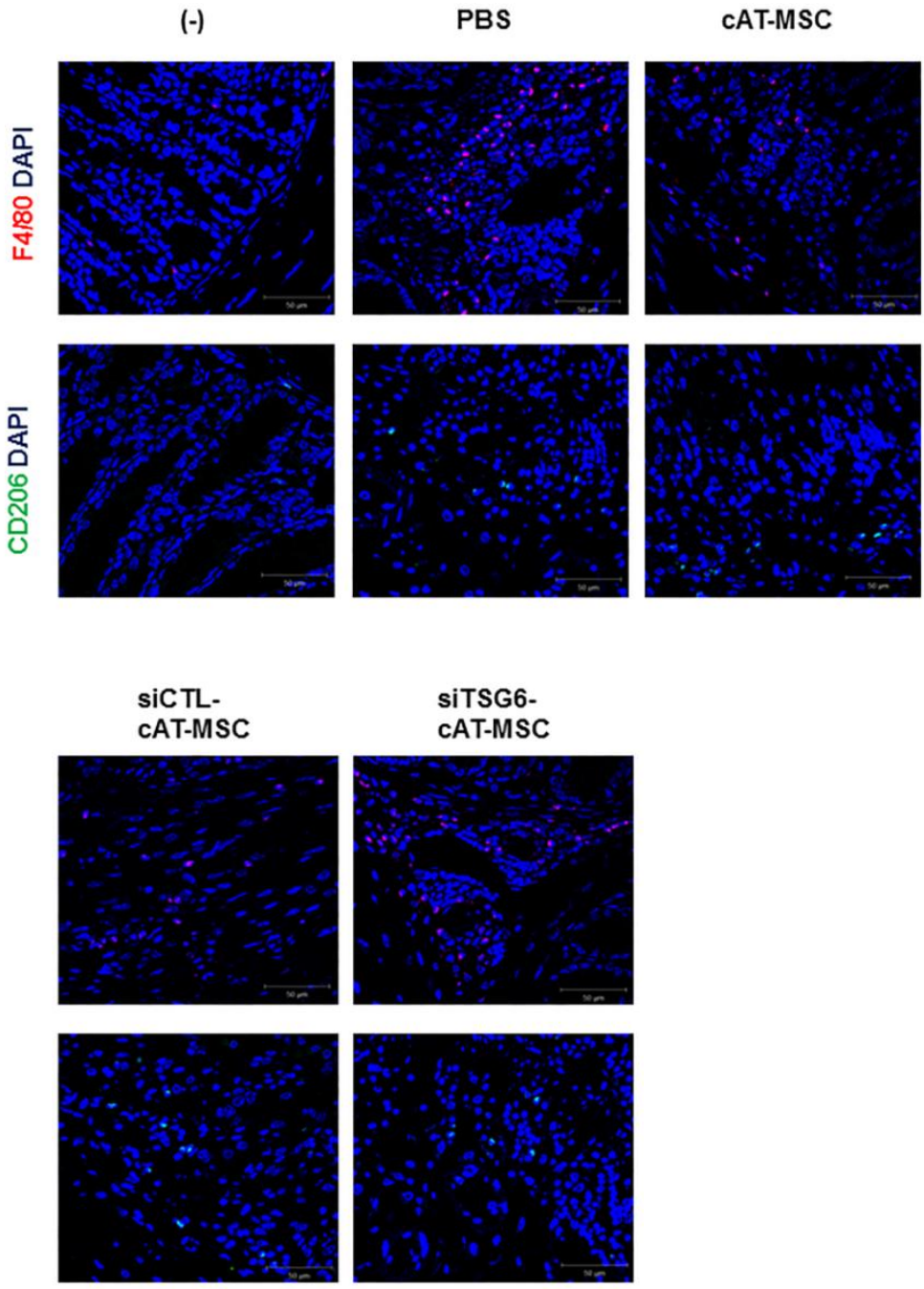

Figure 39. (See legends on next page)

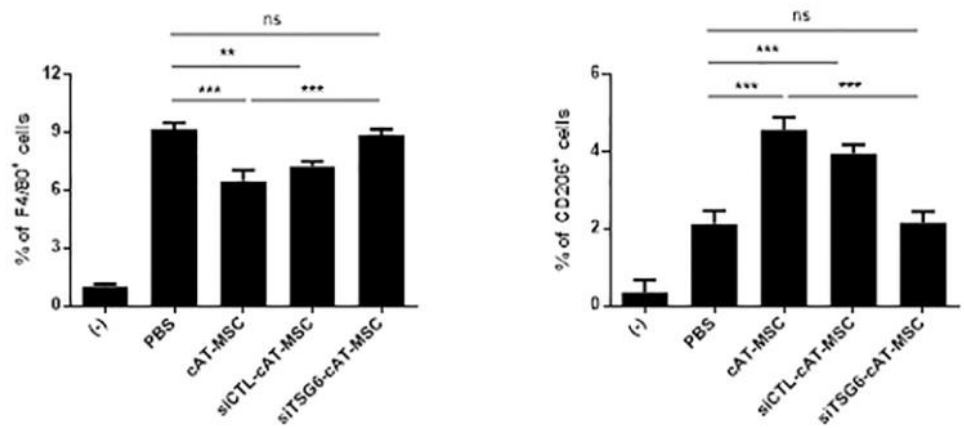

(See figures on previous page)

Figure 39. TSG-6 secreted by cAT-MSCs induces M2 macrophage polarization in inflamed colon. Representative immunofluorescence staining of colon tissue sections using F4/80- or CD206-specific antibodies, and their percentages of F4/80- or CD206-positive cells are shown. Bars = 50 μm. Results are presented as the mean ± standard deviation. **P < 0.01, ***P < 0.001.

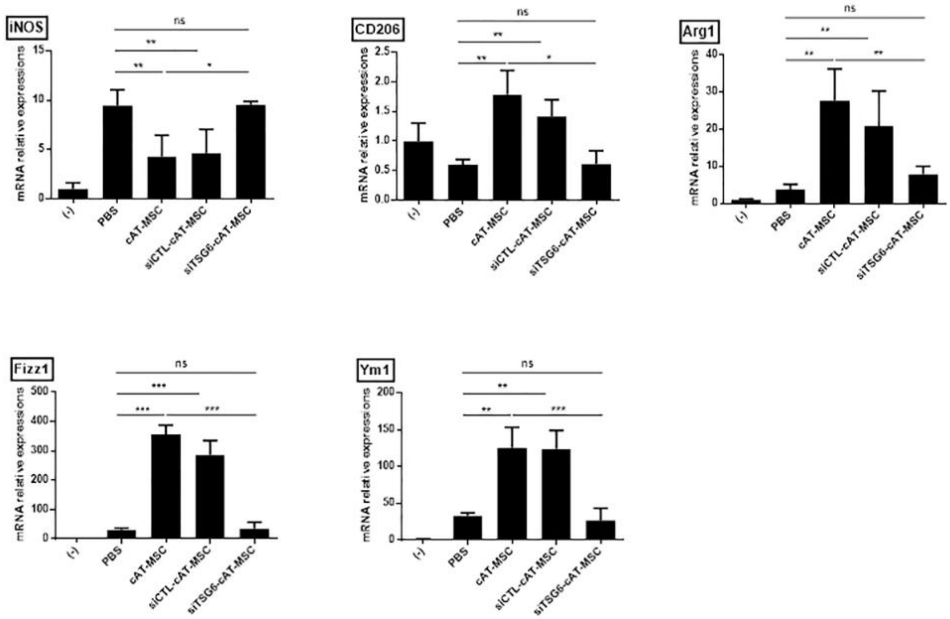

Figure 40. TSG-6 secreted by cAT-MSCs induces M2 macrophage polarization in inflamed colon. The gene expression levels of iNOS, CD206, Arg1, Fizz1, and Ym1 in the colon samples of mice were evaluated. Results are presented as the mean ± standard deviation. *P < 0.05, **P < 0.01, ***P < 0.001.

Table 2. List for primers for the second part of this dissertation

Gene	Forward (5′-3′)	Reverse (5′-3′)
Mouse		
iNOS	AAAGGAAATAGAAACAACAGGAACC	GCATAAAGTATGTGTCTGCAGATGT
IL-6	AGGCTTAATTACACATGTTCTCTGG	TTATATCCAGTTTGGTAGCATCCAT
CD206	AACGGAATGATTGTGTAGTTCTAGC	TACAGGATCAATAATTTTTGGCATT
Arg1	CAGAAGAATGGAAGAGTCAG	CAGATATGCAGGGAGTCACC
Fizz1	GAATCTATTGTGGAGAAAAAGGTCA	AGCCGTGATACTAGTACAGGAGAAA
Ym1	GTGTACTCACCTGATCTATGCCTTT	CAGGAGAGTTTTTAGCTCAGTGTTC
IL-10	GTGATTTTAATAAGCTCCAAGACCA	GATCATCATGTATGCTTCTATGCAG
GAPDH	AGTATGTCGTGGAGTCTACTGGTGT	AGTGAGTTGTCATATTTCTCGTGGT
Canine		
iNOS	AAATTATGTCCTGTCCCCTTTCTAC	TTTAAGTTGAATCTTTTTCCTGTGG
IL-6	ATGATCCACTTCAAATAGTCTACC	AGATGTAGGTTATTTTCTGCCAGTG
CD206	GGAAATATGTAAACAGGAATGATGC	TCCATCCAAATAAACTTTTTATCCA
IL-10	ATTTCTGCCCTGTGAGAATAAGAG	TGTAGTTGATGAAGATGTCAAGCTA
TSG-6	TCCGTCTTAATAGGAGTGAAAGATG	AGATTTAAAAATTCGCTTTGGATCT
GAPDH	TTAACTCTGGCAAAGTGGATATTGT	GAATCATACTGGAACATGTACACCA

CHAPTER III.

Canine Adipose Tissue-derived Mesenchymal Stem Cells Pre-treated with TNF-alpha Enhanced Immunomodulatory Effects on Inflammatory Bowel Disease in Mice

Introduction

Canine inflammatory bowel disease (IBD) leading to gastrointestinal or systemic clinical signs is diagnosed by ruling out the possibility of other diseases such as infection and tumor and performing histopathological assessment (Cerquetella, 2010; Craven et al., 2004). IBD is an intractable autoimmune disease, and immunosuppressive drugs are used to reduce inflammation (Allenspach et al., 2006; Dossin and Lavoue, 2011). However, no alternative treatments exist for dogs with IBD that are not responsive to the conventional therapies. Therefore, mesenchymal stem cells (MSCs) that can effectively modulate inflammation might be an alternative therapeutic option (Iyer and Rojas, 2008).

Recent studies have revealed that soluble factors released by MSCs such as prostaglandin E2 (PGE2), hepatocyte growth factor, indoleamine 2,3-dioxygenase, and TNF-stimulated gene/protein 6 (TSG-6) contribute to immunomodulation (Bassi et al., 2012; Montemurro et al., 2016; Teng et al., 2015). Therefore, MSCs exert strong anti-inflammatory effects, although injected MSCs did not migrate into inflamed tissue (Sala et al., 2015). Kang *et al.* and Chae *et al.* also demonstrated that canine and feline MSCs secrete immunomodulatory soluble factors (Chae et al., 2017; Kang et al., 2008). In addition, my previous results from the first and second parts of this

dissertation have shown that TSG-6 released from human and canine MSCs ameliorated colitis in mice.

In my previous study, I have demonstrated that canine MSCs pre-treated with tumor necrosis factor (TNF)-α and interferon (IFN)-γ exerted enhanced anti-inflammatory effects *in vitro* by releasing higher concentrations of PGE2, an immunomodulatory factor (Yang et al., 2018b). Fan *et al.* also have revealed that human MSCs stimulated with interleukin (IL)-1β showed enhanced efficacy in colitis mice (Fan et al., 2012). In addition, recent studies have demonstrated that MSCs pre-treated with pro-inflammatory cytokines showed enhanced secretory abilities (Broekman et al., 2016; Heo et al., 2011). However, few studies have assessed the therapeutic effects of pro-inflammatory cytokine-stimulated canine MSCs.

Therefore, in this study, I used canine adipose tissue (cAT)-MSCs stimulated with TNF-α, and revealed the therapeutic effects and their mechanisms in IBD model mice.

Materials and methods

Isolation, culture, and characterization of cAT-MSCs

Canine adipose tissues were obtained from healthy 4-year-old dogs using protocols approved by the Institutional Animal Care and Use Committee (IACUC) of Seoul National University performed in accordance with approved guidelines. The dogs were negative for canine parvovirus, canine coronavirus, and canine distemper virus infections. MSCs were isolated and cultured as previously described (Kim et al., 2016). Briefly, adipose tissue samples were washed five times in Dulbecco's phosphate buffered saline (DPBS; PAN-Biotech, Aidenbach, Germany) containing 1% penicillin-streptomycin (PS; PAN-Biotech), and cut into small pieces in a petri dish. The samples were digested with collagenase type IA (0.1%, Gibco/Life Technologies, Carlsbad, CA, USA) for 60 min at 37°C. The samples were neutralized with Dulbecco's modified Eagle's medium (DMEM; PAN-Biotech) containing 10% fetal bovine serum (FBS; PAN-Biotech). After centrifugation of the adipose tissue mixture at 1,200 × *g* for 5 min, the pellet containing MSCs was passed through a 70-μm cell strainer (Thermo Fisher Scientific, Rockford, IL, USA) to remove undigested debris. Cells were resuspended in DMEM containing 10% FBS and 1% PS, seeded onto a cell culture dish at a density of 3000/cm^2, and incubated at 37°C and 5% CO_2. After 5 days, cultures were washed with DPBS to remove non-

adherent cells and incubated with fresh medium. The culture medium was changed every 2–3 days until cells reached 70-80% confluence. The cells were then subcultured and seeded at a density of 10,000/cm^2 in culture dishes.

Before experimentation, the cells were characterized using flow cytometry to evaluate the expression of several stem cell markers. Cells were suspended in DPBS and monoclonal antibodies against the following proteins: cluster of differentiation (CD)29- fluorescein isothiocyante (FITC), CD31-FITC, CD34-phycoerythrin (PE), CD73-PE (BD Biosciences, San Diego, CA, USA), CD45-FITC, and CD90-allophycocyanin (eBiosciences, San Diego, CA, USA). Cell fluorescence was analyzed with a FACS Aria II system (BD Biosciences). Additionally, the abilities of cellular differentiation were evaluated using Stempro adipogenesis, osteogenesis, and chondrogenesis differentiation kits (Gibco, Grand Island, NY, USA) according to the manufacturer's instruction. The differentiated cells were stained with Oil Red O, Alizarin Red, and Alcian Blue.

TNF-α stimulation of cAT-MSCs

cAT-MSCs at approximately 60-70% confluence were stimulated with canine recombinant TNF-α (10 ng/mL; PROSPEC Protein Specialists, NJ, USA) for 24 h. The cells were used for TNF-α-stimulated cAT-MSC groups.

Animal experiments

C57BL/6 J mice (male, 5-week-old) were purchased from Nara Biotech (Seoul, Korea) and housed under standard conditions (controlled temperature, humidity, and light cycle). All procedures involving mice were approved by the IACUC of SNU (protocol no. SNU-171123-2), and the protocols were performed in accordance with approved guidelines. Colitis was induced by 3% dextran sulfate sodium (DSS; 36–50 kDa; MP Biomedical, Solon, OH, USA) in the drinking water from day 0 to day 7, whereas mice offered normal water were used as the naive group. The following experiments were performed on day 1: cAT-MSCs (2×10^6) stimulated with TNF-α in 200 μL PBS; cAT-MSCs (2×10^6) in 200 μL PBS; or the identical volume of PBS was injected intraperitoneally into the DSS-induced colitis mice. Dinitrobenzene sulfonic acid (DNBS; Sigma-Aldrich, St. Louis, MO, USA) colitis was induced by rectal administration of DNBS (5 mg/mouse in a 50% ethanol) into mice. Six hours after DNBS infusion, cAT-MSCs were administered intraperitoneally as described above. The mice were sacrificed on day 10 (for DSS-induced colitis experiments) or day 3 (for DNBS-induced colitis experiments), and colon tissues were collected for further processing.

Evaluation of colitis severity

The disease activity index (DAI) was determined by a scoring system described previously in the second part of this dissertation. Briefly, the body weight loss (grades 0–4), stool consistency (grades 0–2), rectal bleeding (grades 0–2), and general activity (grades 0–2) were monitored every 24 h. For histological analysis, colon tissue samples were fixed in 4% phosphate-buffered formaldehyde for 48-72 h, followed by embedding in paraffin, cutting into 4 μm sections, and staining with hematoxylin and eosin. Ten fields per group were randomly selected and histological examinations were performed. The severity of colitis was calculated using the previously described scoring system. Briefly, the extent of bowel wall thickening (grades 0–3), damage to the crypt (grades 0–3), and infiltration of inflammatory cells (grades 0–2) were examined in a blind manner.

Enzyme-linked immunosorbent assay (ELISA)

TSG-6 and PGE2 in the supernatants from TNF-α-pre-treated or non-treated cAT-MSCs were measured using TSG-6 ELISA kit (MyBiosource, San Diego, CA, USA) and PGE2 ELISA Kit (Cusabio Biotech, MD, USA), respectively. Additionally, for *in vivo* experiments, total proteins were extracted from colon tissue samples using PRO-PREP Protein Extraction Solution (Intron Biotechnology, Seongnam, Korea) and the concentrations of

IL-1β, IL-6, and IL-10 were measured using commercial ELISA kits (all from eBiosciences) according to the manufacturer's instructions.

Flow cytometry analysis

For evaluation of mouse macrophage population, the following monoclonal antibodies mixtures were used for the experiments: anti-F4/80-FITC and anti-inducible nitric oxide synthase (iNOS)-PE; or anti-F4/80-FITC and anti-CD206-PE (Santa Cruz Biotechnology, Santa Cruz, CA, USA) were incubated with cells isolated from digested colon tissues. Flow cytometry was performed using a FACS Aria II system (BD Biosciences) and analyzed using FlowJo software (Tree Star, Ashland, OR, USA).

Statistical analysis

Data are shown as the mean ± standard deviation. Mean values among different groups were compared by one-way analysis of variance using the GraphPad Prism software (v.6.01; GraphPad, Inc., La Jolla, CA, USA). A P value < 0.05 was considered statistically significant.

Results

Phenotypic characterization of cAT-MSCs

Cells isolated from canine adipose tissue were assessed for MSC characteristics. Flow cytometry analysis showed that stem cell markers such as CD29, CD73, and CD90 were highly expressed in these cells. In contrast, there was no detectable expression of hematopoietic markers, including CD31, CD34, and CD45. Additionally, the cells could be differentiated into adipocytes, osteocytes, and chondrocytes (Fig. 41). According to criteria established by International Society for Cellular Therapy, the cells used in this study represent MSCs.

Enhanced secretory abilities for immunomodulatory factors of TNF-α stimulated cAT-MSCs

My previous studies demonstrated that secretory factors from canine MSCs such as TSG-6 and PGE2 play a key role in modulating inflammation. Therefore, cAT-MSCs were stimulated with TNF-α, a pro-inflammatory cytokine, to produce more immunomodulatory factors. TSG-6 and PGE2 concentrations determined from the cAT-MSCs pre-treated with TNF-α were significantly higher than those measured from the naïve cAT-MSCs (Fig. 42).

Improved therapeutic effects of TNF-α stimulated cAT-MSCs on DSS- or DNBS-induced colitis mice

Next, I evaluated whether administration of cAT-MSCs or TNF-α stimulated cAT-MSCs could reduce colitis in mice. Consistent with previous studies, administration of cAT-MSCs exhibited a general reduction in body weight loss, DAI, and colon length shortening in DSS- or DNBS-induced colitis (Fig. 2A-C, 3A-C). In addition, further improvement was confirmed in colitis mice injected TNF-α-stimulated cAT-MSCs (Figs. 43-45, 47-49).

Additionally, histopathology in the inflamed colon tissue was evaluated. Colons of mice treated with DSS or DNBS showed severe submucosal thickening, crypt damage, and infiltration of inflammatory cells. In contrast, the mice experienced a slight improvement via administration of cAT-MSCs, and were additionally enhanced by administration of TNF-α-stimulated cAT-MSCs (Figs. 46, 50).

Enhanced anti-inflammatory effects of TNF-α primed cAT-MSCs on DSS-induced colitis mice

I next explored whether cAT-MSCs or TNF-α stimulated cAT-MSCs could improve the anti-inflammatory effects in DSS-induced colitis. In the colons of mice treated with naïve cAT-MSCs, the production of IL-1β and IL-6 was significantly decreased, and that of IL-10 was increased considerably

compared to that in the colons of mice treated with PBS, as expected from previous studies. Similar to the above results, the intestinal inflammation was further improved in colons from mice treated with TNF-α-stimulated cAT-MSCs (Fig. 51).

Increased alteration of macrophage phenotype in the inflamed colon of mice administered TNF-α primed cAT-MSCs

Given that the cytokines (IL-1β, IL-6, and IL-10) modulated in the above results are mainly secreted from macrophages, I further investigated whether cAT-MSCs or TNF-α-stimulated cAT-MSCs could alter macrophage phenotypes in the inflamed colon. My previous study demonstrated that TSG-6 secreted from cAT-MSCs could increase M2 macrophages in the colons of mice treated with DSS. Consistent with the study, the M2 macrophage population ($F4/80^+/CD206^+$) in colons of DSS-induced colitis mice treated with cAT-MSCs was significantly increased compared with that in mice treated with PBS. In addition, the M1 macrophage population ($F4/80^+/iNOS^+$) was decreased in the cAT-MSCs-treated group. The phenotypic population of macrophages was further altered in the TNF-α stimulated cAT-MSCs-treated group (Fig. 52).

Discussion

Recently, a number of studies have shown that MSCs can effectively reduce IBD in rodent models (Gonzalez-Rey et al., 2009; Tanaka et al., 2008; Wang et al., 2014). Furthermore, the administration of MSCs as a therapeutic option for IBD in small clinical trials (both in humans and dogs) has also shown considerable promise (Kim et al., 2017; Perez-Merino et al., 2015). In this dissertation, I have demonstrated that TSG-6 released from human and canine MSCs plays a crucial role in immunomodulation by inducing an M2 macrophage switch. In addition, studies from other groups have shown that PGE2 secreted from human MSCs could exert anti-inflammatory effects in rodent models (Yang et al., 2018a). Therefore, by up-regulating the secretion of the soluble factors, MSCs could enhance the immunomodulatory effects. Overall, these findings highlight the efficacy of TNF-α stimulated cAT-MSCs against DSS- or DNBS-induced colitis in mice.

In this study, I demonstrated that intraperitoneal injection of TNF-α stimulated cAT-MSCs showed higher therapeutic efficacy compared to naïve cAT-MSCs administration in IBD mice models. For example, body weight loss and DAI were further improved in the TNF-α-stimulated cAT-MSCs-treated mice by 6% and 20%, respectively, compared to the naive cAT-MSCs-treated group. In addition, evaluation of colon length and histopathologic analysis highlight the increased therapeutic effects of TNF-α-stimulated cAT-

MSCs. In addition, concentrations of inflammatory cytokines in the inflamed colons were significantly altered in the TNF-α-cAT-MSC group compared with those in the cAT-MSC group.

Previous studies have revealed that human MSCs stimulated with pro-inflammatory cytokines (such as TNF-α and IL-1β) could improve the secretory effects of immunomodulatory soluble factors (Broekman et al., 2016; Heo et al., 2011). Here, I also showed that TNF-α-stimulated cAT-MSCs released significantly higher concentrations of TSG-6 (2.5-fold) and PGE2 (3-fold), relative to naive cAT-MSCs. TSG-6 and PGE_2 are well-known immunomodulatory factors secreted from human and canine MSCs, and recent studies have demonstrated that these factors play important roles in ameliorating atopic dermatitis, rheumatoid arthritis, acute pancreatitis, and IBD (Chae et al., 2017; Kim et al., 2016; Kim et al., 2015; Mao et al., 2017; Shin et al., 2016). Consistent with these studies, my results indicate that cAT-MSCs stimulated with TNF-α further reduced DSS- or DNBS-induced colitis by releasing higher concentrations of TSG-6 and PGE_2.

Macrophages are important innate immune cells that play a key role in releasing inflammatory cytokines and transferring information to acquired immune cells such as T cells. It is well established that two types of macrophages (M1 and M2) are observed in the inflamed tissues (Mosser and Edwards, 2008; Stout and Suttles, 2004), and these cells play an important

role in regulating inflammatory responses. Melief *et al.* demonstrated that human MSCs induce monocytes into $CD206^+$ M2 macrophages, and consequently increase $Foxp3^+$ regulatory T cells (Melief et al., 2013). In addition, recent studies have revealed that soluble factors (such as TSG-6 and PGE_2) released from human MSCs could increase M2 macrophage phenotype and reduce inflammation in mouse models of rheumatoid arthritis and wound healing (Shin et al., 2016; Zhang et al., 2010). Additionally, I previously demonstrated that TSG-6 released from canine MSCs could induce M2 macrophage phenotypic changes *in vitro* and *in vivo* in the second part of this dissertation. In this study, TNF-α stimulated cAT-MSCs increased macrophage alteration to M2 phenotype ($F4/80^+/CD206^+$) in the colons of IBD mice, whereas M1 macrophages ($F4/80^+/iNOS^+$) were decreased in the inflamed colons. Consistent with previous studies and my results, TNF-α stimulated cAT-MSCs reduced inflammation through altering macrophage phenotypic changes by secreting higher concentrations of TSG-6 and PGE_2.

Recent studies have suggested other mechanisms by which MSCs might contribute to reduction of colitis. For example, MSCs may stimulate epithelial regeneration (Sémont et al., 2013; Sémont et al., 2006; Valcz et al., 2011). It is well established that MSCs upregulate $Ki67^+$ cells in inflamed tissues (Nakagawa et al., 2015; Wu et al., 2007). In addition, Chen *et al.* have demonstrated that MSCs increased $Lgr5^+$ intestinal stem cells in colonic

tissues of IBD model mice (Chen et al., 2013). Another potential mechanism of MSC-dependent improvement in IBD involves microbiome changes. However, in this study, TNF-α-stimulated MSCs, which release higher concentrations of immunomodulatory soluble factors, showed further improved colitis in mice (Soontararak et al., 2018). Therefore, I demonstrated here that the anti-inflammatory effects of MSCs play an important role in their overall therapeutic effects on colitis, although MSCs might reduce IBD through diverse mechanisms.

It should be acknowledged that I was not able to perform microarray screening of TNF-α-stimulated cAT-MSCs, although I evaluated increased TSG-6 and PGE2 from TNF-α stimulated cAT-MSCs. However, it is well demonstrated that TSG-6 and PGE2 secreted from MSCs could induce macrophage phenotypic alteration. Therefore, my findings suggest that increased TSG-6 and PGE2 released from TNF-α stimulated cAT-MSCs play a key role in reducing inflammation in an IBD mouse model.

In summary, I demonstrated that TNF-α-stimulated cAT-MSCs further ameliorated IBD via their enhanced anti-inflammatory effects. Additionally, I showed that cAT-MSCs pre-treated with TNF-α could release higher immunomodulatory factors such as TSG-6 and PGE2, which contribute to induce macrophages phenotypic alteration. These results may

suggest a novel cell-based therapeutic option for treating autoimmune disease such as IBD.

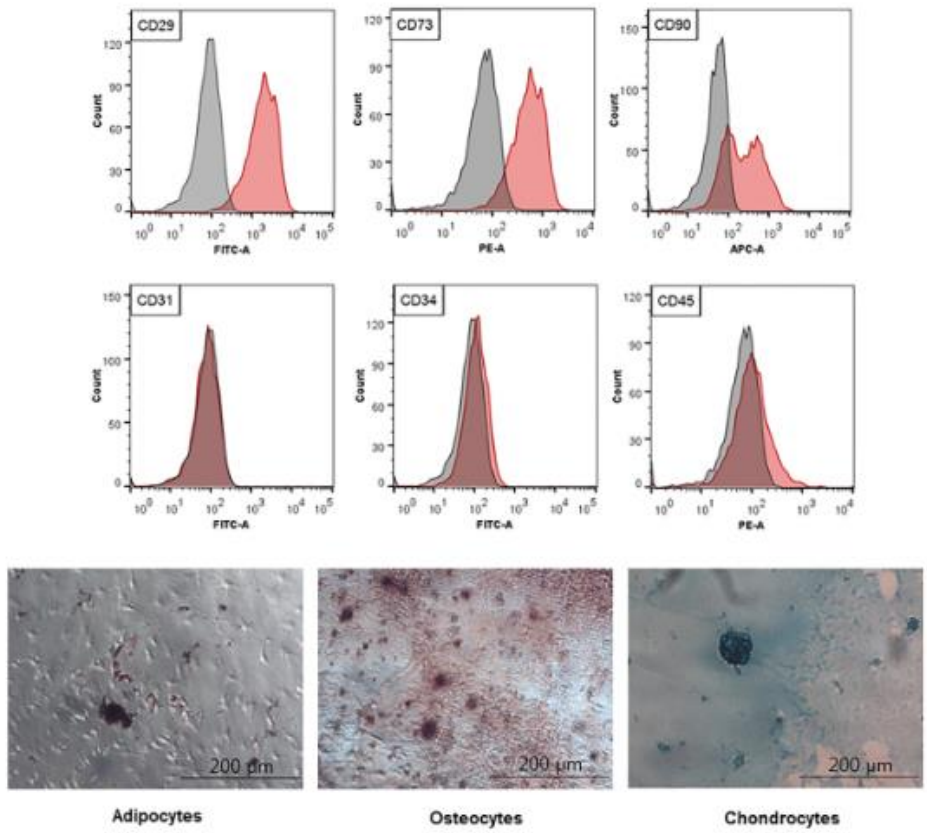

Figure 41. Cells isolated from canine adipose tissues were characterized before their use in this study by flow cytometry analysis, as well as adipogenic, osteogenic, and chondrogenic differentiation analysis.

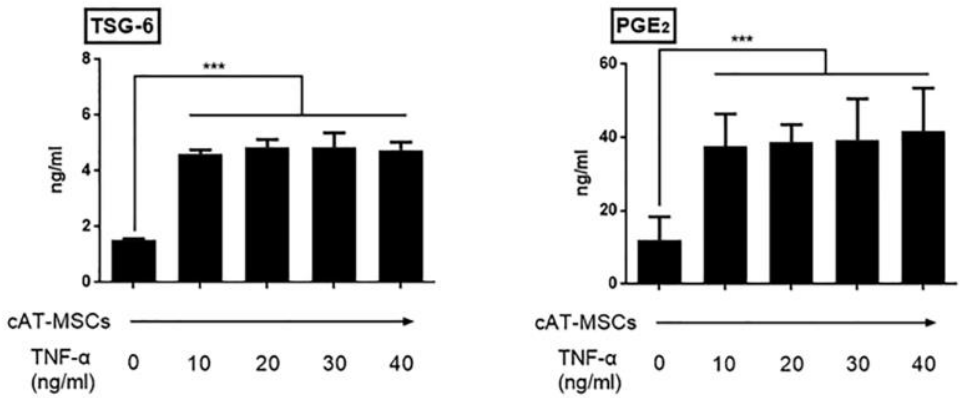

Figure 42. Canine adipose tissue-derived mesenchymal stem cells (cAT-MSCs) stimulated with TNF-α released higher concentrations of immunomodulatory factors such as TSG-6 and PGE2. Results are shown as the mean ± standard deviation of three independent experiments. ***P < 0.001.

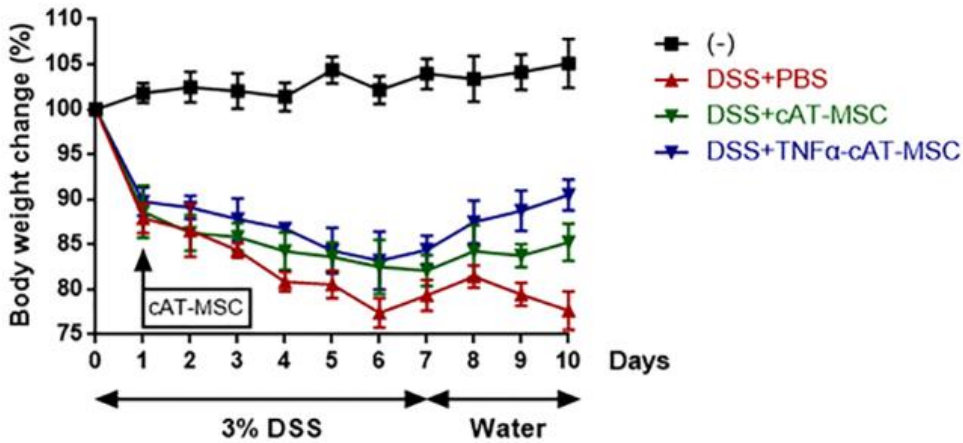

Figure 43. cAT-MSCs stimulated with TNF-α showed enhanced therapeutic effects on dextran sodium sulfate (DSS)-induced colitis in mice. Therapeutic abilities of cAT-MSCs were assessed by body weight change.

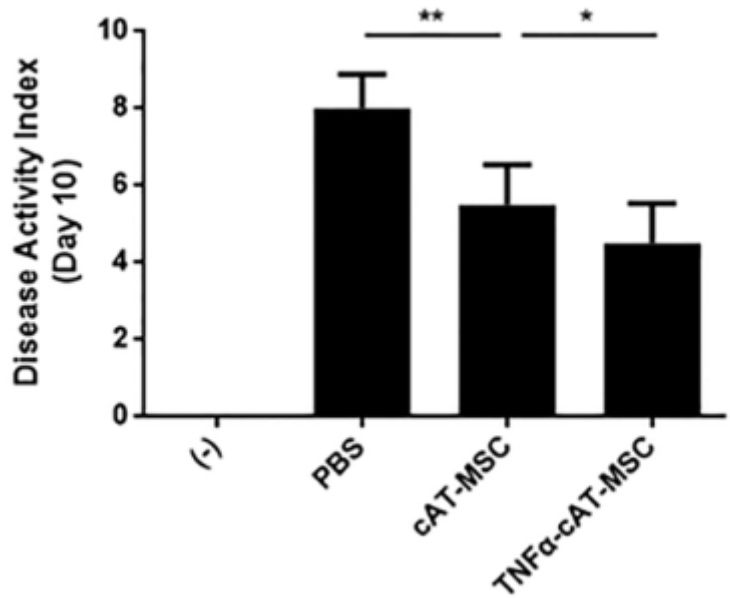

Figure 44. cAT-MSCs stimulated with TNF-α showed enhanced therapeutic effects on dextran sodium sulfate (DSS)-induced colitis in mice. Therapeutic abilities of cAT-MSCs were assessed by disease activity index. Results are shown as the mean ± standard deviation. *P < 0.05, **P < 0.01.

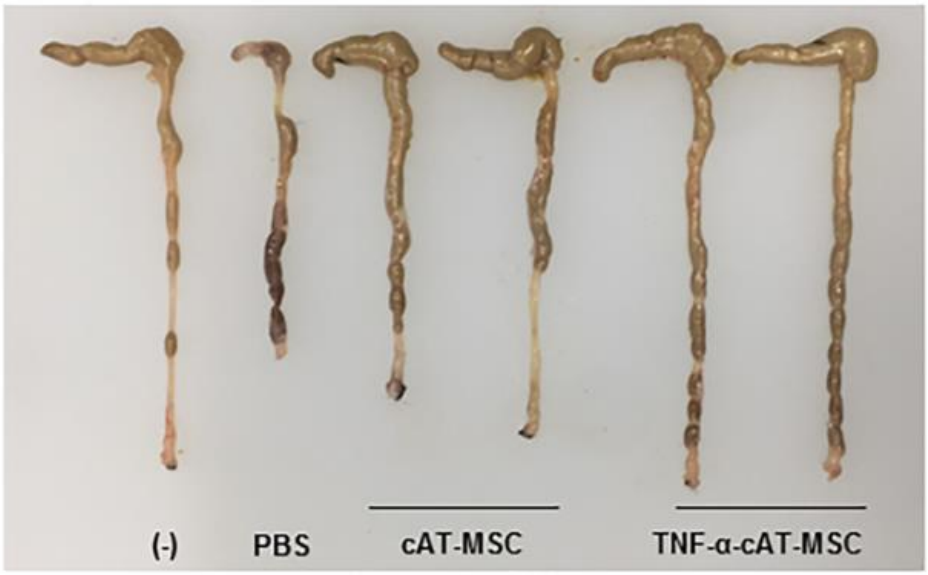

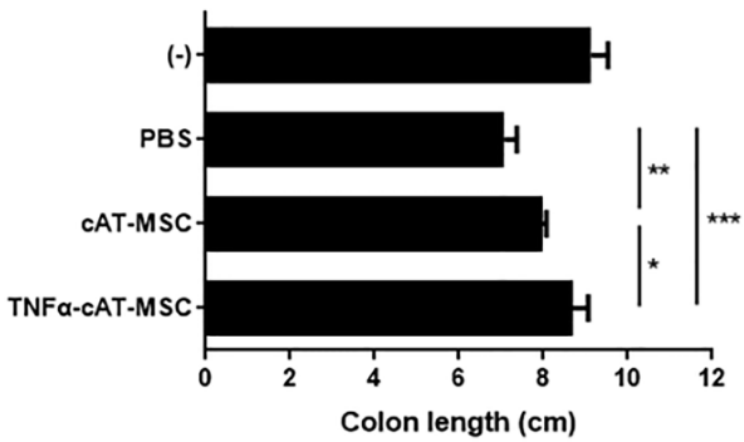

Figure 45. cAT-MSCs stimulated with TNF-α showed enhanced therapeutic effects on dextran sodium sulfate (DSS)-induced colitis in mice. Therapeutic abilities of cAT-MSCs were assessed by colon length. Results are shown as the mean ± standard deviation. *P < 0.05, **P < 0.01, ***P < 0.001.

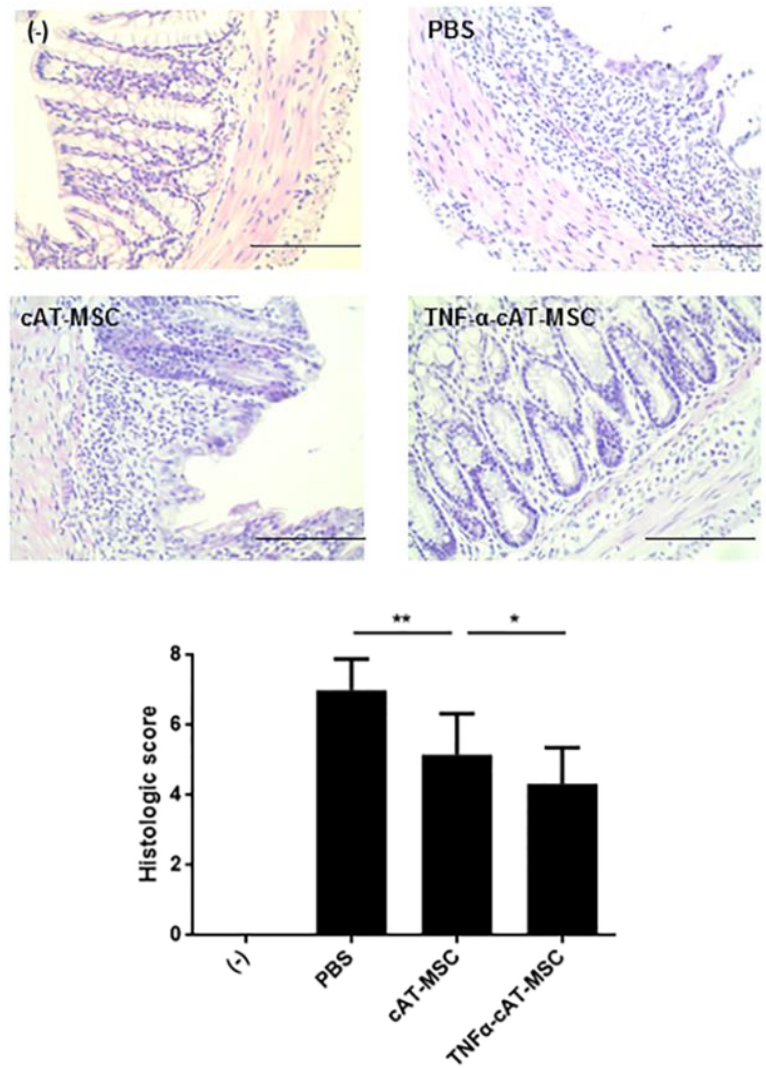

Figure 46. cAT-MSCs stimulated with TNF-α showed enhanced therapeutic effects on dextran sodium sulfate (DSS)-induced colitis in mice. Therapeutic abilities of cAT-MSCs were assessed by histopathologic analysis Results are shown as the mean ± standard deviation. *P < 0.05, **P < 0.01.

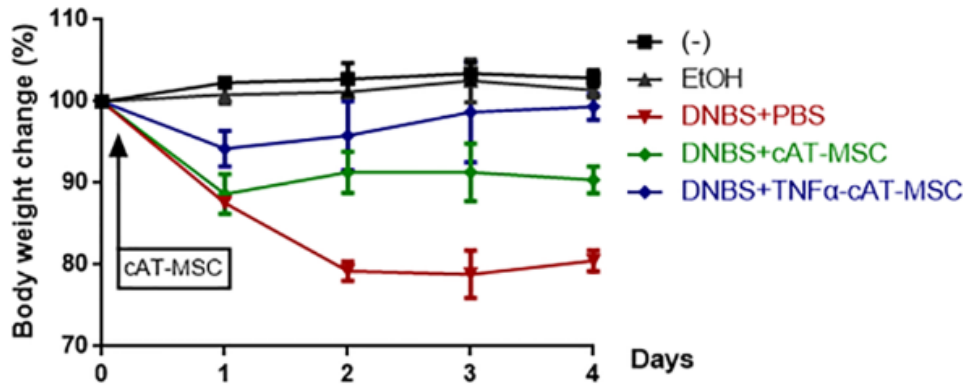

Figure 47. cAT-MSCs stimulated with TNF-α showed enhanced therapeutic effects on dinitrobenzene sulfonic acid (DNBS)-induced colitis in mice. Therapeutic abilities of cAT-MSCs were assessed by body weight change.

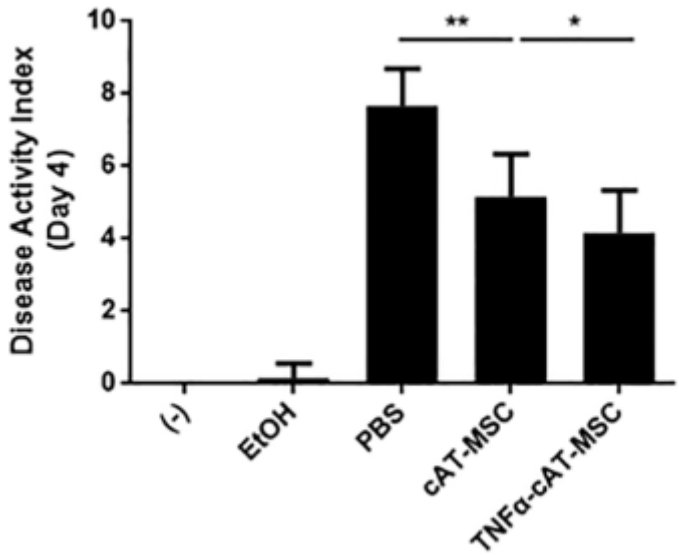

Figure 48. cAT-MSCs stimulated with TNF-α showed enhanced therapeutic effects on dinitrobenzene sulfonic acid (DNBS)-induced colitis in mice. Therapeutic abilities of cAT-MSCs were assessed disease activity index. Results are shown as the mean ± standard deviation. *P < 0.05, **P < 0.01.

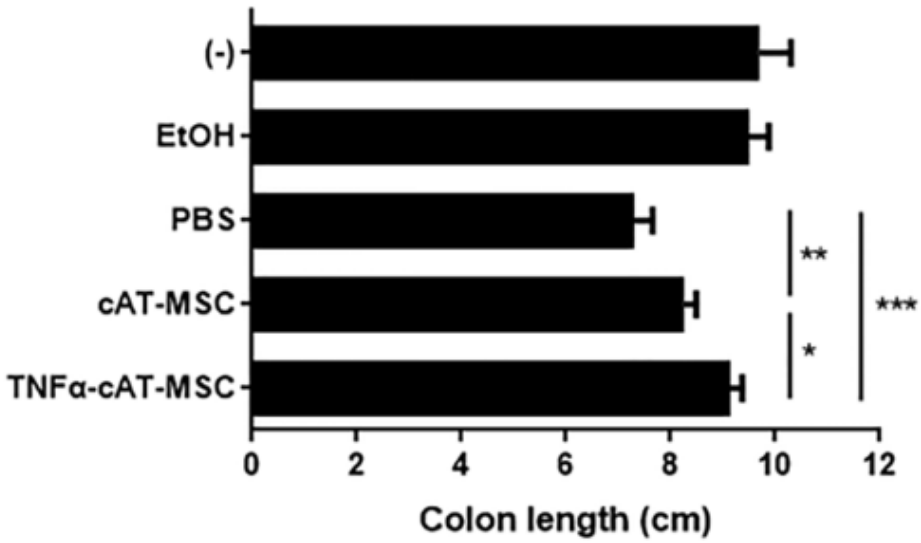

Figure 49. cAT-MSCs stimulated with TNF-α showed enhanced therapeutic effects on dinitrobenzene sulfonic acid (DNBS)-induced colitis in mice. Therapeutic abilities of cAT-MSCs were assessed by colon length. Results are shown as the mean ± standard deviation. *P < 0.05, **P < 0.01, ***P < 0.001.

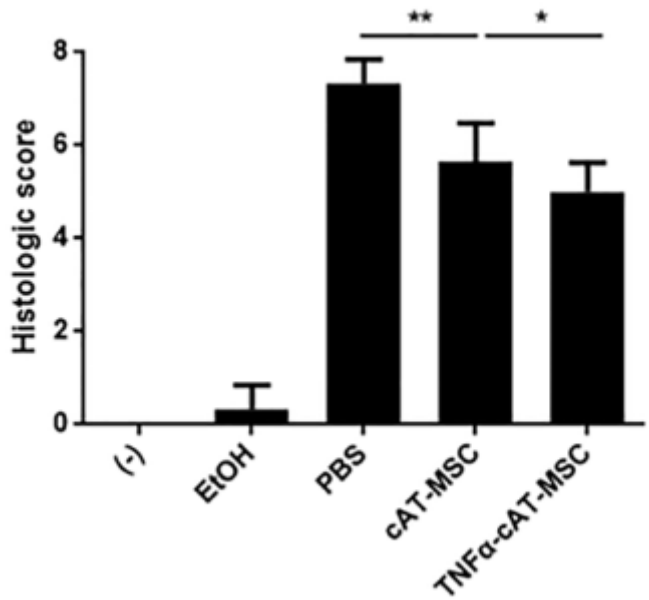

Figure 50. cAT-MSCs stimulated with TNF-α showed enhanced therapeutic effects on dinitrobenzene sulfonic acid (DNBS)-induced colitis in mice. Therapeutic abilities of cAT-MSCs were assessed histopathologic analysis. Results are shown as the mean ± standard deviation. *P < 0.05, **P < 0.01.

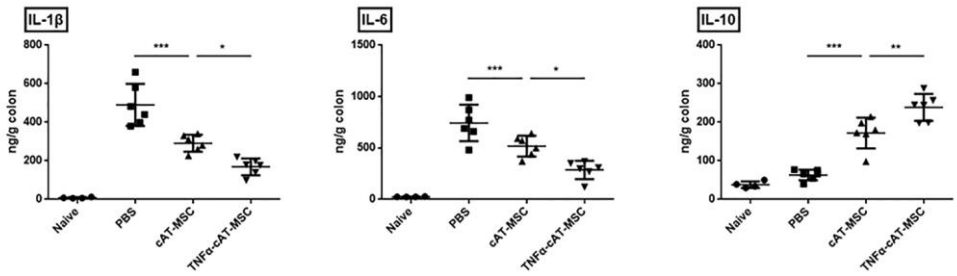

Figure 51. cAT-MSCs stimulated with TNF-α decreased expression of pro-inflammatory cytokines (IL-1β, IL-6) and increased expression of one anti-inflammatory cytokine (IL-10) in colon samples from DSS-induced colitis mice. Results are shown as the mean ± standard deviation. *P < 0.05, **P < 0.01, ***P < 0.001.

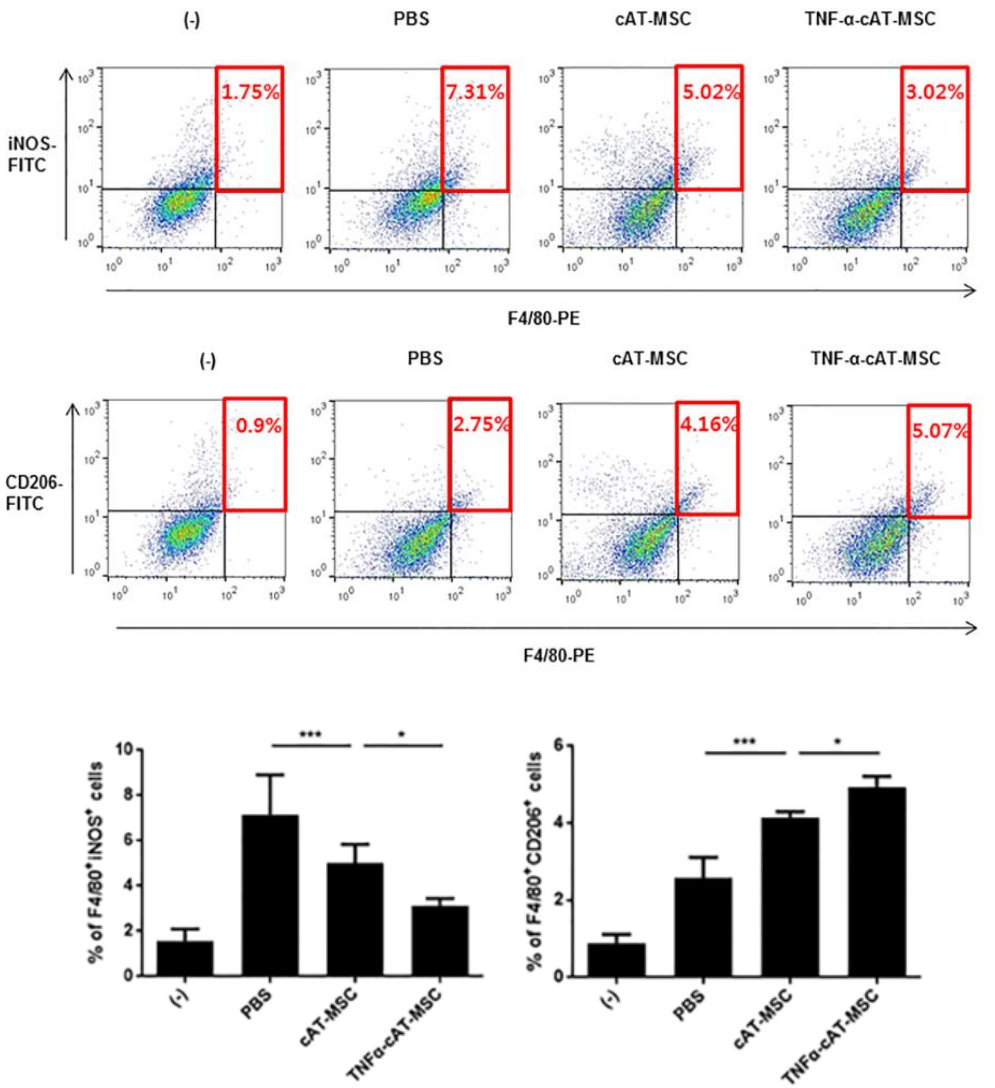

Figure 52. cAT-MSCs stimulated with TNF-α further decreased M1 macrophages ($F4/80^+/iNOS^+$ cells) and increased M2 macrophages ($F4/80^+/CD206^+$ cells) in colons from DSS-induced colitis mice. Results are shown as the mean ± standard deviation. *$P < 0.05$, ***$P < 0.001$.

GENERAL CONCLUSION

The purpose of this study was to investigate the immunomodulatory effects of human or canine adipose tissue-derived mesenchymal stem cells (MSCs) in mouse models of inflammatory bowel disease. First, I assessed the effects of human adipose tissue-derived (hAT)-MSCs on a dextran sulfate sodium (DSS)-induced colitis model in mice, together with the effect on phenotypic switch in macrophages. Additionally, I aimed to elucidate the mechanisms underlying these processes. The second study was designed to evaluate the anti-inflammatory effects and their mechanisms of canine adipose tissue-derived (cAT)-MSCs in a DSS-induced colitis model. In the last study, I used cAT-MSCs stimulated with TNF-α, and revealed the therapeutic effects and their mechanisms in IBD model mice. The conclusions are as follows;

In the first experiment;

1. I showed that the application of hAT-MSCs to DSS-induced colitis mouse model may alleviate the symptoms of this disease, and that the weight loss and disease activity index (DAI) were improved.
2. The intraperitoneally administration of hAT-MSCs modulates the expression of the inflammatory cytokines by inducing the cell

differentiation into M2 macrophages in the colon, alleviation the inflammatory responses.

3. Most of hAT-MSCs administered intraperitoneally might form aggregates in the peritoneal cavity and reduce colitis by inducing M2 macrophages distant from the inflamed colon through secretory factors.
4. TSG-6 secreted by hAT-MSCs plays a crucial role in the regulation of M1 to M2 phenotypic switch *in vitro*.
5. TSG-6 secreted by hAT-MSCs plays an important role in the alteration of macrophages to M2 phenotype in the inflamed mouse colons.

In conclusion, I demonstrated that hAT-MSC-secreted TSG-6 induces the phenotypic switch of macrophages that infiltrated into colon to M2 type, which leads to the regulation of inflammatory cytokine expression and the alleviation of DSS-induced colitis symptoms in mice.

In the second experiment;

1. I showed that TSG-6 secreted from intraperitoneally infused cAT-MSCs may ameliorate the symptoms of DSS-induced colitis and that weight loss and DAI were reduced.

2. TSG-6 released from cAT-MSCs played an important role in modulating inflammatory cytokines such as TNF-α, IL-6, and IL-10 in the colon.
3. Intraperitoneally injected cAT-MSCs formed aggregates in the peritoneal cavity and alleviated DSS-induced colitis at sites distant from the colon through soluble factors, such as TSG-6.
4. TSG-6 secreted from cAT-MSCs contributed to the decrease in the expression levels of M1 markers such as iNOS and IL-6, and the increase in the expression levels of M2 markers such as CD206 *in vitro*.
5. I demonstrated that TSG-6 secreted by cAT-MSCs plays an essential role in the switching phenotype of macrophages from M1 to M2 in the inflamed colon.

In conclusion, I demonstrated that TSG-6 secreted by cAT-MSCs ameliorated DSS-induced colitis in mice by inducing macrophages to switch to the M2 phenotype.

In the third experiment;

1. In this study, I demonstrated that intraperitoneal injection of TNF-α stimulated cAT-MSCs showed higher therapeutic efficacy

compared to naïve cAT-MSCs administration in IBD mice models.

2. I also showed that TNF-α-stimulated cAT-MSCs released significantly higher concentrations of TSG-6 and PGE2, relative to naive cAT-MSCs.
3. TNF-α stimulated cAT-MSCs increased macrophage alteration to M2 phenotype ($F4/80^{+}/CD206^{+}$) in the colons of IBD mice, whereas M1 macrophages ($F4/80^{+}/iNOS^{+}$) were decreased in the inflamed colons.

In conclusion, I demonstrated that TNF-α-stimulated cAT-MSCs further ameliorated IBD via their enhanced anti-inflammatory effects. Additionally, I showed that cAT-MSCs pre-treated with TNF-α could release higher immunomodulatory factors such as TSG-6 and PGE2, which contribute to induce macrophages phenotypic alteration.

REFERENCES

Abdel Salam AG, Ata HM, Salman TM, Rashed LA, Sabry D, Schaalan MF. 2014. Potential therapeutic utility of mesenchymal stem cells in inflammatory bowel disease in mice. *International Immunopharmacololgy*, 22, 515-521

Allenspach K, Rüfenacht S, Sauter S, Gröne A, Steffan J, Strehlau G, Gaschen. 2006. Pharmacokinetics and clinical efficacy of cyclosporine treatment of dogs with steroid-refractory inflammatory bowel disease. *Journal of Veterinary Internal Medicine*, 20, 239-244

Allenspach, K, Wieland, B, Gröne, A, Gaschen, F. 2007. Chronic enteropathies in dogs: evaluation of risk factors for negative outcome. *Journal of Veterinary Internal Medicine*, 21, 700-708

Anderson P, Souza-Moreira L, Morell M, Caro M, O'valle F, Gonzalez-Rey E, Delgado M. 2012. Adipose-derived mesenchymal stromal cells induce immunomodulatory macrophages which protect from experimental colitis and sepsis. *Gut*, gutjnl-2012-302152

Ando Y, Inaba M, Sakaguchi Y, Tsuda M, Quan GK, Omae M, Okazaki K, Ikehara S. 2008. Subcutaneous adipose tissue-derived stem cells facilitate colonic mucosal recovery from 2,4,6-trinitrobenzene sulfonic acid (TNBS)-induced colitis in rats. *Inflammatory Bowel Disease*, 14, 826-838

Bassi Ê J, de Almeida DC, Moraes-Vieira PMM, Câmara. 2012. Exploring the role of soluble factors associated with immune regulatory properties

of mesenchymal stem cells. *Stem Cell Reviews and Reports*, 8, 329-342

Bazhanov N, Ylostalo JH, Bartosh TJ, Tiblow A, Mohammadipoor A, Foskett A, Prockop D. 2016. Intraperitoneally infused human mesenchymal stem cells form aggregates with mouse immune cells and attach to peritoneal organs. *Stem Cell Research & Therapy*, 7, 27

Bouma G, Strober W. 2003. The immunological and genetic basis of inflammatory bowel disease. *Nature Reviews Immunology*, 3, 521-533

Broekman W, Amatngalim GD, de Mooij-Eijk Y, Oostendorp J, Roelofs H, Taube C, Stolk J, Hiemstra. 2016. TNF-α and IL-1β-activated human mesenchymal stromal cells increase airway epithelial wound healing in vitro via activation of the epidermal growth factor receptor. *Respiratory Research*, 17, 3

Carrade Holt DD, Wood JA, Granick JL, Walker NJ, Clark KC, Borjesson DL. 2014. Equine mesenchymal stem cells inhibit T cell proliferation through different mechanisms depending on tissue source. *Stem Cells and Development*, 23, 1258-1265

Castelo-Branco MT, Soares ID, Lopes DV, Buongusto F, Martinusso CA, do Rosario A Jr, Souza SA, Gutfilen B, Fonseca LM, Elia C, Madi K, Schanaider A, Rossi MI, Souza HS. 2012. Intraperitoneal but not intravenous cryopreserved mesenchymal stromal cells home to the inflamed colon and ameliorate experimental colitis. *Plos One*, 7, e33360

Cerquetella M. 2010. Inflammatory bowel disease in the dog: Differences and similarities with humans. *World Journal of Gastroenterology*, 16, 1050-1056

Chae HK, Song WJ, Ahn JO, Li Q, Lee BY, Kweon K, Park SC, Youn HY. 2017. Immunomodulatory effects of soluble factors secreted by feline adipose tissue-derived mesenchymal stem cells. *Veterinary Immunology and Immunopathology*, 191, 22-29

Chávez-Galán L, Olleros ML, Vesin D, Garcia I. 2015. Much more than M1 and M2 macrophages, there are also CD169+ and TCR+ macrophages. *Frontiers in Immunology*, 6, 263

Chen Q-Q, Yan L, Wang C-Z, Wang W-H, Shi H, Su B-B, Zeng Q-H, Du H-T, Wan JJ. 2013. Mesenchymal stem cells alleviate TNBS-induced colitis by modulating inflammatory and autoimmune responses. *World Journal of Gastroenterology*, 19, 4702

Cho DI, Kim MR, Jeong HY, Jeong HC, Jeong MH, Yoon SH, Kim YS, Ahn Y. 2014. Mesenchymal stem cells reciprocally regulate the M1/M2 balance in mouse bone marrow-derived macrophages. *Experimental Molecular Medicine*, 46, e70

Choi EW, Lee M, Song JW, Shin IS, Kim SJ. 2016. Mesenchymal stem cell transplantation can restore lupus disease-associated miRNA expression and Th1/Th2 ratios in a murine model of SLE, *Scientific Reports*, 6, 38237

Choi H, Lee RH, Bazhanov N, Oh JY, Prockop DJ. 2011. Anti-inflammatory protein TSG-6 secreted by activated MSCs attenuates zymosan-

induced mouse peritonitis by decreasing TLR2/NF-kappaB signaling in resident macrophages. *Blood*, 118, 330-338

Cook A, Breitschwerdt E, Levine J, Bunch S, Linn L. 1993. Risk factors associated with acute pancreatitis in dogs: 101 cases (1985-1990). *Journal of the American Veterinary Medical Association*, 203, 673-679

Craig M. 2013 Disease facts: pemphigus foliaceus in the dog and cat. *Companion Animal*, 18, 374-377

Craven M, Simpson J, Ridyard A, Chandler M. 2004. Canine inflammatory bowel disease: retrospective analysis of diagnosis and outcome in 80 cases (1995–2002). *Journal of Small Animal Practice*, 45, 336-342

Danchuk S, Ylostalo JH, Hossain F, Sorge R, Ramsey A, Bonvillain RW, Lasky JA, Bunnell BA, Welsh DA, Prockop D. 2011. Human multipotent stromal cells attenuate lipopolysaccharide-induced acute lung injury in mice via secretion of tumor necrosis factor-α-induced protein 6. *Stem Cell Research & Therapy*, 2, 1

da Silva Meirelles L, Chagastelles PC, Nardi NB. 2006. Mesenchymal stem cells reside in virtually all post-natal organs and tissues. *Journal of Cell Science*, 119, 2204-2213

Dominici M, Le Blanc K, Mueller I, Slaper-Cortenbach I, Marini F, Krause D, Deans R, Keating A, Prockop D, Horwitz E. 2006. Minimal criteria for defining multipotent mesenchymal stromal cells. *The International Society for Cellular Therapy position statement Cytotherapy*, 8, 315-317

Dossin O, Lavoue R. 2011. Protein-losing enteropathies in dogs Veterinary Clinics of North America. *Small Animal Practice*, 41, 399-418

Fan H, Zhao G, Liu L, Liu F, Gong W, Liu X, Yang L, Wang J, Hou Y. 2012. Pre-treatment with IL-1β enhances the efficacy of MSC transplantation in DSS-induced colitis. *Cellular and Molecular Immunology* 9, 473

Geng Y, Zhang L, Fu B, Zhang J, Hong Q, Hu J, Li D, Luo C, Cui S, Zhu F. 2014. Mesenchymal stem cells ameliorate rhabdomyolysis-induced acute kidney injury via the activation of M2 macrophages. *Stem Cell Research & Therapy*, 5, 1

Gomez SM, Morris DO, Rosenbaum MR, Goldschmidt MH. 2004. Outcome and complications associated with treatment of pemphigus foliaceus in dogs: 43 cases (1994–2000). *Journal of American Veterinary Medical Association*, 224, 1312-1316

Gonzalez-Rey E, Gonzalez MA, Rico L, Buscher D, Delgado M. 2009. Human adult stem cells derived from adipose tissue protect against experimental colitis and sepsis. *Gut*, 58, 929-939

Gonzalez MA, Gonzalez-Rey E, Rico L, Buscher D, Delgado M. 2009. Adipose-derived mesenchymal stem cells alleviate experimental colitis by inhibiting inflammatory and autoimmune responses. *Gastroenterology*, 136, 978-989

Gonzalo-Gil E, Perez-Lorenzo MJ, Galindo M, Diaz de la Guardia R, Lopez-Millan B, Bueno C, Menendez P, Pablos JL, Criado G. 2016. Human embryonic stem cell-derived mesenchymal stromal cells ameliorate

collagen-induced arthritis by inducing host-derived indoleamine 2,3 dioxygenase. *Arthritis Research & Therapy*, 18, 77

Gross TL, Ihrke PJ, Walder EJ, Affolter VK. 2008. Skin diseases of the dog and cat: clinical and histopathologic diagnosis. *John Wiley & Sons*

Hall M, Rosenkrantz WS, Hong J, Griffin CE, Mendelsohn CJ. 2010. Evaluation of the potential use of adipose-derived mesenchymal stromal cells in the treatment of canine atopic dermatitis: a pilot study. *Veterinary Therapeutics*, 11, 1-14

He Z, Hua J, Qian D, Gong J, Lin S, Xu C, Wei G, Meng H, Yang T, Zhou B. 2016. Intravenous hMSCs Ameliorate Acute Pancreatitis in Mice via Secretion of Tumor Necrosis Factor-α Stimulated Gene/Protein 6. *Scientific Reports*, 6, 38438

Heo SC, Jeon ES, Lee IH, Kim HS, Kim MB, Kim JH. 2011. Tumor necrosis factor-α-activated human adipose tissue–derived mesenchymal stem cells accelerate cutaneous wound healing through paracrine mechanisms. *Journal of Investigative Dermatology*, 131, 1559-1567

Hess R, Saunders H, Van TW, Shofer F, Washabau R. 1998. Clinical, clinicopathologic, radiographic, and ultrasonographic abnormalities in dogs with fatal acute pancreatitis: 70 cases (1986-1995). *Journal of the American Veterianry Medical Association*, 213, 665-670

Hillier A, Griffin C. 2001. The ACVD task force on canine atopic dermatitis (I): incidence and prevalence. *Veterinary Immunology and Immunopathology*, 81, 147-151

Iyer SS, Rojas MJ. 2008. Anti-inflammatory effects of mesenchymal stem cells: novel concept for future therapies. *Expert Opinion on Biological Therapy*, 8, 569-581

Jang S-E, Han MJ, Kim S-Y, Kim D-H. 2014. Lactobacillus plantarum CLP-0611 ameliorates colitis in mice by polarizing M1 to M2-like macrophages. *International Immunopharmacology*, 21, 186-192

Jergens AE, Schreiner CA, Frank DE, Niyo Y, Ahrens FE, Eckersall P, Benson TJ, Evans RJ. 2003. A scoring index for disease activity in canine inflammatory bowel disease. *Journal of Veterinary Internal Medicine*, 17, 291-297

Jung KH, Song SU, Yi T, Jeon MS, Hong SW, Zheng HM, Lee HS, Choi MJ, Lee DH, Hong SS. 2011. Human bone marrow-derived clonal mesenchymal stem cells inhibit inflammation and reduce acute pancreatitis in rats. *Gastroenterology*, 140, 998-1008

Kang JW, Kang K-S, Koo HC, Park JR, Choi EW, Park YH. 2008. Soluble factors–Mediated immunomodulatory effects of canine adipose tissue–derived mesenchymal stem cells. *Stem Cells and Development*, 17, 681-694

Kennelly H, Mahon BP, English K. 2016. Human mesenchymal stromal cells exert HGF dependent cytoprotective effects in a human relevant pre-clinical model of COPD. *Scientific Reports*, 6, 38207

Kern S, Eichler H, Stoeve J, Klüter H, Bieback K. 2006. Comparative analysis of mesenchymal stem cells from bone marrow, umbilical cord blood, or adipose tissue. *Stem Cells*, 24, 1294-1301

Kim HS, Lee JH, Roh KH, Jun HJ, Kang KS, Kim TY. 2017. Clinical Trial of Human Umbilical Cord Blood-Derived Stem Cells for the Treatment of Moderate-to-Severe Atopic Dermatitis: Phase I/IIa Studies. *Stem Cells*, 35, 248-255

Kim HS, Shin TH, Lee BC, Yu KR, Seo Y, Lee S, Seo MS, Hong IS, Choi SW, Seo KW, Nunez G, Park JH, Kang KS. 2013. Human umbilical cord blood mesenchymal stem cells reduce colitis in mice by activating NOD2 signaling to COX2. *Gastroenterology*, 145, 1392-1403

Kim HS, Yun JW, Shin TH, Lee SH, Lee BC, Yu KR, Seo Y, Lee S, Kang TW, Choi SW, Seo KW, Kang KS. 2015. Human umbilical cord blood mesenchymal stem cell-derived PGE2 and TGF-beta1 alleviate atopic dermatitis by reducing mast cell degranulation. *Stem Cells*, 33, 1254-1266

Kim HW, Song WJ, Li Q, Han SM, Jeon KO, Park SC, Ryu MO, Chae HK, Kyeong K, Youn HY. 2016. Canine adipose tissue-derived mesenchymal stem cells ameliorate severe acute pancreatitis by regulating T cells in rats. *Journal of Veterinary Science*, 17, 539-548

Knights D, Lassen KG, Xavier RJ. 2013. Advances in inflammatory bowel disease pathogenesis: linking host genetics and the microbiome. *Gut*, 62, 1505-1510

Le Blanc K, Tammik C, Rosendahl K, Zetterberg E, Ringdén O. 2003. HLA expression and immunologic propertiesof differentiated and undifferentiated mesenchymal stem cells. *Experimental Hematology*, 31, 890-896

Lee JW, Fang X, Krasnodembskaya A, Howard JP, Matthay MA. 2011. Concise review: Mesenchymal stem cells for acute lung injury: role of paracrine soluble factors. *Stem Cells*, 29, 913-919

Lee RH, Pulin AA, Seo MJ, Kota DJ, Ylostalo J, Larson BL, Semprun-Prieto L, Delafontaine P, Prockop D. 2009. Intravenous hMSCs improve myocardial infarction in mice because cells embolized in lung are activated to secrete the anti-inflammatory protein TSG-6. *Cell Stem Cell*, 5, 54-63

Legaki E, Roubelakis M, Theodoropoulos G, Lazaris A, Kollia A, Karamanolis G, Marinos E, Gazouli M. 2016. Therapeutic potential of secreted molecules derived from human amniotic fluid mesenchymal stem/stroma cells in a mice model of colitis. *Stem Cell Reviews and Reports*, 12, 604-612

Liang L, Dong C, Chen X, Fang Z, Xu J, Liu M, Zhang X, Gu DS, Wang D, Du W, Zhu D, Han ZC. 2011. Human umbilical cord mesenchymal stem cells ameliorate mice trinitrobenzene sulfonic acid (TNBS)-induced colitis. *Cell Transplant*, 20, 1395-1408

Liu L, Song H, Duan H, Chai J, Yang J, Li X, Yu Y, Zhang X, Hu X, Xiao M. 2016. TSG-6 secreted by human umbilical cord-MSCs attenuates severe burn-induced excessive inflammation via inhibiting activations of P38 and JNK signaling. *Scientific Reports*, 6, 30121

Liu W, Zhang S, Gu S, Sang L, Dai C. 2015. Mesenchymal stem cells recruit macrophages to alleviate experimental colitis through TGFbeta1. *Cellular Physiology and Biochemistry*, 35, 858-865

Liu Y, Mu R, Wang S, Long L, Liu X, Li R, Sun J, Guo J, Zhang X, Guo J. 2010. Therapeutic potential of human umbilical cord mesenchymal stem cells in the treatment of rheumatoid arthritis. *Arthritis Research & Therapy*, 12, 1

Locati M, Mantovani A, Sica A. 2012. Macrophage activation and polarization as an adaptive component of innate immunity. *Advances in Immunology*, 120, 163-184

Lopez-Santalla M, Mancheño-Corvo P, Menta R, Lopez-Belmonte J, DelaRosa O, Bueren JA, Dalemans W, Lombardo E, Garin MI. 2015. Human Adipose-Derived Mesenchymal Stem Cells Modulate Experimental Autoimmune Arthritis by Modifying Early Adaptive T Cell Responses. *Stem Cells*, 33, 3493-3503

Maeda S, Ohno K, Fujiwara-Igarashi A, Uchida K, Tsujimoto H. 2016. Changes in Foxp3-Positive Regulatory T Cell Number in the Intestine of Dogs With Idiopathic Inflammatory Bowel Disease and Intestinal Lymphoma. *Veterinary Pathololog*y, 53, 102-112

Manichanh C, Borruel N, Casellas F, Guarner F. 2012. The gut microbiota in IBD. *Nature Reviews Gastroenterology and Hepatology*, 9, 599-608

Mansfield C. 2012. Acute pancreatitis in dogs: advances in understanding, diagnostics, and treatment. *Veterinary Immunology and Immunopatholgy*, 27, 123-132

Mantovani A, Biswas SK, Galdiero MR, Sica A, Locati M. 2013. Macrophage plasticity and polarization in tissue repair and remodelling. *The Journal of Pathology*, 229, 176-185

Mao F, Tu Q, Wang L, Chu F, Li X, Li H Xu S. 2017. Mesenchymal stem cells and their therapeutic applications in inflammatory bowel disease. *Oncotarget*, 8, 38008

Martinez FO, Gordon S, Locati M, Mantovani A. 2006. Transcriptional profiling of the human monocyte-to-macrophage differentiation and polarization: new molecules and patterns of gene expression. *The Journal of Immunology*, 177, 7303-7311

Medleau L, Hnilica K. 2006. Small animal dermatology–a color atlas and therapeutic guide. *Saunders Elsevier*

Melief SM, Schrama E, Brugman MH, Tiemessen MM, Hoogduijn MJ, Fibbe WE, Roelofs. 2013. Multipotent stromal cells induce human regulatory T cells through a novel pathway involving skewing of monocytes toward anti-inflammatory macrophages. *Stem Cells*, 31, 1980-1991

Mittal M, Tiruppathi C, Nepal S, Zhao Y-Y, Grzych D, Soni D, Prockop DJ, Malik AB. 2016. TNFα-stimulated gene-6 (TSG6) activates macrophage phenotype transition to prevent inflammatory lung injury. *Proceedings of the National Academy of Sciences*, 113, E8151-E8158

Momin E, Mohyeldin A, Zaidi H, Vela G, Quiñones-Hinojosa A. 2010. Mesenchymal stem cells: new approaches for the treatment of neurological diseases. *Current Stem Cell Research & Therapy*, 5, 326-344

Montemurro T, Viganò M, Ragni E, Barilani M, Parazzi V, Boldrin V, Lavazza C, Montelatici E, Banfi F, Lauri E. 2016. Angiogenic and

anti-inflammatory properties of mesenchymal stem cells from cord blood: soluble factors and extracellular vesicles for cell regeneration. *European Journal of Cell Biology*, 95, 228-238

Morris R. 1994. Modes of action of FK506, cyclosporin A, and rapamycin. *Transplantation proceedings*, 3272

Mosser DM, Edwards. 2008. Exploring the full spectrum of macrophage activation. *Nature Reviews Immunology*, 8, 958

Murray PJ, Wynn TA. 2011. Protective and pathogenic functions of macrophage subsets. *Nature Reviews Immunology*, 11, 723-737

Nakagawa Y, Muneta T, Kondo S, Mizuno M, Takakuda K, Ichinose S, Tabuchi T, Koga H, Tsuji K, Sekiya. 2015. Synovial mesenchymal stem cells promote healing after meniscal repair in microminipigs. *Osteoarthritis and Cartilage*, 23, 1007-1017

Nakajima H, Uchida K, Guerrero AR, Watanabe S, Sugita D, Takeura N, Yoshida A, Long G, Wright KT, Johnson WE, Baba H. 2012. Transplantation of mesenchymal stem cells promotes an alternative pathway of macrophage activation and functional recovery after spinal cord injury. *Journal of Neurotrauma*, 29, 1614-1625

Neurath MF. 2014. Cytokines in inflammatory bowel disease. *Nature Reviews Immunology*, 14, 329-342

Nishikawa K, Seo N, Torii M, Ma N, Muraoka D, Tawara I, Masuya M, Tanaka K, Takei Y, Shiku H. 2014. Interleukin-17 induces an atypical m2-like macrophage subpopulation that regulates intestinal inflammation. *Plos One*, 9, e108494

Norman J. 1998. The role of cytokines in the pathogenesis of acute pancreatitis. *The American Journal of Surgery*, 175, 76-83

Pandiyan P, Zheng L, Ishihara S, Reed J, Lenardo M. 2007. CD4+ CD25+ Foxp3+ regulatory T cells induce cytokine deprivation–mediated apoptosis of effector CD4+ T cells. *Nature Immunology*, 8, 1353

Parekkadan B, Upadhyay R, Dunham J, Iwamoto Y, Mizoguchi E, Mizoguchi A, Weissleder R, Yarmush M. 2011. Bone marrow stromal cell transplants prevent experimental enterocolitis and require host CD11b+ splenocytes. *Gastroenterology*, 140, 966-975 e964

Perez-Merino EM, Uson-Casaus JM, Zaragoza-Bayle C, Duque-Carrasco J, Marinas-Pardo L, Hermida-Prieto M, Barrera-Chacon R, Gualtieri M. 2015. Safety and efficacy of allogeneic adipose tissue-derived mesenchymal stem cells for treatment of dogs with inflammatory bowel disease: Clinical and laboratory outcomes. *The Veterinary Journal*, 206, 385-390

Prockop DJ, Oh JY. 2012. Mesenchymal stem/stromal cells (MSCs): role as guardians of inflammation. *Molecular Therapy*, 20, 14-20

Qi Y, Jiang D, Sindrilaru A, Stegemann A, Schatz S, Treiber N, Rojewski M, Schrezenmeier H, Vander Beken S, Wlaschek M, Bohm M, Seitz A, Scholz N, Durselen L, Brinckmann J, Ignatius A, Scharffetter-Kochanek K. 2014. TSG-6 released from intradermally injected mesenchymal stem cells accelerates wound healing and reduces tissue fibrosis in murine full-thickness skin wounds. *Journal of Investigative Dermatology*, 134, 526-537

Roddy GW, Oh JY, Lee RH, Bartosh TJ, Ylostalo J, Coble K, Rosa RH Jr, Prockop DJ. 2011. Action at a distance: systemically administered adult stem/progenitor cells (MSCs) reduce inflammatory damage to the cornea without engraftment and primarily by secretion of TNF-alpha stimulated gene/protein 6. *Stem Cells*, 29, 1572-1579

Romanov YA, Svintsitskaya VA, Smirnov VN. 2003. Searching for alternative sources of postnatal human mesenchymal stem cells: candidate MSC-like cells from umbilical cord. *Stem Cells*, 21, 105-110

Sala E, Genua M, Petti L, Anselmo A, Arena V, Cibella J, Zanotti L, D'Alessio S, Scaldaferri F, Luca G. 2015. Mesenchymal stem cells reduce colitis in mice via release of TSG6, independently of their localization to the intestine. *Gastroenterology*, 149, 163-176 e120

Sémont A, François S, Mouiseddine M, François A, Saché A, Frick J, Thierry D, Chapel A. 2006. Mesenchymal stem cells increase self-renewal of small intestinal epithelium and accelerate structural recovery after radiation injury. *Tissue Engineering Springer*, 19-30

Shin T-H, Lee B-C, Choi SW, Shin J-H, Kang I, Lee JY, Kim J-J, Lee H-K, Jung J-E, Choi Y-W. 2017. Human adipose tissue-derived mesenchymal stem cells alleviate atopic dermatitis via regulation of B lymphocyte maturation. *Oncotarget*, 8, 512-522

Shin TH, Kim HS, Kang TW, Lee BC, Lee HY, Kim YJ, Shin JH, Seo Y, Choi, SW, Lee S, Shin K, Seo KW, Kang KS. 2016. Human umbilical cord blood-stem cells direct macrophage polarization and block

inflammasome activation to alleviate rheumatoid arthritis. *Cell Death and Disease*, 7, e2524

Sica A, Erreni M, Allavena P, Porta C. 2015. Macrophage polarization in pathology. *Cellular and Molecular Life Sciences*, 72, 4111-4126

Silini A, Parolini O, Huppertz B, Lang I. 2013. Soluble factors of amnion-derived cells in treatment of inflammatory and fibrotic pathologies. *Current Stem Cell Research & Therapy*, 8, 6-14

Song JY, Kang HJ, Hong JS, Kim CJ, Shim JY, Lee CW, Choi J. 2017. Umbilical cord-derived mesenchymal stem cell extracts reduce colitis in mice by re-polarizing intestinal macrophages. *Scientific Reports*, 7, 9412

Soontararak S, Chow L, Johnson V, Coy J, Wheat W, Regan D, Dow S. 2018. Mesenchymal stem cells (MSCs) derived from induced pluripotent stem cells equivalent to adipose-derived MSC in promoting intestinal healing and microbiome normalization in mouse inflammatory bowel disease model. *Stem Cells*, 7, 456-467

Stout RD, Suttles JJ. 2004. Functional plasticity of macrophages: reversible adaptation to changing microenvironments. *Journal of Leukocyte Biology*, 76, 509-513

Tanaka F, Tominaga K, Ochi M, Tanigawa T, Watanabe T, Fujiwara Y, Ohta K, Oshitani N, Higuchi K, Arakawa. 2008. Exogenous administration of mesenchymal stem cells ameliorates dextran sulfate sodium-induced colitis via anti-inflammatory action in damaged tissue in rats. *Life Science*, 83, 771-779

Teng X, Chen L, Chen W, Yang J, Yang Z, Shen Z. 2015. Mesenchymal stem cell-derived exosomes improve the microenvironment of infarcted myocardium contributing to angiogenesis and anti-inflammation. *Cellular Physiology and Biochemistry*, 37, 2415-2424

Tsuda H, Yamahara K, Otani K, Okumi M, Yazawa K, Kaimori J, Taguchi A, Kangawa K, Ikeda T, Takahara S. 2014. Transplantation of allogenic fetal membrane-derived mesenchymal stem cells protects against ischemia/reperfusion-induced acute kidney injury. *Cell Transplantation*, 23, 889-899

Uccelli A, Moretta L, Pistoia V. 2008. Mesenchymal stem cells in health and disease. *Nature Reviews Immunology*, 8, 726

Valcz G, Krenács T, Sipos F, Leiszter K, Tóth K, Balogh Z, Csizmadia A, Műzes G, Molnár B, Tulassay Z. 2011. The role of the bone marrow derived mesenchymal stem cells in colonic epithelial regeneration. *Pathology Oncology Research*, 17, 11-16

van Beelen Granlund A, Flatberg A, Ø stvik AE, Drozdov I, Gustafsson BI, Kidd M, Beisvag V, Torp, SH, Waldum, HL, Martinsen, TC. 2013. Whole genome gene expression meta-analysis of inflammatory bowel disease colon mucosa demonstrates lack of major differences between Crohn's disease and ulcerative colitis. *Plos One*, 8, e56818

van den Broek LJ, Kroeze KL, Waaijman T, Breetveld M, Sampat-Sardjoepersad SC, Niessen FB, Middelkoop E, Scheper RJ, Gibbs S. 2013. Differential response of human adipose tissue-derived mesenchymal stem cells, dermal fibroblasts, and keratinocytes to burn

wound exudates: potential role of skin-specific chemokine CCL27. *Tissue Engineering Part A*, 20, 197-209

Vasandan AB, Jahnavi S, Shashank C, Prasad P, Kumar A, Prasanna SJ. 2016. Human Mesenchymal stem cells program macrophage plasticity by altering their metabolic status via a PGE2-dependent mechanism. *Scientific Reports*, 6, 38308

Viana KF, Aguiar-Soares RD, Roatt BM, Resende LA, Silveira-Lemos D, Correa-Oliveira R, Martins-Filho OA, Moura SL, Zanini MS, Silva MS, Reis AB, Giunchetti RC. 2013. Analysis using canine peripheral blood for establishing in vitro conditions for monocyte differentiation into macrophages for Leishmania chagasi infection and T-cell subset purification. *Veterinary Parasitology*, 198, 62

Wang C, Chen J, Sun L, Liu Y. 2014. TGF-beta signaling-dependent alleviation of dextran sulfate sodium-induced colitis by mesenchymal stem cell transplantation. *Molecular Biology Reports*, 41, 4977-4983

Wang M, Liang C, Hu H, Zhou L, Xu B, Wang X, Han Y, Nie Y, Jia S, Liang J. 2016. Intraperitoneal injection (IP), Intravenous injection (IV) or anal injection (AI)? Best way for mesenchymal stem cells transplantation for colitis. *Scientific Reports*, 6, 30696

Wang N, Li Q, Zhang L, Lin H, Hu J, Li D, Shi S, Cui S, Zhou J, Ji J, Wan J, Cai G, Chen X. 2012. Mesenchymal stem cells attenuate peritoneal injury through secretion of TSG-6. *Plos One*, 7, e43768

Wang Y, Chen X, Cao W, Sh, Y. 2014. Plasticity of mesenchymal stem cells in immunomodulation: pathological and therapeutic implications. *Nature Immunology*, 15, 1009-1016

Wang Y, Wang Y, Zheng G, Lee V, Ouyang L, Chang D, Mahajan D, Coombs J, Wang Y, Alexander S. 2007. Ex vivo programmed macrophages ameliorate experimental chronic inflammatory renal disease. *Kidney International*, 72, 290-299

Wise AF, Williams TM, Kiewiet MB, Payne NL, Siatskas C, Samuel CS, Ricardo SD. 2014. Human mesenchymal stem cells alter macrophage phenotype and promote regeneration via homing to the kidney following ischemia-reperfusion injury. *American Journal of Physiology-Renal Physiology*, 306, F1222-1235

Whitcomb DC, Gorry MC, Preston RA, Furey W, Sossenheimer MJ, Ulrich CD, Martin SP, Gates LK, Amann ST, Toskes PP. 1996. Hereditary pancreatitis is caused by a mutation in the cationic trypsinogen gene. *Nature Genetics*, 14, 141

White SD, Carlotti DN, Pin D, Bonenberger T, Ihrke PJ, Monet E, Nishifuji K, Iwasaki T, Papich M. 2002. Putative drug-related pemphigus foliaceus in four dogs. *Veterinary Dermatology*, 13, 195-202

Wu Y, Chen L, Scott PG, Tredget EE. 2007. Mesenchymal stem cells enhance wound healing through differentiation and angiogenesis. *Stem Cells*, 25, 2648-2659

Wynn TA, Chawla A, Pollard JW. 2013. Macrophage biology in development, homeostasis and disease. *Nature*, 496, 445-455

Yang FY, Chen R, Zhang X, Huang B, Tsang LL, Li X, Jiang X. 2018a. Preconditioning Enhances the Therapeutic Effects of Mesenchymal Stem Cells on Colitis Through PGE2-Mediated T-Cell Modulation. *Cell Transplantation*, 27, 1352-1367

Yang H-M, Song W-J, Li Q, Kim S-Y, Kim H-J, Ryu M-O, Ahn J-O, Youn H-Y. 2018b. Canine mesenchymal stem cells treated with TNF-α and IFN-γ enhance anti-inflammatory effects through the COX-2/PGE2 pathway. *Research in Veterinary Science*, 119, 19-26

Ylöstalo JH, Bartosh TJ, Coble K, Prockop DJ. 2012. Human mesenchymal stem/stromal cells cultured as spheroids are self-activated to produce prostaglandin E2 that directs stimulated macrophages into an anti-inflammatory phenotype. *Stem Cells*, 30, 2283-2296

Zhang Q, Atsuta I, Liu S, Chen C, Shi S, Shi S, Le AD. 2013. IL-17-mediated M1/M2 macrophage alteration contributes to pathogenesis of bisphosphonate-related osteonecrosis of the jaws. *Clinical Cancer Research*, 19, 3176-3188

Zhang QZ, Su WR, Shi SH, Wilder-Smith P, Xiang AP, Wong A, Nguyen AL, Kwon CW, Le AD. 2010. Human gingiva-derived mesenchymal stem cells elicit polarization of m2 macrophages and enhance cutaneous wound healing. *Stem Cells*, 28, 1856-1868

Zhu W, Yu J, Nie Y, Shi X, Liu Y, Li F, Zhang XL. 2014. Disequilibrium of M1 and M2 macrophages correlates with the development of experimental inflammatory bowel diseases. *Immunological Investigations*, 43, 638-652

국 문 초 록

염증성 장질환 마우스 모델에서 사람과 개의 지방유래 중간엽줄기세포가 분비하는 TSG-6 에 의한 대식세포 표현형 조절

송우진
(지도교수 윤화영)

서울대학교 대학원
수의과대학 임상수의학 (수의내과학) 전공

염증성 장 질환은 삶의 질을 떨어뜨리는 난치성 자가 면역 질환이다. 스테로이드와 같은 전신적 면역 억제제나 항 TNF-α 약물인 infliximab 등의 약물이 사용되나, 해당 약물에 반응이 미비하거나 없는 경우도 있다. 따라서 염증이 있는 조직에서 염증 인자의 조절을 통해 염증을 완화시키는 역할을 하는 중간엽줄기세포는 인의와 수의에서 염증성 장질환의 치료 대안 중 하나로 촉망받고 있다. 게다가, tumor necrosis factor-alpha-induced gene/protein-6 (TSG-6)와 같은 중간엽줄기세포가 분비하는 염증 조절 인자가 중요한 역할을 담당함이 잘 알려져 있다. 그러나, 사람과 개의 지방유래 중간엽줄기세포가 분비하는 염증 조절

인자들이 염증성 장질환에서 어떠한 기전으로 증상을 완화시키는지 자세히 알려져 있지 않다. 따라서, 이번 연구의 목표는 사람과 개의 지방유래 중간엽줄기세포를 이용해 염증성 장질환 생쥐 모델에서의 치료 효과를 평가하고, 그 기전에 대해서 연구하는 것이다.

이 학위 논문은 세 부분으로 나눌 수 있다.

첫번째 부분에서는 dextran sulfate sodium (DSS)에 의해 대장염이 유발된 생쥐에서 사람 지방유래 중간엽줄기세포의 치료 효과와 그 기전에 대하여 연구하였다. DSS 의 투여로 대장염이 유발된 생쥐에 사람 지방유래 중간엽줄기세포를 복강내 투여한 후, 열흘 째 되는 날에 부검을 하여 대장 조직을 얻었다. 투여한 사람 지방유래 중간엽줄기세포는 대장 조직에서 M2 대식세포의 발현양을 증가시키며, 염증 사이토카인의 발현 정도를 조절하였다. 대장으로 이주한 줄기세포의 양적 분석을 위한 real-time PCR 검사에서, 주입한 전체 줄기세포의 0.001%에 해당하는 20 개 미만의 세포가 확인되었다. 따라서 이러한 치료 효과가 분비 인자의 영향을 크게 받은 것이라 가정할 수 있었다. 생체 외 실험을 통해 사람 유래 중간엽줄기세포의 분비 인자에 대한 치료 효과를 평가하기 위해 transwell co-culture 시스템을 사용하였다. 이를 통해 사람 지방유래 중간엽줄기세포에서 분비하는 tumor necrosis factor-alpha-induced gene/protein 6 (TSG-6)가 M2 대식세포의 증가를 유도함을 확인하였다. 또한, 생쥐를 이용한 실험을 통해 복강 내로

투여한 TSG-6 에 대한 small interfering RNA (siRNA) 처리를 한 중간엽줄기세포를 투여하였을 때에는 M2 대식세포의 유도 및 염증성 장질환의 치료 효과가 관찰되지 않음을 확인하였다. 이를 통해, 사람 지방유래 중간엽줄기세포에서 분비되는 TSG-6 가 DSS 로 유발된 생쥐 장 염증성 장질환 모델에서 M2 대식세포의 증가 유도 및 증상의 완화에 중요한 역할을 함을 증명하였다.

두번째 부분에서는 개 지방유래 중간엽줄기세포에서 분비되는 TSG-6 가 생쥐 염증성 장질환 모델에서 증상의 완화 및 염증의 감소에 어떠한 역할을 하는지 연구하였다. 생체 외 실험에서 개 지방유래 중간엽줄기세포가 분비하는 TSG-6 의 효과를 확인하기 위해, transwell co-culture 시스템을 이용하였다. 개 지방유래 중간엽줄기세포에서 분비한 TSG-6 가 M1 으로 유도된 개 대식세포를 M2 대식세포로 전환하는 것을 확인할 수 있었다. 이러한 M2 대식세포의 증가는 생쥐 모델의 대장에서도 확인할 수 있었다.

마지막 부분에서는 TNF-α 로 자극한 개 지방유래 중간엽줄기세포가 생쥐의 염증성 장질환 모델에서 치료효과를 증대시킬 수 있는지 연구하였다. TNF-α 를 24 시간동안 10 ng/ml 로 자극한 개 지방유래 중간엽줄기세포는 높은 농도의 TSG-6 와 prostaglandin E2 (PGE2)를 분비하였다. DSS 또는 dinitrobenzene sulfonic acid (DNBS)에 의해 대장염이 유발된 생쥐에 TNF-α 를 자극시킨 개 지방유래

중간엽줄기세포를 복강 내로 투여하였다. 이후 생쥐에서 부검을 통해 대장 조직을 얻었으며 조직학적 검사와 유세포 분석을 진행하였다. TNF-α 를 자극한 개 지방유래 중간엽줄기세포는 대장염 유발 생쥐의 증상을 크게 개선시켰으며, 대장에서의 염증 사이토카인의 발현양을 강력히 감소시켰다. 또한 대장에서 M1 대식세포 (F4/80+/iNOS+ 세포)의 감소 및 M2 대식세포 ($F4/80^{+}/CD206^{+}$ 세포)의 증가를 강력하게 유도하였다.

결론적으로, 이 학위 논문을 통해 사람과 개의 지방유래 중간엽줄기세포에서 분비하는 TSG-6 가 염증성 장 질환 생쥐 모델에서 치료 효과를 나타냄을 증명하였다. 게다가, TNF-α 를 자극한 개 지방유래 중간엽줄기세포는 염증 조절 인자인 TSG-6 와 PGE2 를 더 많이 분비함으로써 염증이 있는 조직에서의 M2 대식세포의 증가와 증상의 개선을 더욱 강력히 개선함을 확인하였다. 이러한 결과는 IBD 에 이환된 개에서 세포 치료를 적절히 활용하는 데에 기여할 것이다.

주요어: 염증성 장 질환 / 자가면역 질환 / 중간엽 줄기세포 / TSG-6 / 면역 조절 / 항염증 / 개

학번: 2013-21558